FINAL REPORT

on

R&D Project

EXPERIMENTAL STUDY ON LABYRINTH / PIANO KEY SPILLWAY

SPONSORED BY

INDIAN NATIONAL COMMITTEE ON HYDRAULICS (INCH)
MINISTRY OF WATER RESOURCES
GOVT. OF INDIA

PREPARED BY

WATER RESOURCES DEVELOPMENT & MANAGEMENT
INDIAN INSTITUTE OF TECHNOLOGY
ROORKEE
ROORKEE -247 667, INDIA

TEAM OF INVESTIGATORS

Principal Investigator
> **Dr. Nayan Sharma**
> *Professor & Head*
> *Water Resources Development &*
> *Management*
> *IIT-Roorkee*

Co- Principal Investigator
> **Dr. C. S. P. Ojha**
> *Professor*
> *Civil Engineering Department*
> *IIT-Roorkee*

Research Associate
> **Mr. Gopal Das Singhal**
> *Research Associate*
> *Water Resources Development &*
> *Management*
> *IIT-Roorkee*

Supporting Staff
> **Mr. Neeraj Kumar**
> *Computer Operator*
> *Water Resources Development &*
> *Management*
> *IIT-Roorkee*

CONTENTS

LIST OF FIGURES

iv

LIST OF PLATES

LIST OF TABLES

LIST OF NOTATIONS

The following symbols are used in this thesis

Symbol		Description	Units
a	=	Width of inlet cell	cm
A	=	Flow area upstream of weir	m^2
b	=	Width of outlet cell	cm
B	=	Length of elements	cm
C_d	=	Discharge coefficient of rectangular sharp crested weir; and discharge coefficient of V-notch	---
C_{dm}	=	Discharge magnification coefficient	---
Fr	=	Froude number	---
g	=	Gravitational acceleration	cm/sec^2
H	=	Total depth of water in channel	cm
h	=	Head over the crest (at one meter u/s of the P. K. Weir)	cm
H_e	=	Effective depth of water above vertex at the upstream of V-notch;	cm
K_h	=	Combined effects of fluid properties	----
L	=	Perimeter of Piano Key weir	cm
L/W	=	Length magnification ratio	---
p	=	Crest Height of Piano Key weir	cm
Q	=	Discharge over a rectangular notch	cm^3/sec Q_L
	=	Discharge through sharp crested weir	cm^3/sec
Q_{PK}	=	Discharge through Piano Key weir	cm^3/sec
r	=	ratio of Piano Key Weir discharge to linear weir discharge	---
R^2	=	Squared correlation coefficient	---
W	=	Width of channel	cm
Z	=	Height of crest	cm
ΔQ	=	Difference of Piano Key weir discharge and Rectangular sharp crested weir discharge	cm^3/sec
θ	=	Angle of the V-notch	degree

1.1   GENERAL

A weir is built across a river (or stream) in order to raise level of water on the upstream side and to allow the excess water to flow over its entire length to the downstream side. Thus a weir is similar to a small dam constructed across river, with the difference that whereas in the case of a dam excess water flows to the downstream side, only through a small portion called spillway, the same in the case of a weir flow over its entire length. Spillways represent a substantial portion of total project costs and they play a major role in ensuring safety (Modi and Seth, 1991). Weirs may be classified according to the shape of opening, the shape of crest, the effect of sides on the issuing the nappe and the discharge condition. According to the shape of opening, the weirs may be classified as rectangular, triangular and trapezoidal weirs. According to the shape of the crest, the weirs may be classified as sharp crested weir, narrow crested weir, broad crested weir and ogee shaped weir.

As projects are reassessed for safety, provision for an increased estimate of the probable maximum flood (PMF) has to be made in many cases. It is therefore necessary to provide more flood storage and/or larger capacity for spillways to pass the PMF safely. If the dam can not adequately pass the updated flood, the structure requires modification by increasing the flood storage space, increasing the spillway capacity or using combinations of these two solutions. An innovative and effective way of increasing the spillway capacity is to use a Labyrinth weir. The concept of the Labyrinth weir is to vary the plan shape of the crest to increase the effective crest length (Lempérière and Jun, 2005; and Baud et al. 2002). This increases the discharge per unit width of the spillway for a given operating head.

The ability of the Labyrinth to pass large flows at comparatively low heads has led to many applications. The primary use of Labyrinth weir has been as a spillway for dams. It is particularly suited for use where the spillway width is restricted, or where the flood surcharge space is limited. The Labyrinth is relatively low cost when compared with gated spillways and this has led to its use in conjunction with the raising of dams for increased storage space. Labyrinth weirs can be highly effective in many circumstances (Blanc and Lempérière, 2001).

A Labyrinth weir has advantages compared to the straight over flow weir and the standard ogee crest. The total length of Labyrinth weir is typically three to four times the spillway width. Its capacity varies with head and is typically about twice that of a standard weir or over flow crest of the same width. Labyrinth weirs can be used to increase outlet capacity for a given spillway crest elevation and length or to increase storage by raising the crest while maintaining spillway capacity.

1.2   LABYRINTH WEIR

Labyrinth weirs are polygonal walls, designed to provide a much longer overtopped crest than the length of the spillway. The Labyrinth weir is particularly well-suited for cases where the length of the structure has to be restricted or for rehabilitation of existing spillways (Emiroglu and Baylar, 2005; and Hay and Taylor, 1970). The concept involves a structure where the crest length is developed by triangular or trapezoidal elements which are much longer than the spillway chute width.

This type of spillway is characterized by a broken-axis weir in plan, generally with the same polygonal pattern repeated periodically. Hence, for the same total width, the Labyrinth weir spillway will present larger crest lengths than the same solution.

A Labyrinth weir can pass large discharge at a relatively low head. Its advantage includes relatively low construction and maintenance costs, and more reliable operation, compared with gated spillways. As their application is sometimes difficult in rehabilitation projects due to inappropriate supporting conditions, a new concept of Labyrinth weirs has been proposed with a new shape, called Piano Key Weir (Chi et al., 2006; and Lempérière and Ouamane, 2003). This innovative alternative of Labyrinth weir provides an increase in the stability of the structure which can be placed on the top of most existing or new gravity dams.

1.3   PIANO KEY WEIR

A new concept of a Labyrinth weir has been proposed with a new shape like black and white Piano keys when viewed in plan, this new concept was called the Piano Key Weir (Lempérière and Ouamane, 2003). This innovative design solves most of the problem presented by the original Labyrinth weir, and is also more efficient. Compared with the traditional Labyrinth weir:

- Plan view of the Piano Key Weir is not trapezoidal, but rectangular

- Vertical walls founded on a flat area are replaced by lateral vertical walls and sloping slabs upstream and downstream of the crest. These slabs are partially a cantilever structure, upstream and downstream. Therefore the overall structure is self balanced

- The Piano Key Weir can be positioned on the top of the crest of new or existing gravity dams.

- Application can cover a wide range of specific flows, from 3 to 1000 $m^3/s/ml$.

- Piano Key Weir can increase by a factor about 1.50 to 4.00 times than the specific discharge capacity of straight sharp crested weir.

- From a structural point of view, Piano Key Weir is extremely hyper-static structures, which are solid and simple.

This innovative alternative of Labyrinth weir has a considerably higher specific flow. The Piano Key Weir can increase safety and the storage and/or the flood control efficiency of existing/new dams. For increasing the storage capacity of reservoir, sediment passage from reservoir area through Piano Key Weir ramp is an additional benefit. The outcome of this study is very much relevant to address the dam safety concerns in developing and developed nation in the current context of adverse hydrological consequences due to ongoing global warming phenomenon, intense rainfall like cloud burst and erratic hydrologic condition.

A Piano Key Weir has advantages compared with the straight overflow weir and the standard ogee crest. The total length of the Piano Key Weir is typically three to seven times the spillway width. Its discharging capacity varies with head and is typically about twice that of a straight sharp crested weir or overflow crest of the same width. Piano Key Weir can be used to increase outlet capacity for a given spillway crest elevation and length or to increase storage by raising the crest while maintaining spillway capacity.

The flow downstream of a Piano Key Weir is considerably aerated as per a system of air injection. Consequently the risks of erosion or cavitation are considerably reduced and the cost of new downstream structures or the maintenance of existing ones is reduced. To avoid vibrations in Piano Key Weir, it is advisable to aerate the nappe.

The Piano Key Weir is particularly well suited for cases where the length of the structure has to be restricted or for the rehabilitation of existing spillways. A Piano Key Weir can pass large discharge at a relatively low head. Its advantages include relatively low construction and maintenance costs and more reliable operation, compared with gated

spillways. In addition for a given maximum operation head, a Piano Key Weir can be an economical alternative in terms of dam crest elevation and reservoir storage volume. The ability of the Piano Key Weir to pass large flows at comparatively low heads has led to many applications. The primary use of Piano Key Weir has been as a spillway for dams. It is particularly suited for use where the spillway width is restricted or where the flood surcharge space is limited.

1.4   OBJECTIVES OF THE STUDY

Keeping in view the relatively reported better performance of Piano Key Weirs in comparison to linear and Labyrinth weirs, following objectives are considered for the present study.

1. Investigation of Piano Key Weir behaviour covering h/p ratio values in the higher ranges of h/p.
2. Hydraulic performance of different shapes and dimensions from the stand point of Piano Key Weir effect.
3. Study of jet interaction and its effect on labyrinth behaviour at higher h/p ratios.
4. Study of length magnification ratio (L/W) vis-à-vis (h/p) ratio on Piano Key Weir effect.
5. Preparation of standardized design covering higher ranges of h/p ratio above 0.5.
6. Investigation into hydraulic and structural effects of Piano Key Weir by different degree of cement mortar filling.
7. Investigation of energy loss behaviour in the flow domain around different models of Piano Key Weir.

With the above objectives in view, the relevant details of the experimental programme have been done.

CHAPTER – 2

LITERATURE REVIEW

2.1   GENERAL

Considering the importance of Piano Key Weir in comparison to other type of weirs, present chapter looks into available practices with particular reference to labyrinth weir/spillway. It also deals with review related to variation of Labyrinth weir discharge coefficient. Finally, it deals with very limited research work on Piano Key Weir to emphasize the need for the present study.

2.2   DEVELOPMENT AND FIELD APPLICATIONS OF LABYRINTH WEIR

Most spillways consist of some form of a weir. The weirs are normally placed perpendicular to the flow direction. The most significant parameters in determining the capacity of a weir are its height relative to the upstream depth, the crest shape and the crest length (Afshar, 1988; and Falvey, 2003). Here, capacity refers to the flow rate or discharge for a given depth of flow over the crest of the weir. Of these parameters, the crest length has the greatest influence on the spillway capacity. In this section, certain examples of existing dams are provided where attempt has been made to increase the crest length.

As the emphasis on dam safety has increased, many spillways must be rehabilitated to increase their capacity without changing the reservoir storage. However, for many spillways, the width of the approach channel or the downstream chute cannot be widened. To increase the crest length but keep the spillway width constant, the crest is often placed at an angle to the centerline of the chute. If the crest is placed parallel with the chute centerline, it is called a side channel spillway (Pinheiro and Silva, 1999), as shown in Fig. 2.1
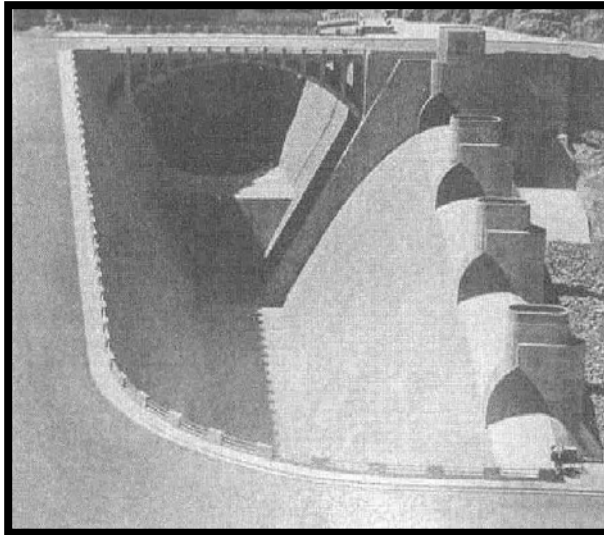
Fig. 2.1 Side channel spillway – Arizona spillway at Hoover dam, USA (Pinheiro and Silva, 1999)

The length can be increased further and can still keep the downstream dimension small by folding the weir into several sections. One implementation of this idea is the duckbill spillway, as shown in Fig. 2.2.
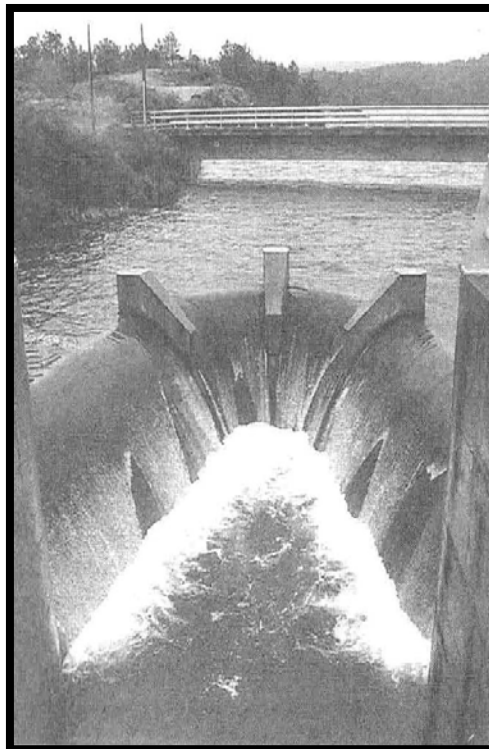
Fig. 2.2 Duckbill spillway – Apartadura spillway, Portugal (Pinheiro and Silva, 1999)

Several cycles of this type of spillway can be placed together to further increase the spillway length. A variation of the duckbill spillway is tile bathtub spillway, as shown in Fig. 2.3. This shape is rectangular instead of the approximately triangular shape of the duckbill.
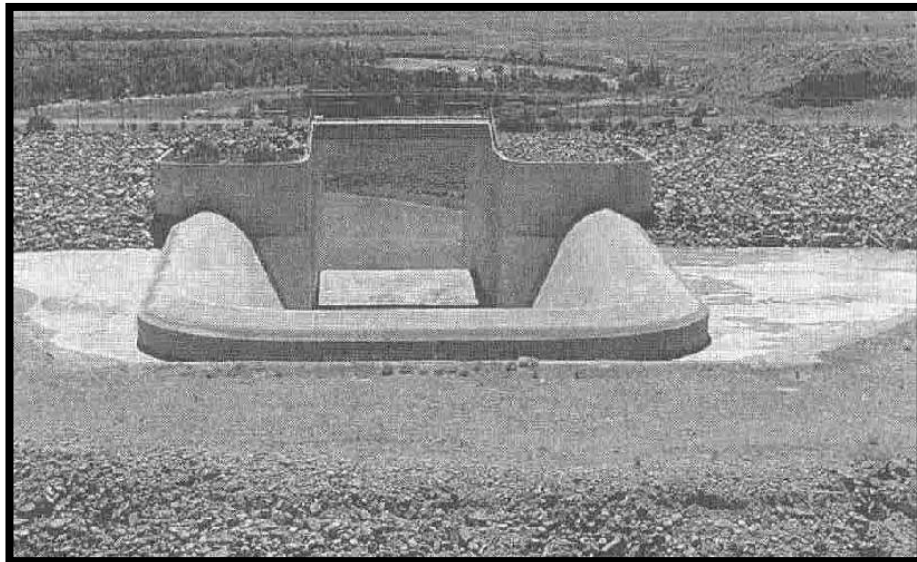
Fig. 2.3 Bathtub spillway – Fontenelle dam, USA (Falvey, 2003)

Several cycles of the bathtub shape can be placed side by side. These weirs are called corrugated, accordion, or folded weirs. If several cycles of the duckbill spillway are placed side by side, the weir is called a Labyrinth weir, as shown in Fig. 2.4.
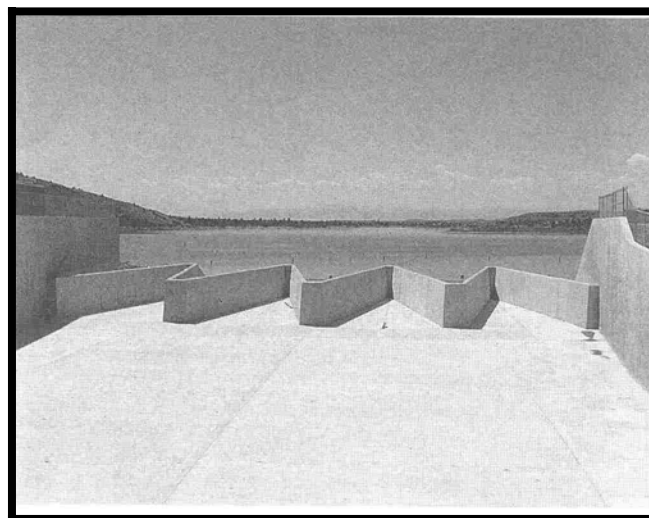
Fig. 2.4 Labyrinth weir- Tongue River dam, USA (Falvey, 2003)

Hydraulic model studies have been conducted at the Portuguese National Laboratory for Harrezza dam (Algeria) in 1980, Dungo dam (Angola) in 1981 and Keddara dam (Algeria) in 1984, and the details are narrated below.

Harrezza Dam

Harrezza dam is a 41 m high earthfill dam. Initial design included an ogee spillway of straight crest, without gates, with three bridge piers and its was located next to the left abutment. At the foot of the spillway there was stilling basin, connected downstream to a 700 m long excavated, rather steep transition channel to the natural river. The weir width was 64.50 m (Four 15.00 m wide spans and three 1.50 m thick piers)

The model tests indicated an upstream head over crest of 2.08 m for a design discharge of 350 m^3/sec. The downstream transition channel to the natural river was to be built in a very soft clay soil. In consequence, the hydraulic model tests led the way to include in the design an armored blanket to protect the transition channel. The existence of this apron made the initially designed spillway non economic solution.

Therefore, a new spillway was designed, next to the right abutment. The downstream transition of the river becoming significantly shorter, but the available width for the entrance zone and spillway weir becoming rather smaller, due to topographical constraints.

The new spillway presents a Labyrinth weir followed by a 230 m long steep channel with variable width (30, 40 to 20 m), a 35 m long stilling basin and finally a transition channel which become almost horizontal.

The Labyrinth weir has three cycles with a total length of 90 m and width 30 and 40 m, includes on the upstream side, three piers, which serve as splitters also.

Model test indicated, for this new solution a quite good behaviour, with an upstream head over crest of 1.90 m for a design discharge of 350 m^3/sec.

Dungo Dam

Dungo dam is a 19 m high earth fill dam. The initial design included a straight ogee crest spillway to be built next to the dam right abutment, without gates, with four bridge piers, and followed downstream by a canal and a stilling basin. The weir total width was approximately 72.50 m. The design discharge of 576 m^3/sec would correspond to an upstream head over crest of 2.50 m.

A large flood occurred during the spillway construction, destroyed the spillway crest and the canal. To rebuild the same spillway was too expensive, so a new spillway was designed located now at the dam left abutment.

The new spillway, much narrower than the initial one, has a Labyrinth weir, followed, similarly, by a canal and a stilling basin. The Labyrinth weir has a total length of 115.50 m and total width of 40.10 m, it has four cycles, and includes splitter piers at both sides upstream and downstream.

The model test confirmed the excellence of this solution, which was finally adopted for construction. The design discharge of 576 m^3/sec was set to an upstream head over crest of 2.40 m.

<u>Keddara Dam</u>

Keddara dam is a 108 m high rockfill dam. The spillway was designed for a 250 m^3/sec discharge and it includes, essentially a Labyrinth weir, a canal and a stilling basin. In this case the Labyrinth weir was adopted since the beginning as the most economical solution. It consists of two cycles and has a total length of 53.77 and a total width of 19.00 m and it includes two bridge splitter piers at the upstream end. The model tests confirmed a well behaved solution with an upstream head over crest of 2.46 m for a design discharge of 250 m^3/sec.

Thus, for dams in operation it is sometimes required to increase the spillway discharge capacity, which may be done either by proposing another spillway or by changing the spillway in weir form.

2.3 LABYRINTH WEIR

2.3.1 General

Labyrinth weirs are polygonal walls, designed to provide a much longer overtopped crest than the length of the spillway. The Labyrinth weir is particularly well-suited for cases where the length of the structure has to be restricted or for rehabilitation of existing spillways. The concept involves a structure where the crest length is developed by triangular or trapezoidal elements which are much longer than the spillway chute width.

This type of weir is characterized by a broken-axis weir in plan, generally with the same polygonal pattern repeated periodically. Hence, for the same total width, the Labyrinth weir will present larger crest lengths than the same total width.

A Labyrinth weir has advantages compared to the straight over flow weir and the standard ogee crest. The total length of Labyrinth weir is typically three to four times the spillway width. Its capacity varies with head and is typically about twice that of a standard weir or over flow crest of the same width. Labyrinth weirs can be used to

increase outlet capacity for a given spillway crest elevation and length or to increase storage by raising the crest while maintaining the spillway capacity.

A Labyrinth weir can pass large discharge at a relatively low head. Its advantage includes relatively low construction and maintenance costs, and more reliable operation, compared with gated spillways.

In addition, for a given maximum operation head, a Labyrinth weir can be an economical alternative in terms of dam crest elevation and reservoir storage volume. Although it has a broad range of applications, its complex flow conditions and design have been considered a drawback by designers.

2.3.2 Characteristics of Flows Over Labyrinth Weir

The distinguishing characteristic of this spillway is that the plan shape is not linear but varies using a repeating plan-form. The repeating plan-forms that have been used are U, V and trapezoidal shapes. Using these plan-form shapes for spillways result in a complex flow pattern. Ideally the discharge passing over the Labyrinth should increase in direct proportion of an increase in crest length. However, this is only the case for Labyrinth weirs with low design heads. Qualitatively, as the upstream head increases, the flow pattern using a Labyrinth weir sequentially passes through four basic phases. These phases are fully aerated, partially aerated, transitional and suppressed (Wormleaton and Tsang, 2000).

The fully aerated condition occurs at low upstream heads when the flow falls freely over the entire length of the Labyrinth crest. In this flow condition, the thickness of the nappe and depth of fall of water do not affect the discharge capability of the spillway. As a result, the Labyrinth behaves almost ideally when compared to a linear weir with the same vertical cross section.

In partially aerated phase when head increases, the tail water depth increases particularly between the nappe and the Labyrinth wall, due to convergence of opposing nappes. The higher tail water depths and restricted area at the upstream apexes aeration under the nappe is maintained. A stable air pocket is formed along each side wall and downstream apex of the Labyrinths.

In the transitional phase, the nappe is alternating between intermittent air entrainment and solid water flows. It is difficult at times to distinguish between the partially aerated and transitional phases but transitional region can be easily identified as a discontinuity in the discharge co-efficient curve.

On the suppressed phase, the flow over the Labyrinth crest forms a solid non aerated nappe. The thickness of the nappe and the depth of tail water do not allow air to be drawn under the nappe. As the upstream head increases, this last flow condition eventually leads to full submergence of the Labyrinth weir. Complete submergence of the Labyrinth usually occurs when the flow depth over the crest is greater than the height of the Labyrinth.

2.3.3   Basics Parameters of Labyrinth Weir

The discharge characteristics of Labyrinth weirs are primarily a function of the weir height, p, the depth of flow over the weir, h, the width of the weir, W, the developed length of the Labyrinth, L, and its shape. Thus, the discharge can be expressed as

$$Q = f(h/p, L/W, Shape) \tag{2.1}$$

The shape of a Labyrinth can be rectangular, trapezoidal, or triangular. Analytic development showed that the flow over a skew weir is strongly influenced by the angle the weir forms with the upstream flow direction. For a triangular weir, the angle is related to the L/W ratio by

$$\alpha_{max} = \arcsin(W/L) \tag{2.2}$$

The angle given by this relationship is the maximum value that can be achieved for a Labyrinth weir. For a trapezoidal plan form, the angle is given by

$$\alpha = \arcsin\left(\frac{W - 4a}{L - 4a}\right) \tag{2.3}$$

where α is side wall angle and a is half apex width.

2.3.4   Different Theories of Labyrinth Weir Discharge Coefficient

<u>**Taylor (1968)**</u>

In the experiments conducted by Taylor, (1968), the discharge was made dimensionless by dividing the Labyrinth weir flow by the discharge of a linear weir that has the same channel width. This is a clever method of removing the effects of surface tension in the model tests. In this manner, a family of curves that represent the characteristics is given by

$$\frac{Q_{Lab.}}{Q_L} = f(h/p, Shape) \tag{2.4}$$

in which p is weir height; Q_{Lab} is the total discharge of the Labyrinth weir; Q_L is the

discharge of a linear weir having the same width of the Labyrinth weir; and h is head over the weir.

Design charts prepared by Hay and Taylor (1970) are shown in Figs. 2.5 and 2.6. These curves are for a Labyrinth located in a channel.

The discharge for a linear weir in these studies was determined from the weir equation of Kindsvater and Carter (1959):

$$Q_k = C_s L_e h_e^{3/2} \qquad (2.5)$$

where L_e is equvlent crest length; h_e is equivalent head on the crest.

in which the discharge coefficient C_s is given by

$$C_k = -3.22 + 0.40 \frac{h}{p} \qquad (2.6)$$

TRIANGULAR PLAN FORM
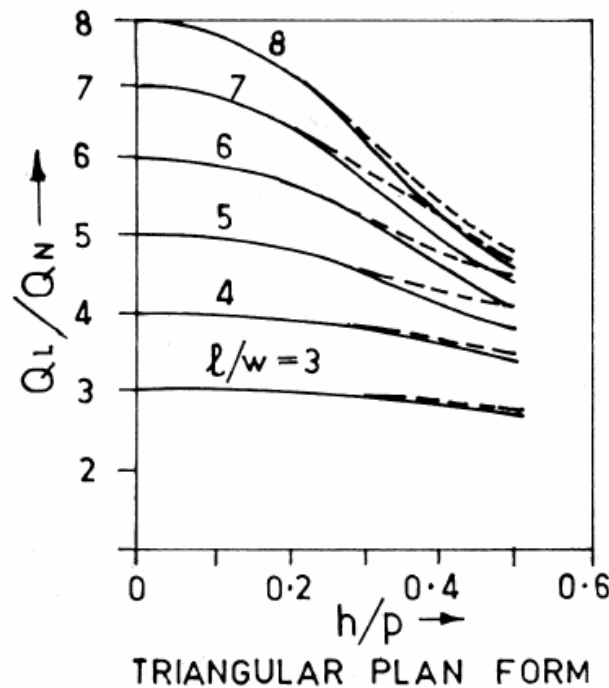
Fig. 2.5 Design curve - triangular -sharp crested weir (Hay and Taylor, 1970)
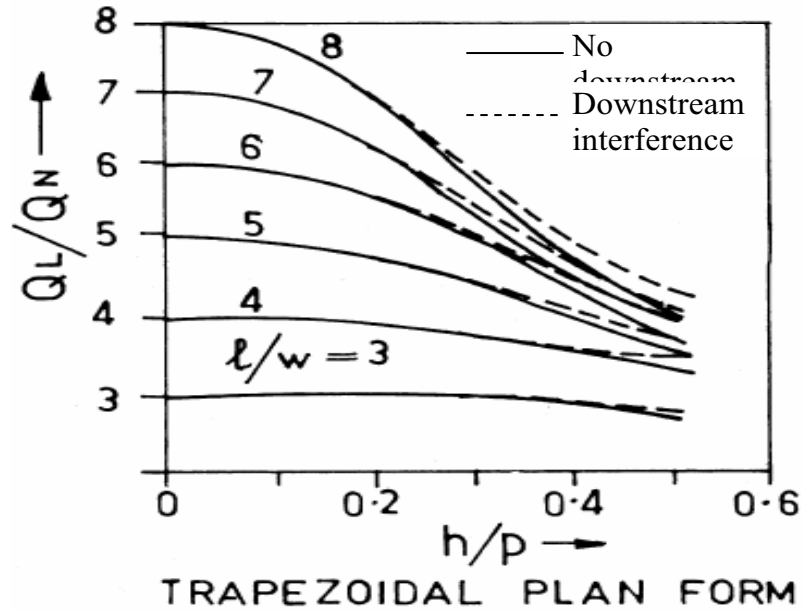
Fig. 2.6 Design curve - trapezoidal - sharp crested weir (Hay and Taylor, 1970)

Darvas (1971)

Darvas (1971) introduced the concept of a discharge coefficient defined as

$$C_W = \frac{Q_{Lab}}{WH_o^{3/2}} \tag{2.7}$$

in which $Q_{Lab.}$ = the total discharge; W = the total width of the Labyrinth weir; C_w is Darvas discharge coefficient; and H_o = the total head on the weir. This coefficient has the units of ft$^{0.5}$/sec. The plots of Darvas are given as a family of curves in which

$$C_w = f(H_o / p, L / W) \tag{2.8}$$

in which L is the development length of the Labyrinth weir and p is weir height. These curves shown in Fig. 2.7
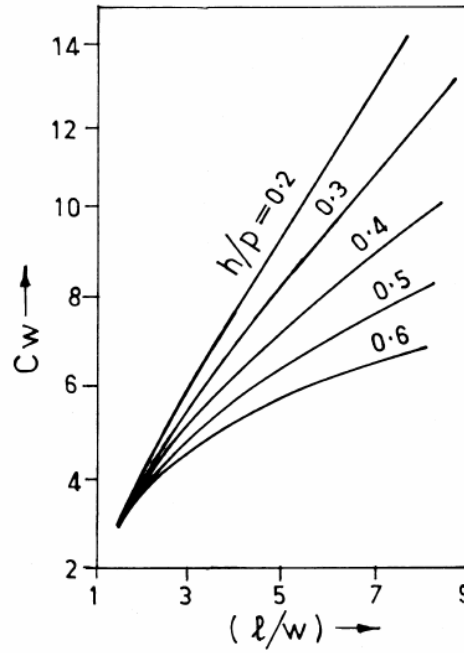
Fig. 2.7 Design curves between C_W Vs L/W (Darvas, 1971)

Mcgalhaes and Lorena (1989)

Megalhaes and Lorena (1989) and Megalhaes (1985) developed curves similar to that of Darvas (1971), except their curves are for a nappe or ogee crest, and the discharge coefficient is given in dimensionless terms by

$$C_p = \frac{Q_{Lab}}{W\sqrt{2g}H_o^{3/2}} \tag{2.9}$$

where H_o is total upstream head; Q_{Lab} is total discharge; C_p is Megalhaes discharge coefficient; W is width of channel; and g is the acceleration of gravity. Design curves are shown in Fig. 2.8.
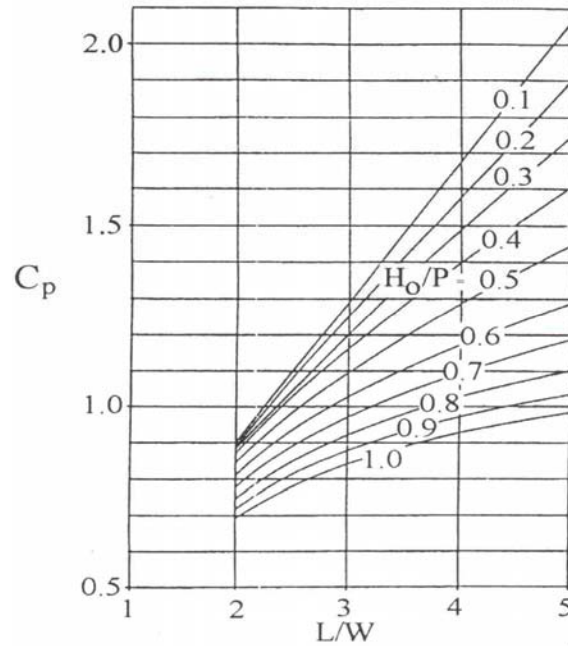
Fig. 2.8 Design curves between C_p Vs L/W (Magalhaes and Lorena, 1989)

Lux (1989)

Lux (1989) introduced another discharge coefficient based on the total upstream head. His relationship for the discharge of one cycle is given by

$$Q_k = C_W \left(\frac{W_c / p}{W_c / (p + k)} \right) W_c H_o \sqrt{g H_o} \tag{2.10}$$

in which k is a shape constant; H_o is the total upstream head; p is height of weir; W_c is width of channel; C_W is Darvas discharge coefficient and g is the acceleration of gravity. These curves are shown in Figs. 2.9 & 2.10.
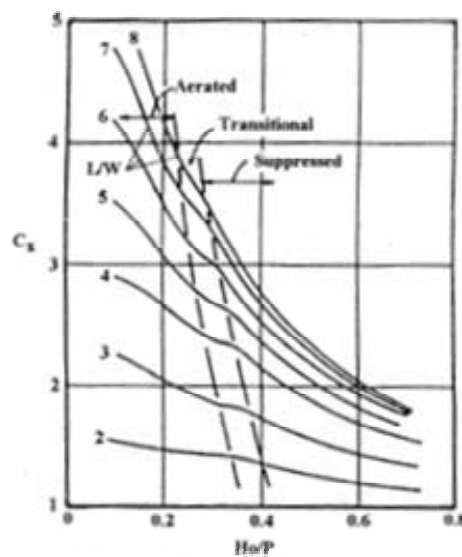
Fig. 2.9 Design curve - triangular weir (Lux, 1985)

15
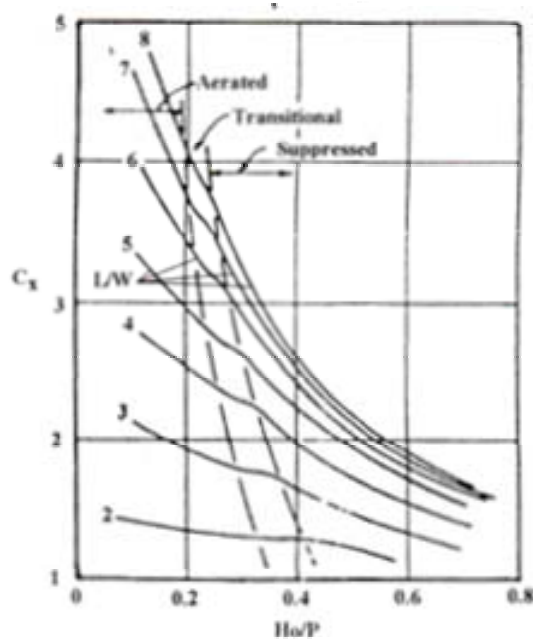
Fig. 2.10 Design curve - trapezoidal weir (Lux, 1985)

Tullis et al. (1995)

Tullis et al. (1995) defined a coefficient that used the total upstream head on the weir. Their equation is

$$Q_{Lab.} = C_T L \frac{2}{3} \sqrt{2g} H^{1.5} \qquad (2.11)$$

where C_T is crest coefficients for a weir, H is head over the crest of weir and L is length of weir crest.

This is similar to the conventional weir discharge equation, except that the head is the total upstream head and not the head or, the weir crest. All of the tests were performed in a channel similar to the investigations of Taylor (1968).

The crest coefficients for a triangular weir with a quarter-round crest are shown in Fig. 2.11 as a function of the angle that the weir makes with the flow.
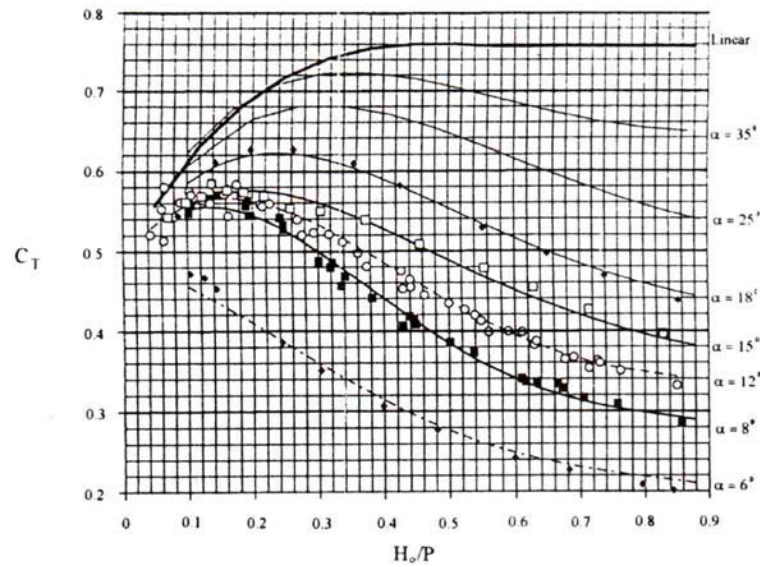
Fig. 2.11 Design curves with quarter-round crest and a triangular weir

(Tullis et al., 1995)

2.4   PIANO KEY WEIR

As for Labyrinth weirs, the advantage of Piano Key Weir is to increase the total effective crest length for a given width (Ouamane and Lempérière, 2006). Consequently, it can be used to increase the discharge capacity for a given head or decrease the head for a given discharge. Therefore, the implementation of such a spillway allows a high crest level which can also increase the storage capacity in the reservoir. In addition, beyond economical considerations, Piano Key Weir is a free flow spillway and has a high level of safety and reliability. Moreover floating debris will easily pass over as the water level increases. A key advantage of Piano Key Weir structures is that they can be placed on the crest of most existing or new gravity dams, unlike traditional Labyrinth weirs.

The flow behaviour compared to the conventional Labyrinth structures is quite different. The flow is divided into two parts, one from the inlet of the Piano Key Weir that overflows as a thin screen and another from the outlet, which flows as a jet at the bottom (Leite et al., 2009).

2.4.1   Flow Characteristics over Piano Key Weir

The flow over Piano Key Weir is complicated further by the interference of the jets at the upstream apex of the Piano Key Weir. That is, at high flows, the jets from adjacent crests strike each other. This creates a nappe that is not aerated and can decrease the discharge coefficient of the weir. The degree of impact increases as the angle between the crests decreases and as the flow depth over the crest increases. As a result, for most Piano Key Weirs, the underside of the nappe gets aerated only for low flow depths.

The interference of the jets from adjacent crests means that Piano Key Weirs become less and less effective as the reservoir level rises. At some depth, the flow over a Piano Key Weir is almost the same as the flow over a straight weir.

The nappes from two weirs placed at an angle with each other will have an impact over a limited length of the weir crest.

This impact is called nappe interference. The effect of the nappe interference is to decrease the discharge. Interference occurs when the jets from the two sidewalls and the sidewall intersect.

2.4.2   Review of the Existing Model Study of Piano Key Weir

An initial model investigations and behavior of Piano Key Weir was studied by Lempérière and Ouamane (2003) in terms of a magnification ratio of the Piano Key Weir against sharp-crested linear weir having the same channel width. The results of the test showed that the Piano Key Weirs are simple solutions as safe and easy to operate as traditional free flow spillways and much more efficient. They may improve the flood control by many existing dams.

Behavior of Piano Key Weir was studied by Barcouda et al. (2006) in terms of a magnification ratio of the Piano Key Weir flow for a sharp-crested linear weir having the same channel width. The results of the test show that the Piano Key Weirs are more efficient than the traditional Labyrinth weir and Piano Key Weirs can be an interesting solution for increasing the active storage of reservoir or for improving the safety of dam during extreme flood.

Some models studies were done by Leite et al. (2007) for rehabilation of St-Marc dam at Laboratory of Hydraulic Constructions (LCH) at the Ecole Polytechnique Federal de Lausanne (EPFL), Switzerland. Experimental tests also demonstrated the efficiency of the Piano Key Weir under low heads also.

In Electricite de France (EDF), Laugier (2007) tested the Piano Key Weir to increase the discharge capacity at Golours Dam, in Southwestern France. The preliminary design was based on Lempérière and Ouamane (2003). Some additional tests were carried out on a hydraulic model constructed at the EDF hydraulic Laboratory (EDF-LNHE), and some configurations were studied. This study represents an innovative solution to increase spillway discharge capacity for flood mitigation.

Thus, a very limited research has been conducted on Piano Key Weir. There are no design criteria, design curve developed from the model studies, as well as shape optimization for generalized Piano Key Weir reported in literature.

2.5   SUMMARY

In this chapter various studies related to Labyrinth weir and Piano Key Weir mechanisms and their applications has been reviewed. It is obvious that Piano Key Weir performance depends on a number of factors including shape geometry, flow pattern and related variables. The opinion defers regarding the relative importance of these factors on performance of Labyrinth weir.

The Piano Key Weir uses simple shapes linked in a repetitive manner to form the structure. These two concepts, simplicity and repetition, makes design and construction of Piano Key Weir easy. Having the Piano Key should be considered as a viable alternative.

3.1 GENERAL

It is obvious that certain preliminary studies on the performance of Piano Key Weir are necessary in order to identify the discharge passing capacity and depth saving. The effect of different shapes and dimensions of Piano Key Weir with different length magnification ratio is also important and needs detailed investigations. With this in view, the experimental programme was organized in five phases. The Piano Key Weir models were made of perspex sheet and all the experiments were performed in a 50 cm wide flume. In this chapter, five phases of experimental campaign on twenty eight Piano Key Weir models are reported. Details of Piano Key Weir shapes are also provided.

3.2 EXPERIMENTAL SET-UP

The experimental set-up consists of the following flow measuring instruments and water conductor infrastructure.

3.2.1 Flow Measuring Instruments

- V-notch: It was used for the measurement of discharge through the P. K. Weir. 900 V-notch was used for the discharge measurement. The V-Notch is shown diagrammatically in Fig. 3.1.
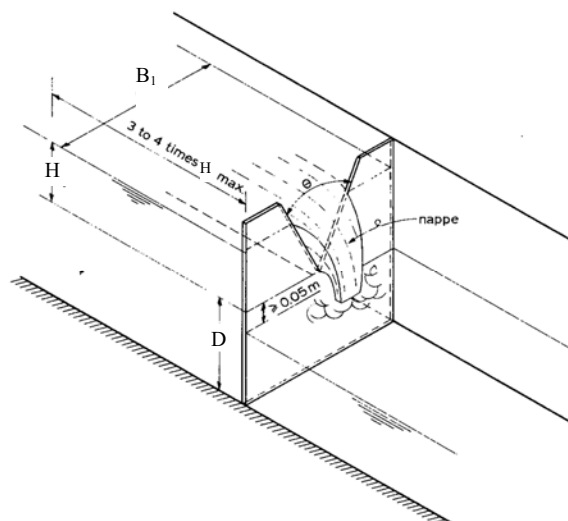
Fig. 3.1 V-notch sharp crested Weir

The following flow regimes are encountered with V-notch sharp-crested or thin-plate weirs:

a) "Partially contracted weir", i.e. in a weir the contractions of which along the sides of the V-notch are not fully developed due to the proximity of the walls and/or bed of the approach channel.

b) "Fully contracted weir", i.e. a weir which has an approach channel whose bed and sides are sufficiently remote from the edges of the V-notch to allow for a sufficiently great approach velocity component parallel to the weir face so that the contraction is fully developed.

These two types of V-notch sharp-crested weirs may be classified by the following limitations on H/D, H/B_1, H, D and B_1. It should be noted that in this classification fully contracted flow is a subdivision of partially contracted flow.

Classification and Limits of Application of V-Notch Sharp-Crested (Thin –Plate) Weirs are shown in below

Partially contracted Weir	Fully contracted Weir
$H/D \leq 1.2$	$H/D \leq 0.4$
$H/B_1 \leq 0.4$	$H/B_1 \leq 0.2$
$0.05\ m < H \leq 0.6\ m$	$0.05\ m < H \leq 0.38\ m$
$D \geq 0.1\ m$	$D \geq 0.45\ m$
$B_1 \geq 0.6\ m$	$B_1 \geq 0.90\ m$

The basic head-discharge equation for a V-notch weir is

$$Q = c_e \frac{8}{15}(2g)^{0.5} \tan\frac{\theta}{2} H^{2.5} \qquad (3.1)$$

To apply this equation to both fully and partially contracted sharp-crested weir it is modified to a form proposed by Kindsvater and Carter

$$Q = c_e \frac{8}{15}(2g)^{0.5} \tan\frac{\theta}{2} H_e^{2.5} \qquad (3.2)$$

where θ equals the angle induced between the sides of the notch and h_e is the effective head which equals $H+K_H$. the quantity k_H represents the combined effects of fluid properties. Empirically defined values for k_H as a function of the notch angle (θ) are shown in Fig. 3.2.
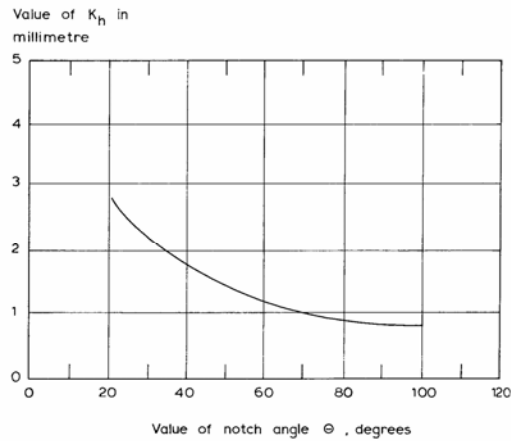
Fig. 3.2 Value of K_h as a function of the notch angle

For water at ordinary temperature, i.e. 5^0C to 30^0C or 40^0F to 85^0F, the effective coefficient of discharge (C_e) for a V-notch sharp-crested weir is a function of three variables:

$$c_e = f\left[\frac{H}{D}, \quad \frac{D}{B_1}, \quad \theta\right] \tag{3.3}$$

If the ratios H/D $\leq$ 0.4 and D/B$_1$ $\leq$ 0.2, the V-notch weir is fully contracted and C_e becomes a function of only the notch angle θ, as illustrated in Fig. 3.3.
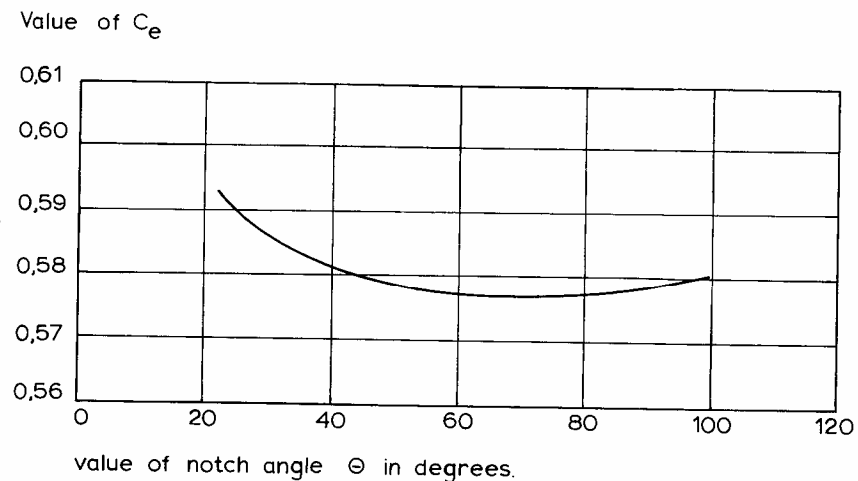
Fig. 3.3 Coefficient of discharge C as a function of notch angle for fully contracted V-notch weirs.

If on the other hand the contraction of the nappe is not fully developed, the effective discharge coefficient (C_e) can be read from Fig. 3.4 for a 90-degree V-notch only.
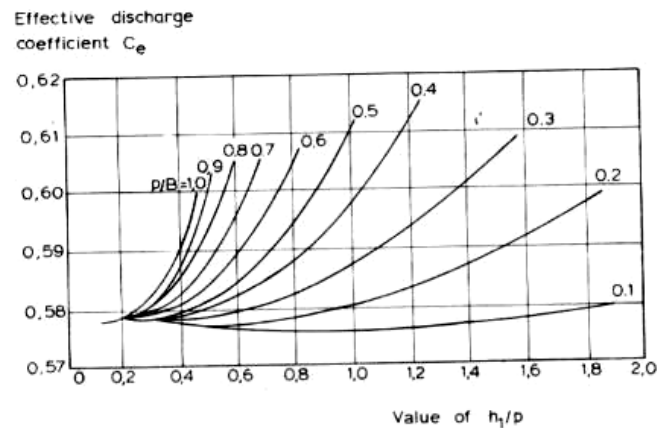
Fig. 3.4 c as a function of h_1/p and p/B for 90-degree V-notch sharp operated weir

- **Point gauge:** It was used to measure the head over crest at the upstream of P. K. Weir and head over the V-notch.

3.2.2 Water Conductor Infrastructure

- **Constant head tank:** An overflowing tank was installed at the upstream head-end to ensure the supply of steady discharge into the experimental flume.
- **Flume:** Rectangular flume of size 50 cm x 80 cm was used for passage of water from upstream head to the P. K. Weir installed in the downstream end.
- **Pipe network and pump:** From downstream of V-notch to upstream of P. K. Weir, the flow network is connected through a pipe system. 20 H.P. pumps are connected to the pipe network for recirculation of water from the storage tank.
- **Piano Key Weir models:** Twenty eight selected models of P. K. Weir have been used for experimentations. The three dimensional view of generalized Piano Key Weir shape is shown in Fig. 3.5.
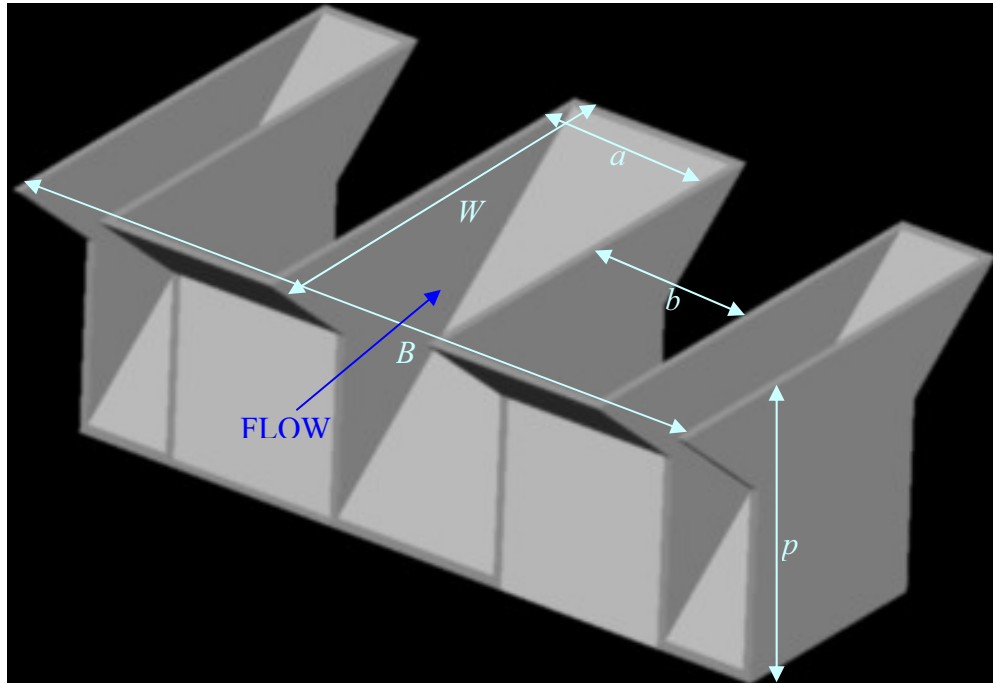
Fig. 3.5 Three dimensional view to generalize Piano Key Weir shape

a = Width of inlet cell

W = Length of elements

b = Width of outlet cell

L = Perimeter of Piano Key Weir crest

p = Crest height of Piano Key Weir

Q_L = Discharge through rectangular sharp crested weir

Q_{PK} = discharge through Piano Key Weir

B = Width of channel

For last elements on the side of the flume, the width of a or b will be divided by 2. The relevant notations used are:

3.3 EXPERIMENTAL PROCEDURE

Experiments were conducted in the following steps:

- Before starting the experiment the side rails of the flume were adjusted and were kept parallel to each other and parallel to the bottom of channel.

- The water was supplied to the flume from constant head tank to upstream tank and upstream tank to flume. Supply pipe connected to the pump and the discharge was controlled by a regulating valve.

- Two rows of perforated plastic sheet walls were provided to dampen the surface disturbances/destroy the excess energy of inflow and distribute the flow uniformly in the entire width of the flume.

- A plastic perspex sheet Piano Key Weir was placed at the down stream end of the flume at 8 cm base platform was made. The models were placed at the platform (pre determined location).

- The water which discharges into the tail box was allowed to flow over 90 degree V-notch. After flowing over the notch, the water was discharged into the sump from where it was re-circulated by pump.

- For the measurement of initial and different nappe depth the pointer gauge fixed to a vertical graduated rod was used. The difference of initial reading and different nappe depth readings gave the nappe depth of different discharges.

- After the Piano Key Weir was placed on the plat-form, discharge was slowly allowed into the flume and covered upto maximum discharge. The experiments were run for 10 to 12 different nappe heights.

3.4 FIRST PHASE MODEL EXPERIMENTS

In the first phase of the experiment programme, six selected models of Piano Key Weir have been used. The dimensions of Piano Key Weir models are as indicated below in Table 3.1. In first three models P_1M_1, P_1M_2, and P_1M_3, element configuration is same but slope is different and same with other three models P_1M_4, P_1M_5, and P_1M_6. Plan and sectional view of Piano Key Weir models are as indicated below in Figs. 3.6-3.11. Length of all elements has been kept as 32 cm.

All the models were run for 10 to 12 different nappe heights, discharges. It was endeavored to run all the models for the value of h/p upto unity. All the models have been studied for the value of Piano Key Weir discharge upto 80 l/s. Running view of all the models is shown in plate no. 3.1 to 3.6. These photos depict the behavior of Piano Key Weir.

Table 3.1: Phase one model dimensions

Model No.	Height of Model (p) (cm)	a (cm)	b (cm)	$a + b$ (cm)	L/W	No. of Element
P_1M_1	12	5.00	5.00	10	7.40	5
P_1M_2	16	5.00	5.00	10	7.40	5
P_1M_3	20	5.00	5.00	10	7.40	5
P_1M_4	12	12.50	12.50	25	3.56	2
P_1M_5	16	12.50	12.50	25	3.56	2
P_1M_6	20	12.50	12.50	25	3.56	2
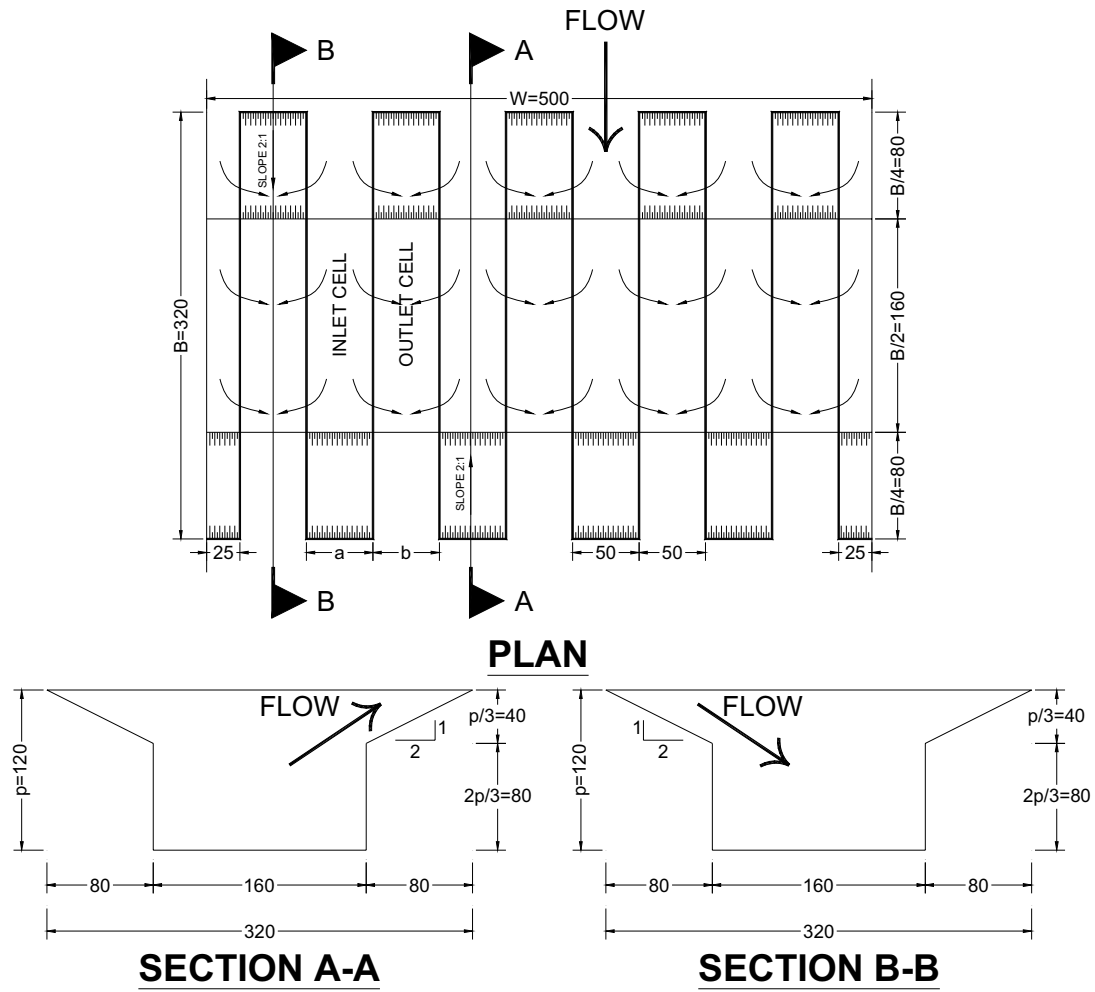
Fig. 3.6 Plan and section of model P_1M_1 (dimensions in mm)

Q_L= 49.23 l/s, Q_{PK}=75.5 l/s, r=1.53, p=12

Plate No. 3.1 Model P_1M_1

PLAN

SECTION A-A
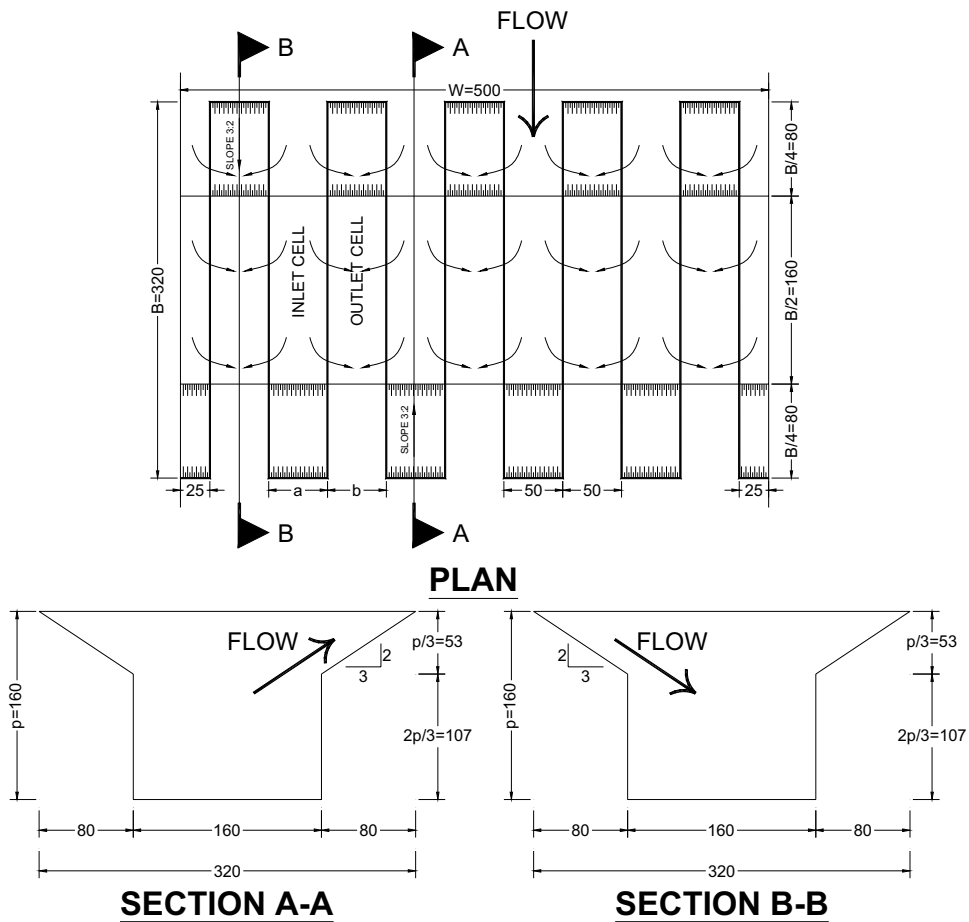
SECTION B-B

Fig. 3.7 Plan and section of model P₁M₂ (dimensions in mm)

Q_L= 43.23 l/s,
Q_{PK}=78.5 l/s,
r=1.81, p=16

Plate No. 3.2 Model P₁M₂

27
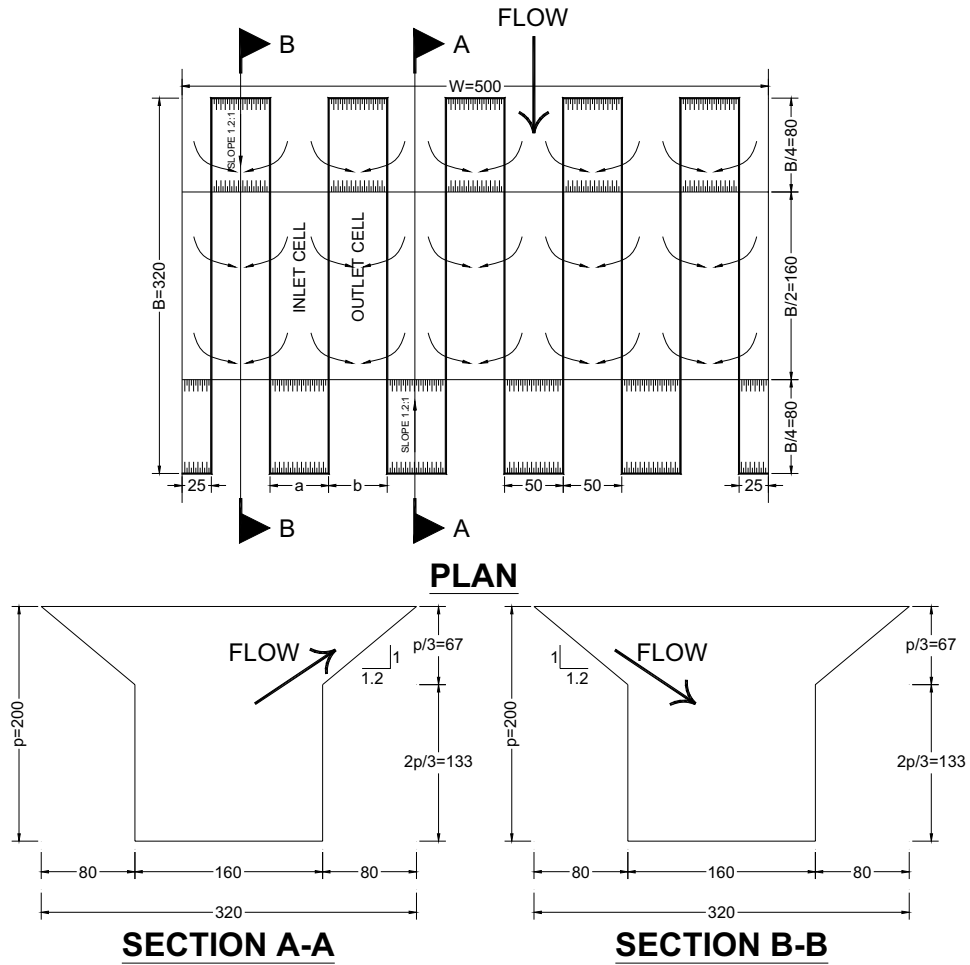
Fig. 3.8 Plan and section of model P₁M₃ (dimensions in mm)

Plate No. 3.3 Model P₁M₃

28
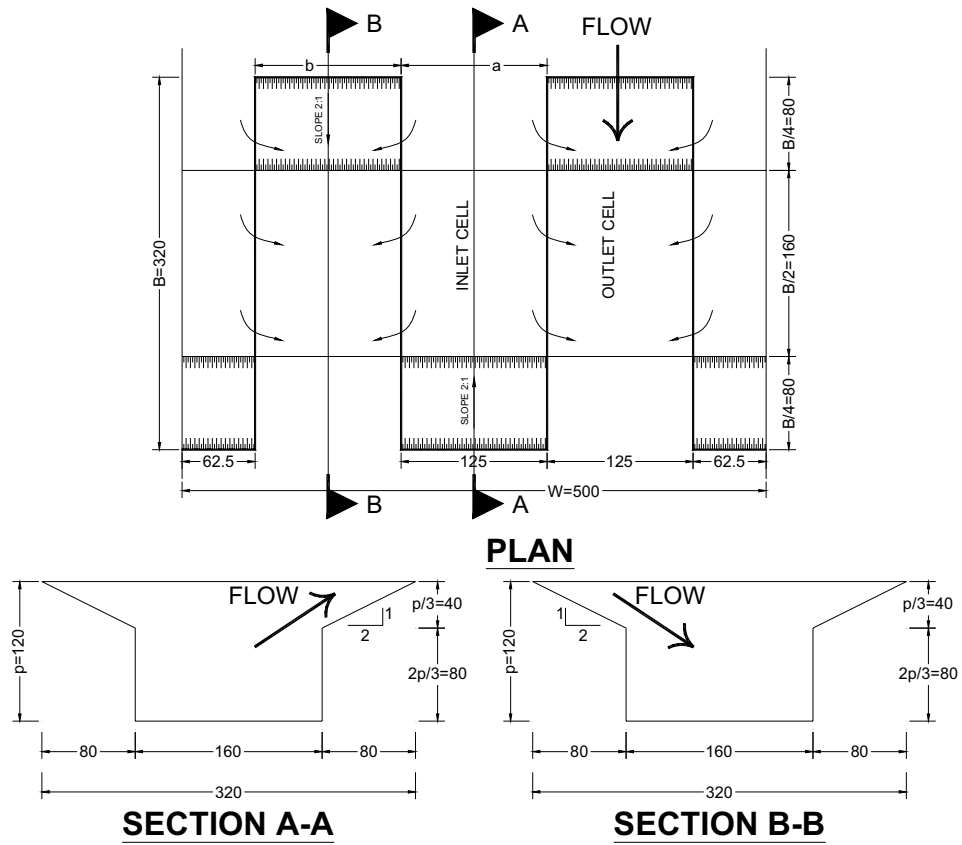
Fig. 3.9 Plan and section of model P_1M_4 (dimensions in mm)

Q_L= 57.32 l/s,
Q_{PK}=80.68 l/s,
r=1.4, p=12 cm

Plate No. 3.4 Model P_1M_4
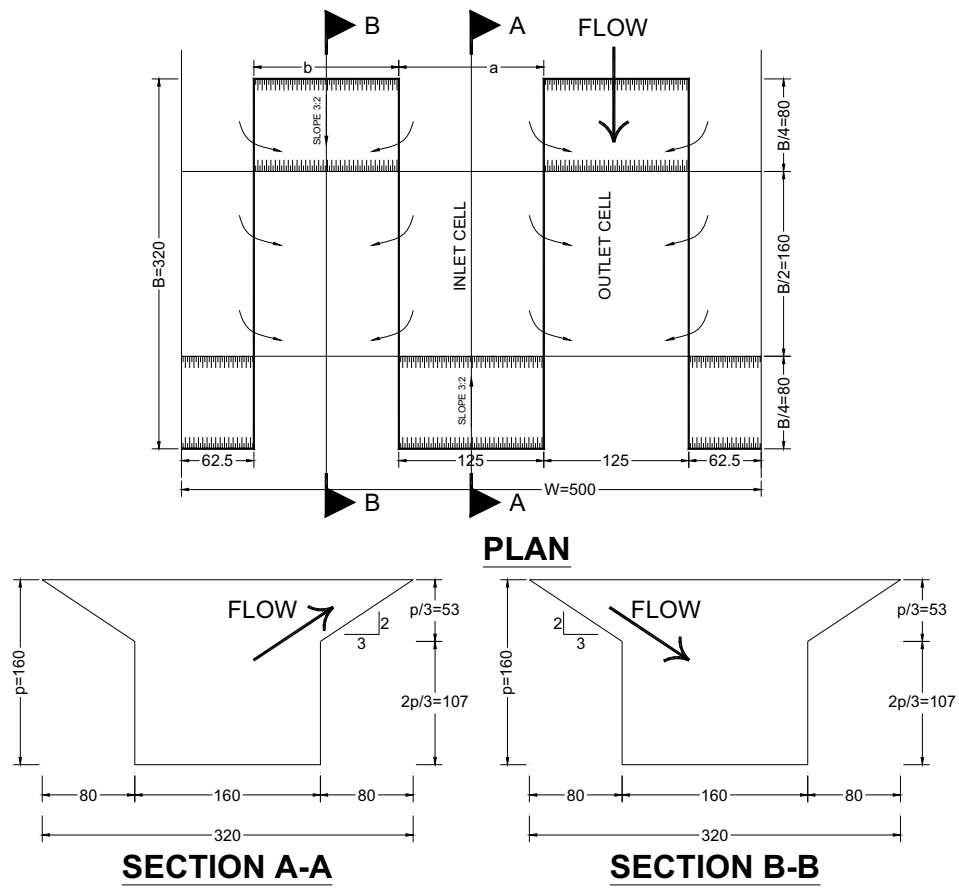
Fig. 3.10 Plan and section of model P₁M₅ (dimensions in mm)

Q_L= 46.38 l/s, Q_{PK}=77.89 l/s, r = 1.68, p =

Plate No. 3.5 Model P₁M₅
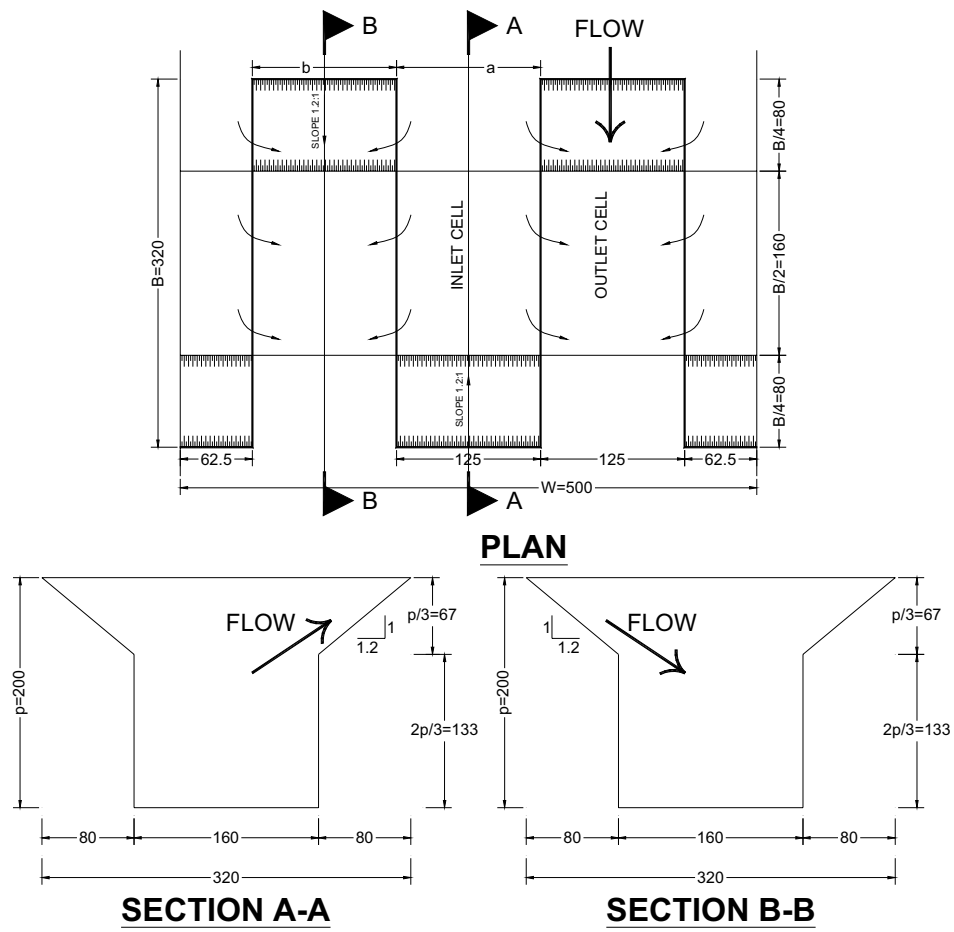
Fig. 3.11 Plan and section of model P_1M_6 (dimensions in mm)

Plate No. 3.6 Model P_1M_6

3.5   PHASE TWO MODEL EXPERIMENTS

From first phase experiment, some modifications have been introduced in the first phase models. In the second phase of the experiment programme, six selected modified models of first phase Piano Key Weir have been used. In the second phase experiment programme, we are providing both sides ramping in the first phase models. The modifications of first phase Piano Key Weir models are shown in Figs. 3.12-3.17. The dimensions of Piano Key Weir models are same as in first phase models.

All the models were run for 10 to 12 different nappe heights and discharges. All the models were tried to run for the value of h/p upto unity. All the models were studied for the value of Piano Key Weir discharge upto 80 l/s. Running view of all the models is shown in plate no. 3.7 to 3.12. These photos show the behavior of Piano Key Weir.
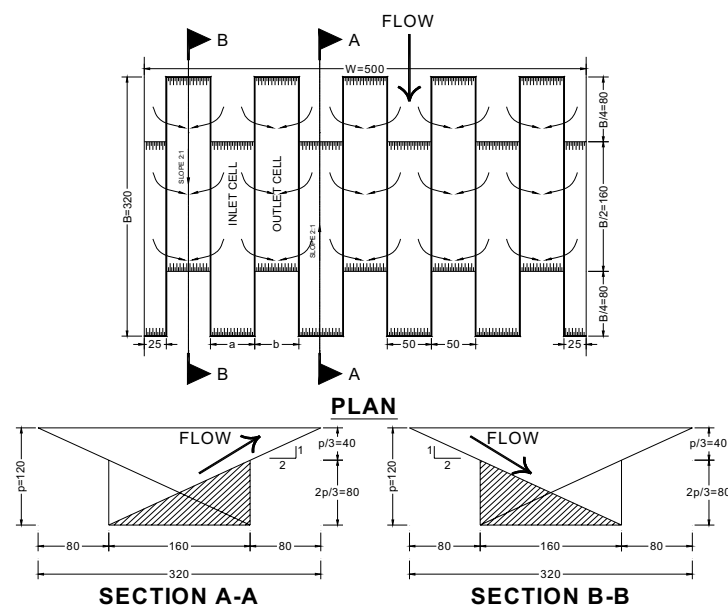
Fig. 3.12 Plan and section of model P$_2$M$_1$ (both sides ramping), (dimensions in mm)

Plate No. 3.7 Model P$_2$M$_1$ (both sides ramping)
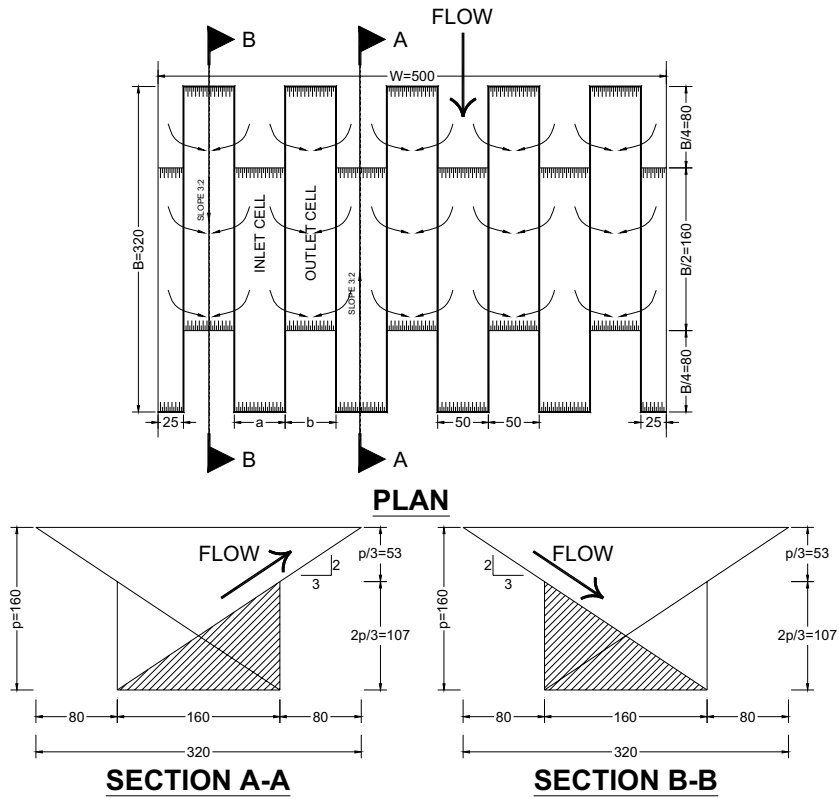
Fig. 3.13 Plan and section of model P₂M₂ (both sides ramping), (dimensions in mm)

Plate No. 3.8 Model P₂M₂ (both sides ramping)
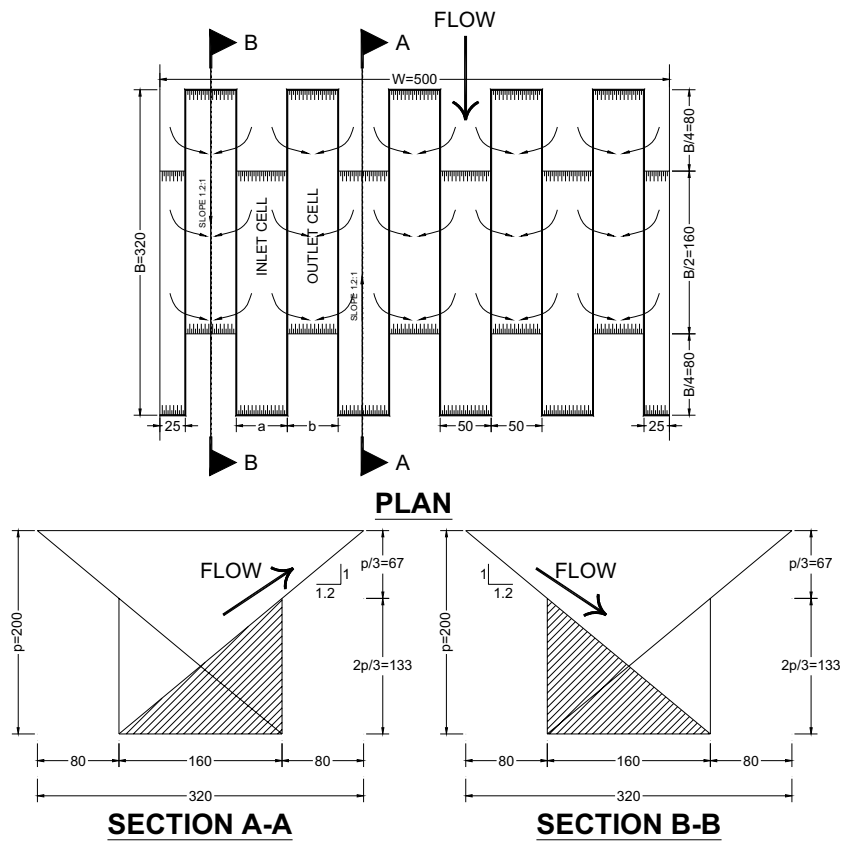
Fig. 3.14 Plan and section of model P₂M₃ (both sides ramping), (dimensions in mm)

Plate No. 3.9 Model P₂M₃ (both sides ramping)
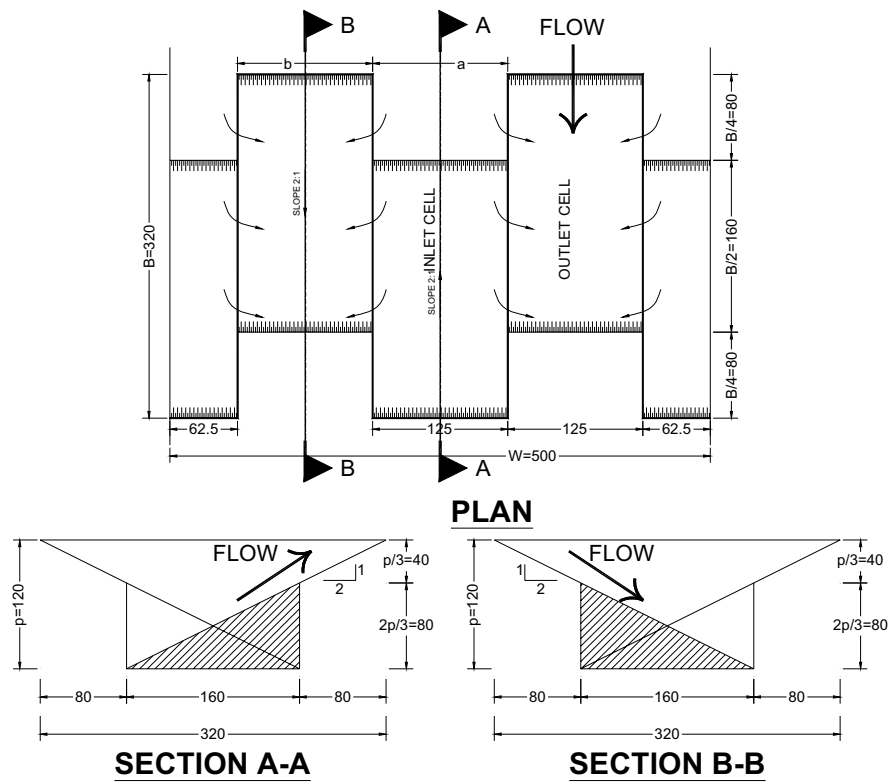
Fig. 3.15 Plan and section of model P₂M₄ (both sides ramping), (dimensions in mm)

Plate No. 3.10 Model P₂M₄ (both sides ramping)
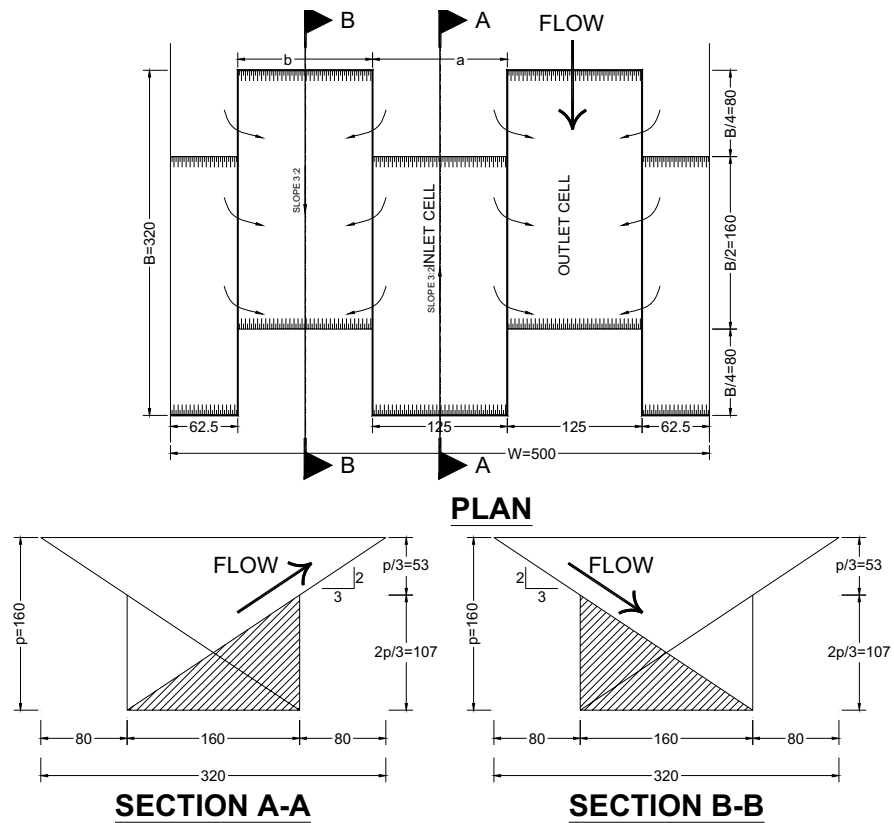
Fig. 3.16 Plan and section of model P$_2$M$_5$ (both sides ramping), (dimensions in mm)

Plate No. 3.11 Model P$_2$M$_5$ (both sides ramping)
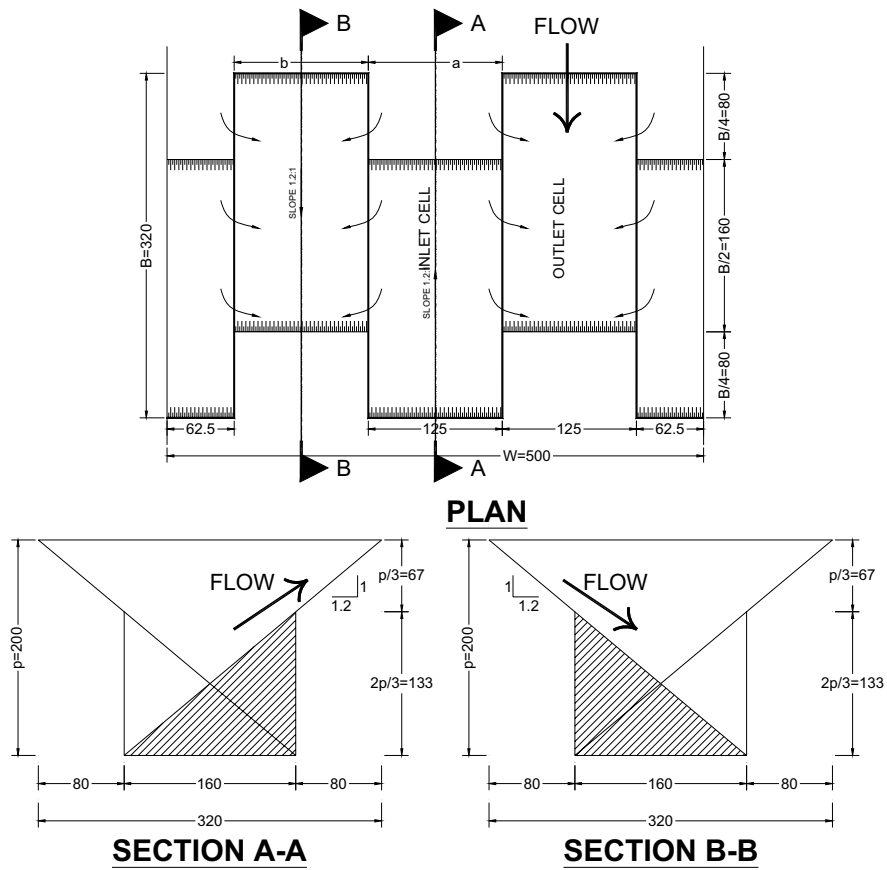
Fig. 3.17 Plan and section of model P$_2$M$_6$ (both sides ramping), (dimensions in mm)

Q$_L$ = 48.88 l/s, Q$_{PK}$=77.10 l/s, r = 1.577, p =

Plate No. 3.12 Model P$_2$M$_6$ (both sides ramping)

3.6   PHASE THREE MODEL EXPERIMENTS

In the third phase of the experiment programme, six selected models of Piano Key Weir have been used. The dimensions of Piano Key Weir models are as indicated below in Table 3.2. In third phase experimental models, all six models P_3M_1, P_3M_2, P_3M_3, P_3M_4, P_3M_5, and P_3M_6 have same slope but element configuration is different. Plan and sectional view of Piano Key Weir models P_3M_1, P_3M_2, P_3M_3, P_3M_4, P_3M_5, and P_3M_6 are as shown in Figs. 3.18-3.23. Running view of all the models is shown in plate no. 3.13 to 3.18.

All the models were run for 10 to 12 different nappe heights and discharges. All the models were run for the value of h/p upto unity. All the models have been experimented for the value of Piano Key Weir discharge upto 80 l/s.

Table 3.2: Phase Three Model dimensions

Model No.	Height of Model (p) (cm)	a (cm)	b (cm)	$a + b$ (cm)	L/W	No. of Element
P_3M_1	16	6.00	4.00	10.00	7.40	5
P_3M_2	16	4.00	6.00	10.00	7.40	5
P_3M_3	16	10.00	6.67	16.67	4.84	3
P_3M_4	16	6.67	10.00	16.67	4.84	3
P_3M_5	16	8.33	8.33	16.67	4.84	3
P_3M_6	16	10.00	15.00	25.00	3.56	2

For last elements on the side of the flume, the width of a or b will be divided by 2.
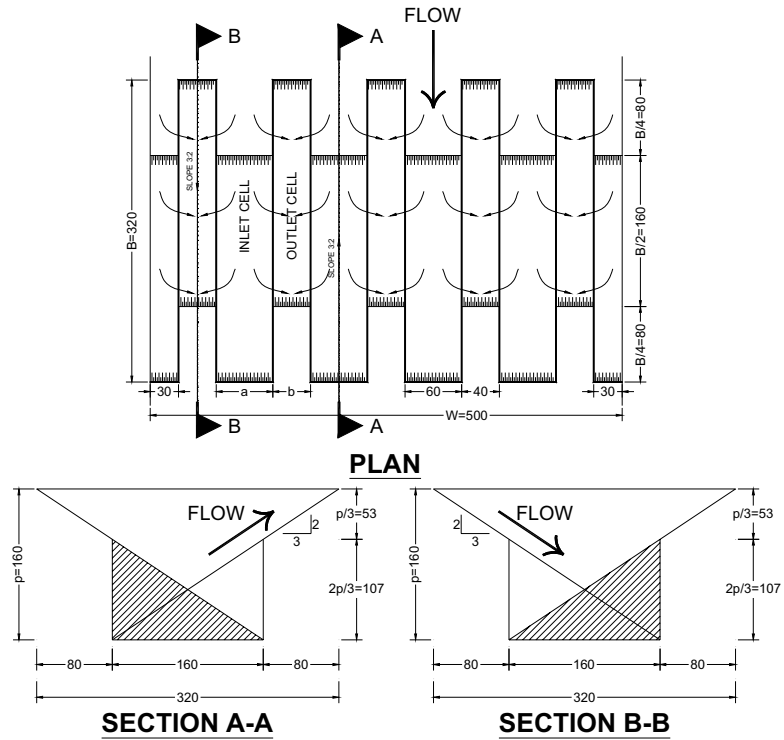
Fig. 3.18 Plan and section of model P₃M₁ (both sides ramping), (dimensions in mm)

Plate No. 3.13 Model P₃M₁ (both sides ramping)
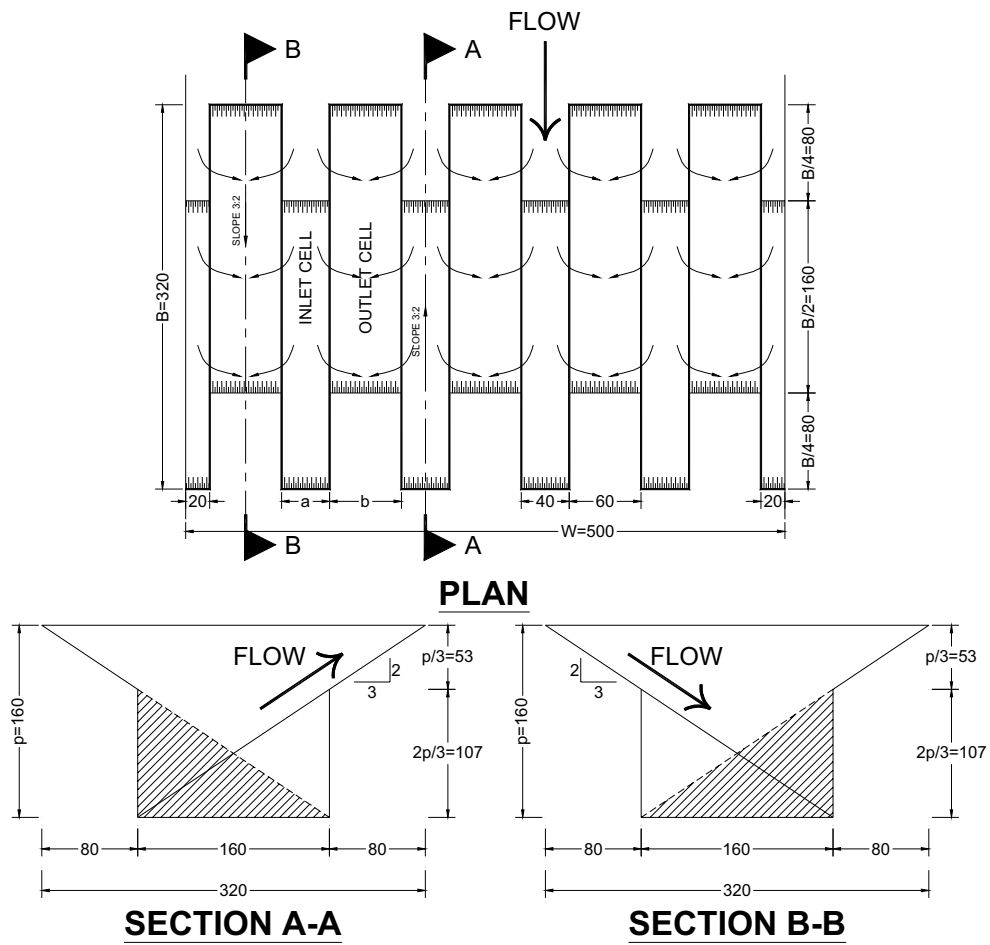
Fig. 3.19 Plan and section of model P₃M₂ (both sides ramping), (dimensions in mm)

Plate No. 3.14 Model P₃M₂ (both sides ramping)
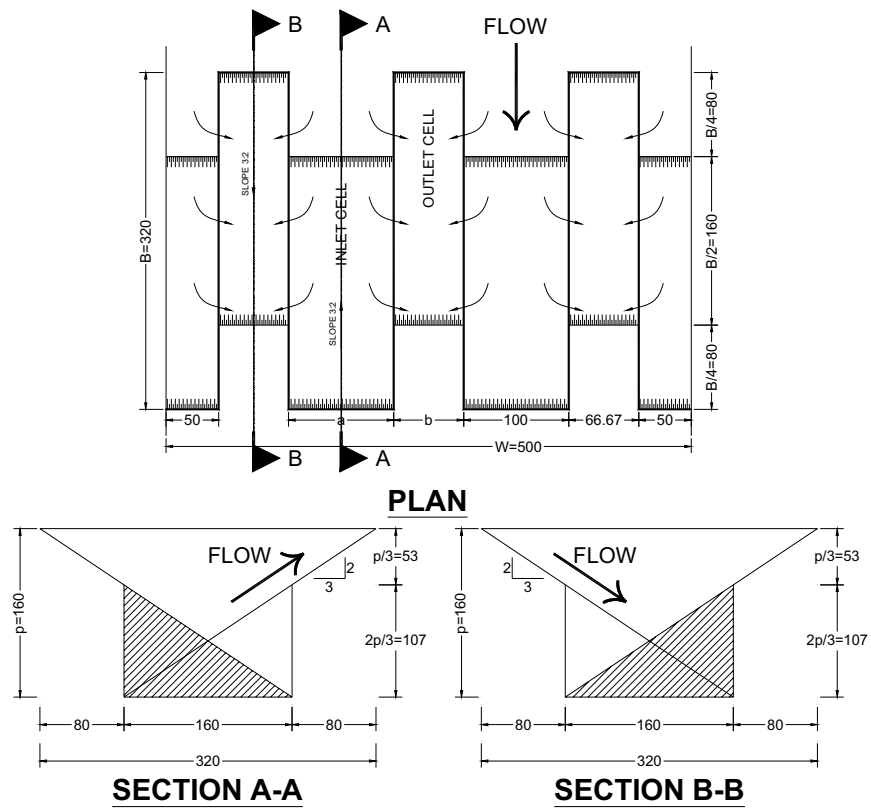
Fig. 3.20 Plan and section of model P₃M₃ (both sides ramping), (dimensions in mm)

Plate No. 3.15 Model P₃M₃ (both sides ramping)
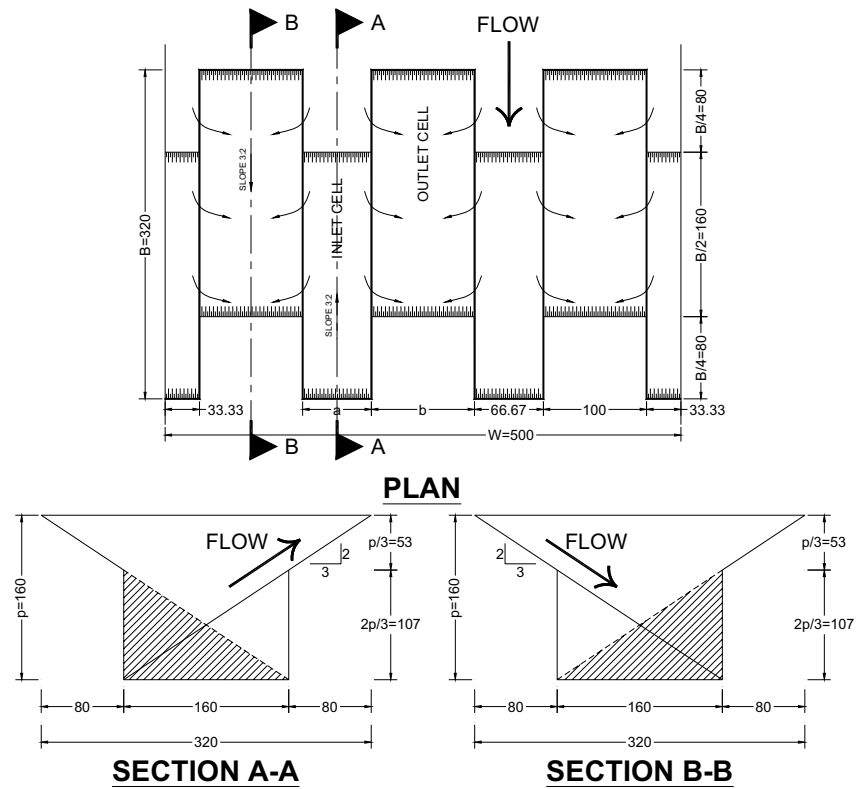
Fig. 3.21 Plan and section of model P₃M₄ (both sides ramping), (dimensions in mm)

QL=52.80 l/s, QPK=77.83 l/s, r=1.474, p=16

Plate No. 3.16 Model P₃M₄ (both sides ramping)
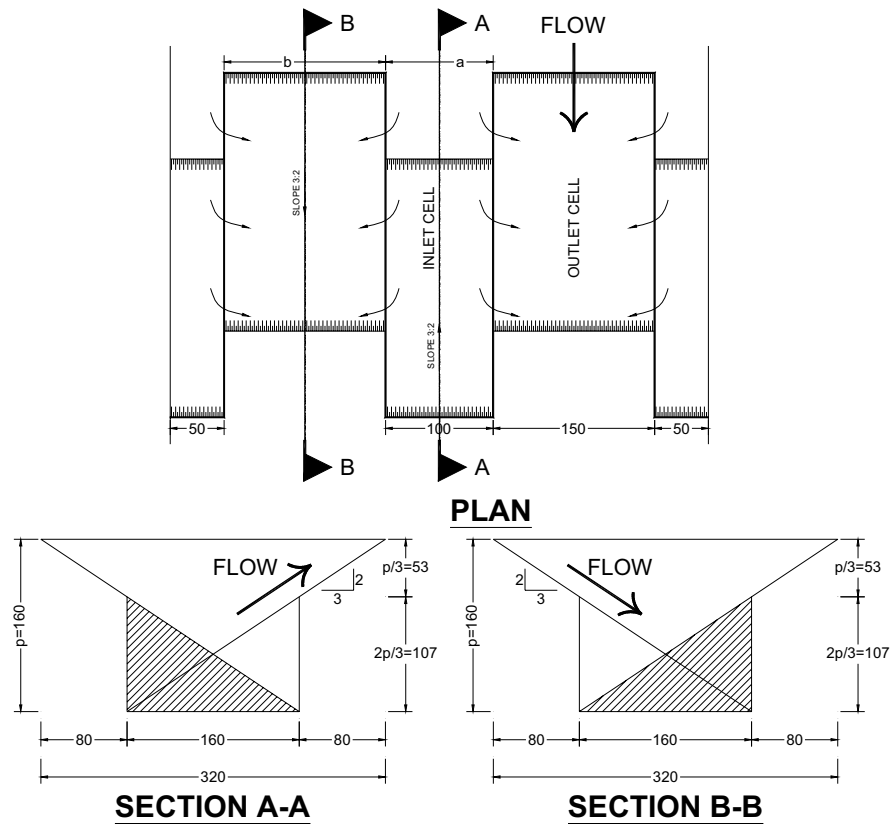
Fig. 3.22 Plan and section of model P₃M₅ (both sides ramping), (dimensions in mm)

Q_L=50.73 l/s, Q_{PK}=78.02 l/s, r = 1.538, p =

Plate No. 3.17 Model P₃M₅ (both sides ramping)
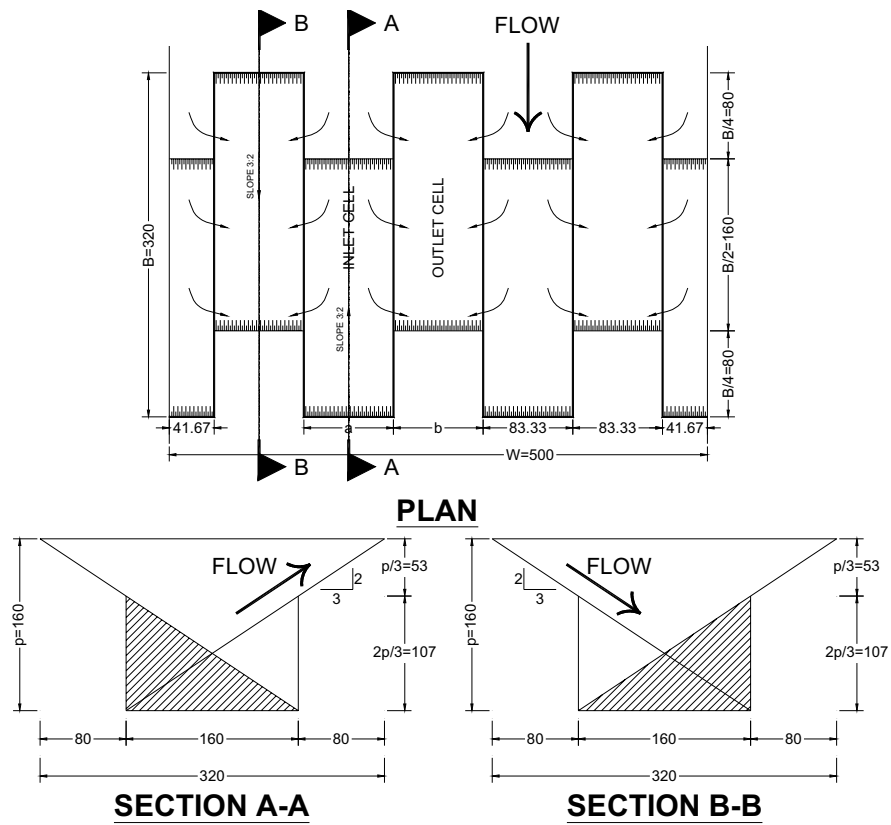
Fig. 3.23 Plan and section of model P_3M_6 (both sides ramping), (dimensions in mm)

Plate No. 3.18 Model P_3M_6 (both sides ramping)

3.7   PHASE FOUR MODEL EXPERIMENTS

In the fourth phase of the experiment programme, five selected models of Piano Key Weir have been used. The dimensions of Piano Key Weir models are as indicated below in Table 3.3. In fourth phase experimental models, P_4M_1, P_4M_2, and P_4M_3, models have same slope but element configuration is different. P_4M_4, and P_4M_5 models have also same slope but different from P_4M_1, P_4M_2, and P_4M_3, and element configuration is different. Here downstream side over hanging only was considered, not upstream side. Plan and sectional view of Piano Key Weir models P_4M_1, P_4M_2, P_4M_3, P_4M_4, and P_4M_5 are shown in Figs. 3.24-3.28. Running view of all the models is shown in plate no. 3.19 to 3.23.

All the models were run for 10 to 12 different nappe heights and discharges. All the models were endeavored to run for the value of h/p upto unity. All the models have been studied for the value of Piano Key Weir discharge upto 80 l/s.

Table 3.3: Phase four model dimensions

Model No.	Height of Model (p) (cm)	a (cm)	b (cm)	$a + b$ (cm)	L/W	No. of Element
P_4M_1	16	5.00	5.00	10.00	7.40	5
P_4M_2	16	12.50	12.5	25.00	3.56	2
P_4M_3	16	8.33	8.33	16.67	4.84	3
P_4M_4	12	8.33	8.33	16.67	4.84	3
P_4M_5	12	10.00	6.67	16.67	4.84	3

For last elements on the side of the flume, the width of a or b will be divided by 2.
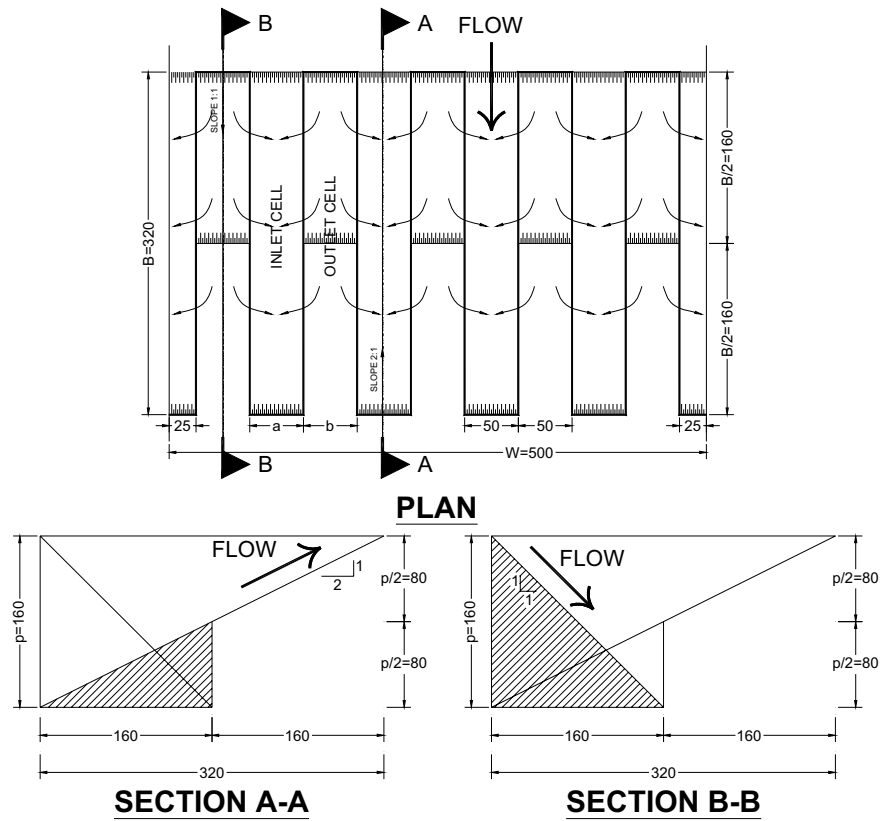
Fig. 3.24 Plan and section of model P$_4$M$_1$ (both sides ramping), (dimensions in mm)

Plate No. 3.19 Model P$_4$M$_1$ (both sides ramping)

46
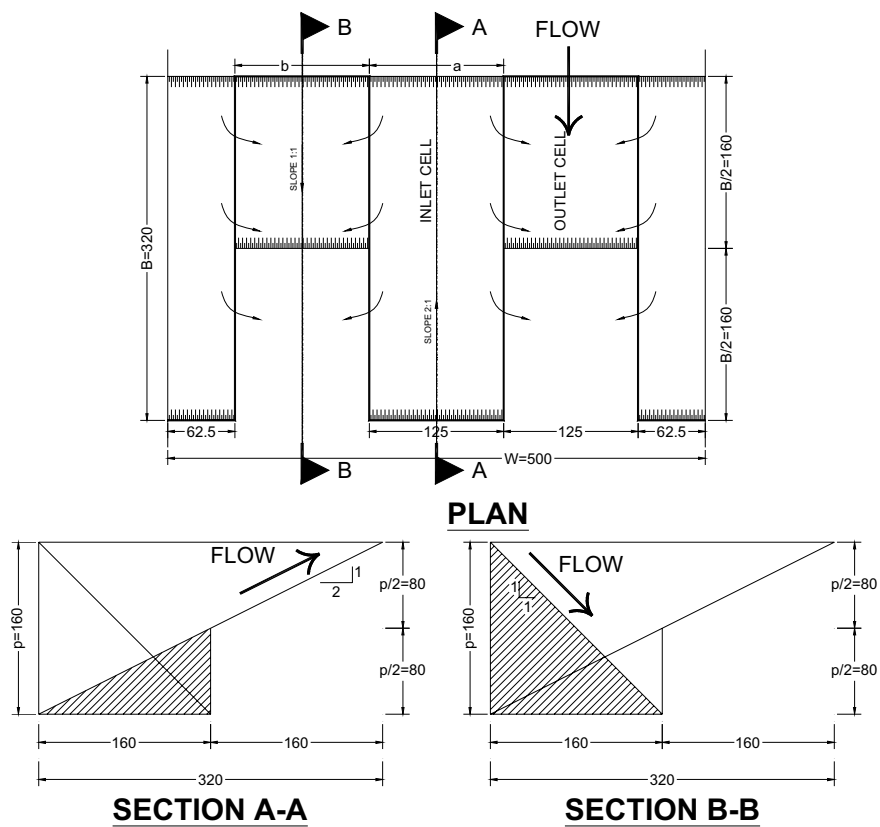
Fig. 3.25 Plan and section of model P$_4$M$_2$ (both sides ramping), (dimensions in mm)

Q$_L$=48.01 l/s, Q$_{PK}$=76.87 l/s, r=1.664, p=16
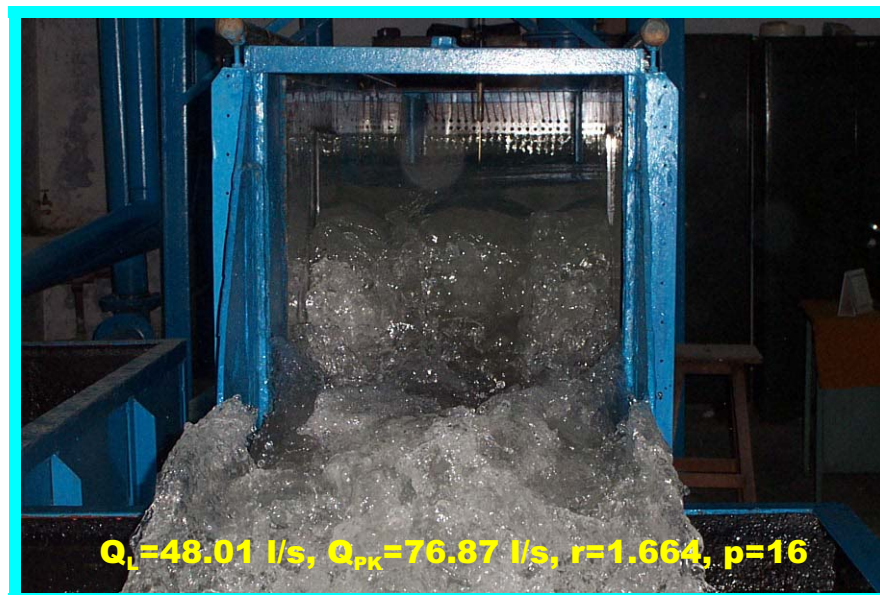
Plate No. 3.20 Model P$_4$M$_2$ (both sides ramping)
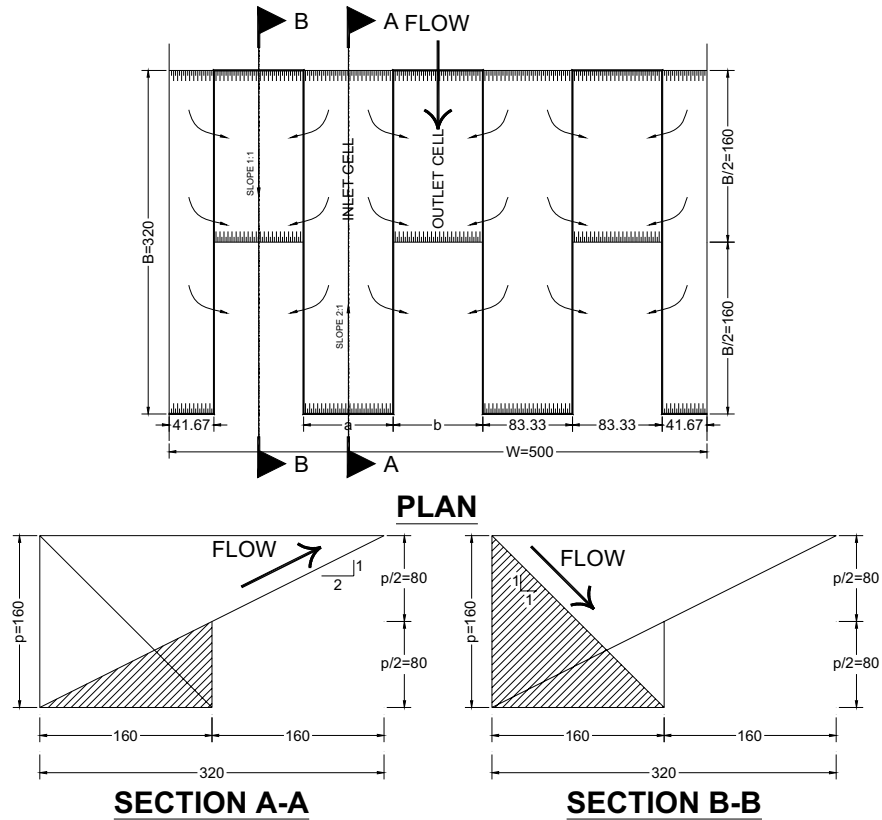
Fig. 3.26 Plan and section of model P$_4$M$_3$ (both sides ramping), (dimensions in mm)
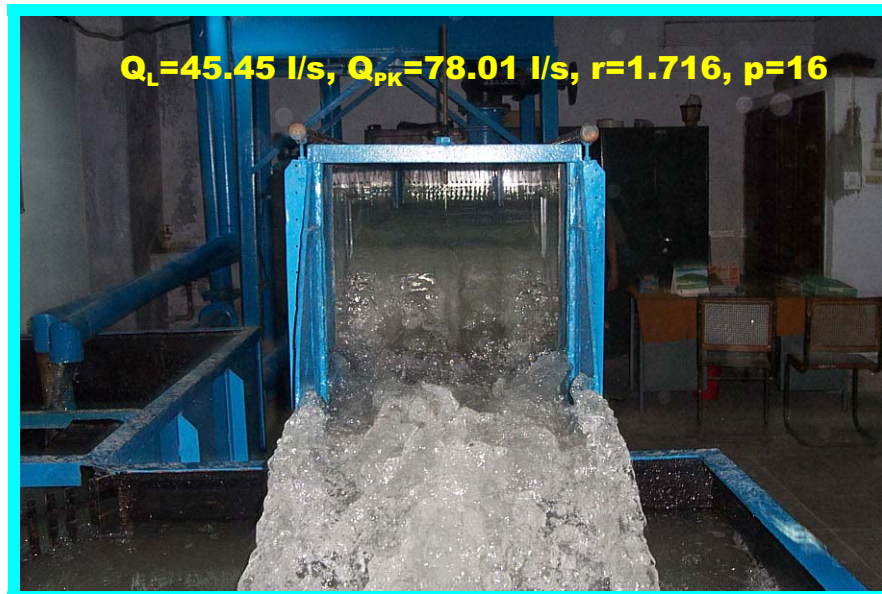
Plate No. 3.21 Model P$_4$M$_3$ (both sides ramping)
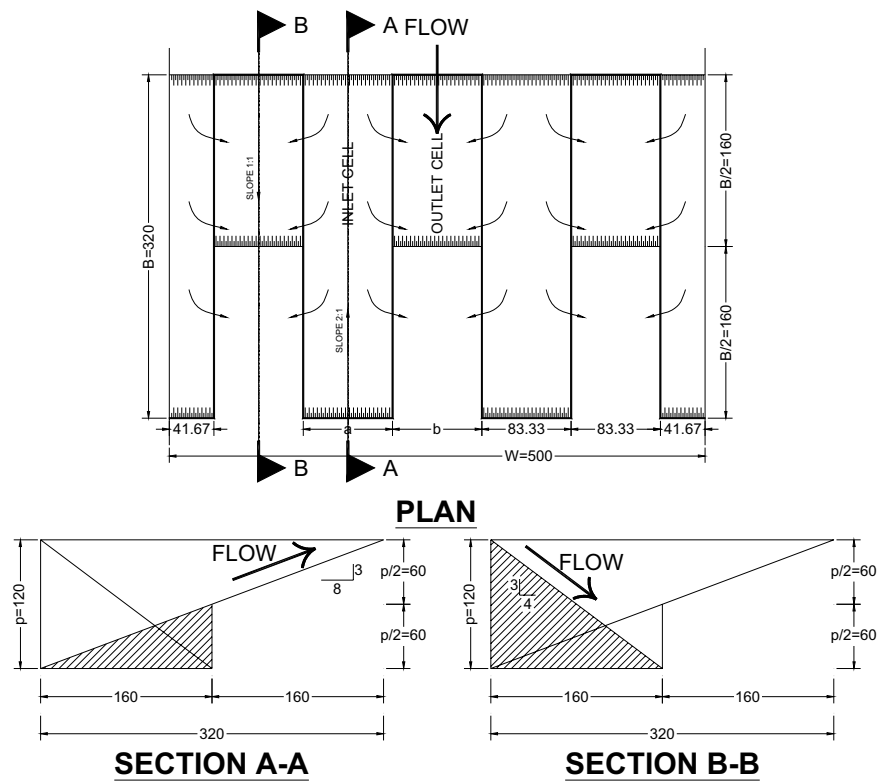
Fig. 3.27 Plan and section of model P₄M₄ (both sides ramping), (dimensions in mm)
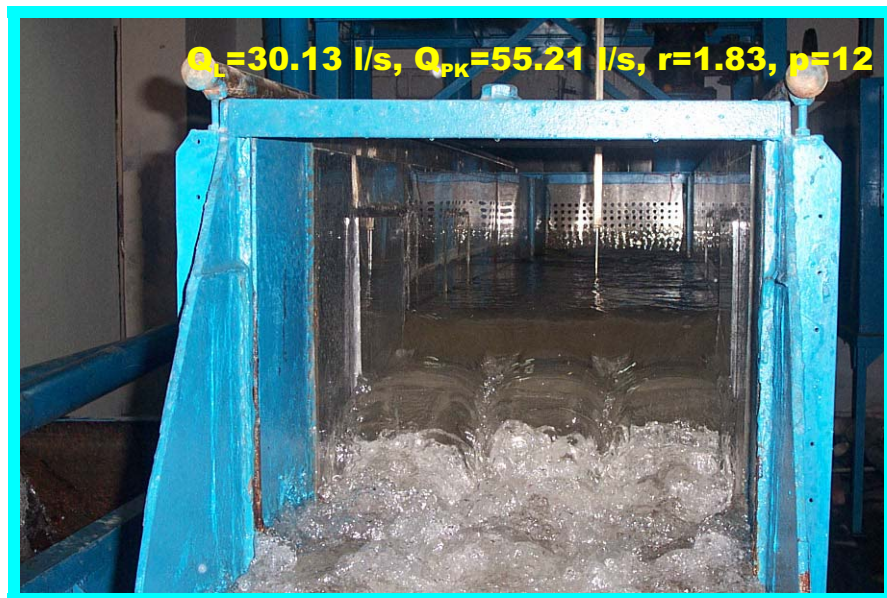
Plate No. 3.22 Model P₄M₄ (both sides ramping)
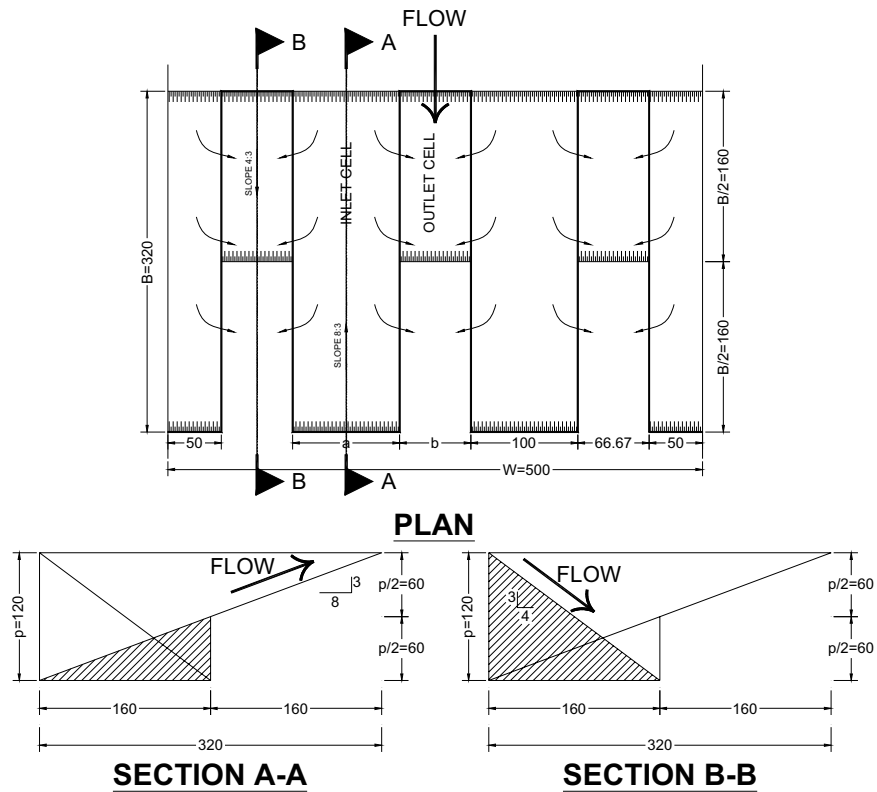
Fig. 3.28 Plan and section of model P$_4$M$_5$ (both sides ramping), (dimensions in mm)

Q$_L$=31.72 l/s, Q$_{PK}$=54.87 l/s, r=1.73, p=12

Plate No. 3.23 Model P$_4$M$_5$ (both sides ramping)

3.8   PHASE FIVE MODEL EXPERIMENTS

In the fifth phase of the experiment programme, five selected models of Piano Key Weir have been used with some modification in previous models. Inlet modification has been done in the model P_2M_4, and P_4M_3. Filling inlet cell modification has been done in the model P_2M_6 and filling outlet cell modification has been done in the model P_2M_2 and P_2M_5. Modification in the selected models of Piano Key Weir is shown in Figs 3.29-3.33 with plan and sectional view. These modifications were incorporated to see the improvement in the performance of Piano Key Weir.
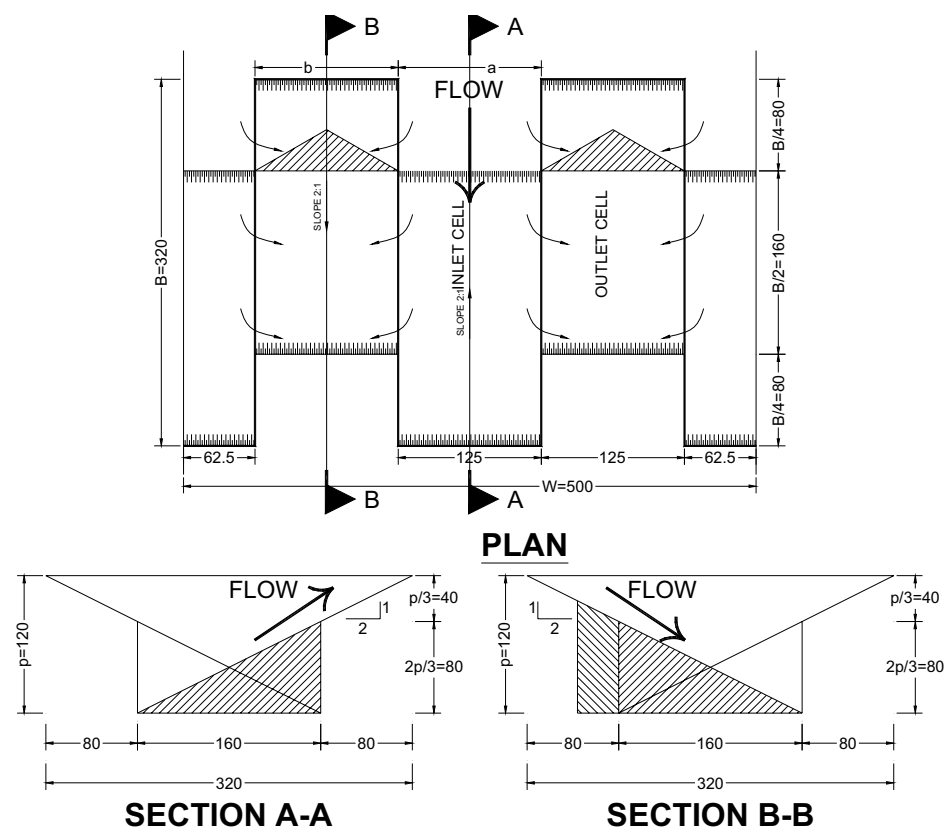
Fig. 3.29 Plan and section of model P_2M_4 with inlet modification (dimensions in mm)

51
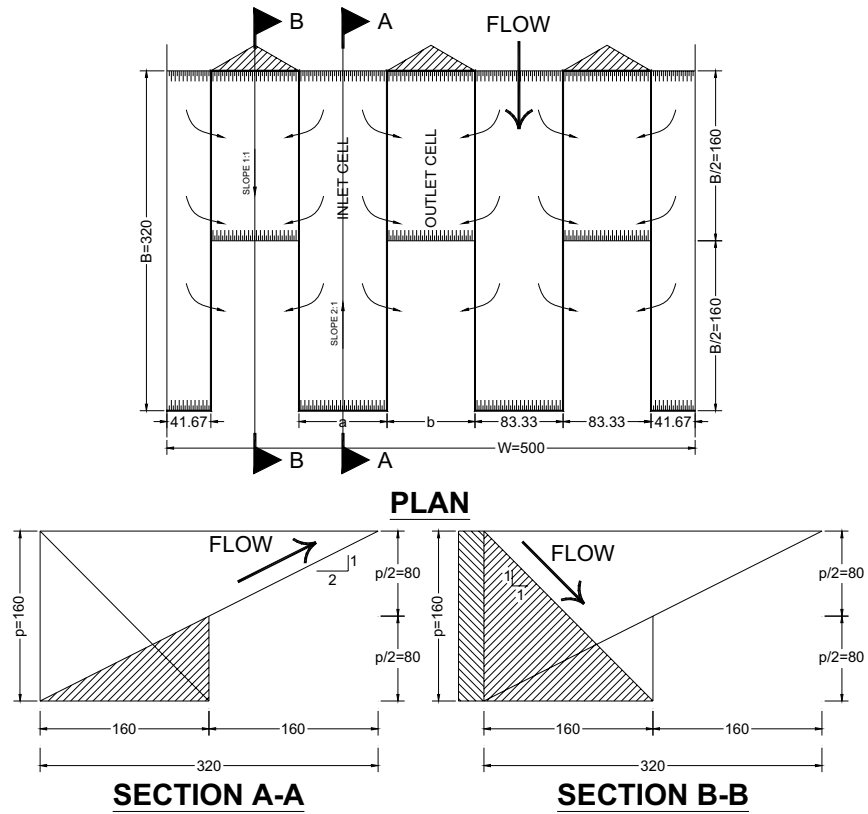
Fig. 3.30 Plan and section of model P_4M_3 with inlet modification (dimensions in mm)
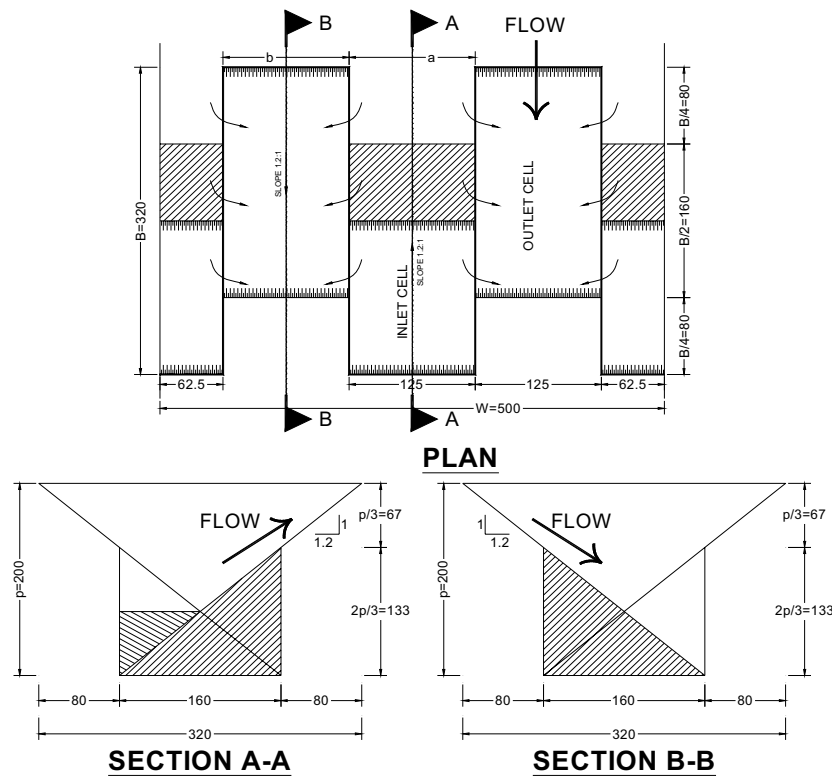
Fig. 3.31 Plan and section of model P_2M_6 with filling inlet cell modification
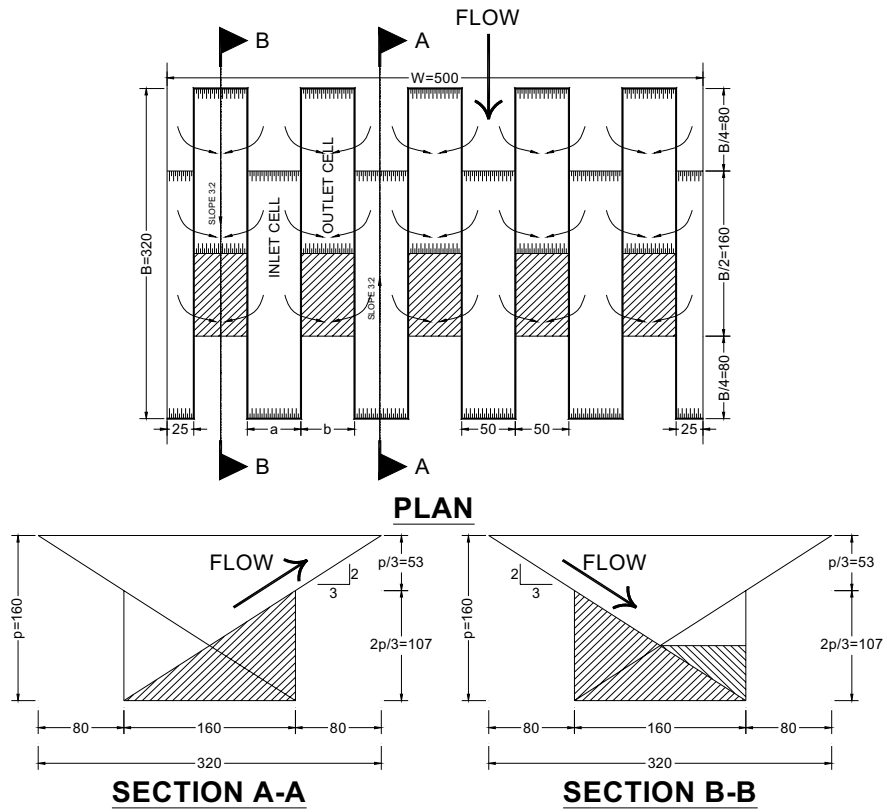
(dimensions in mm)

Fig. 3.32 Plan and section of model P₂M₂ with filling outlet cell modification (dimensions in mm)
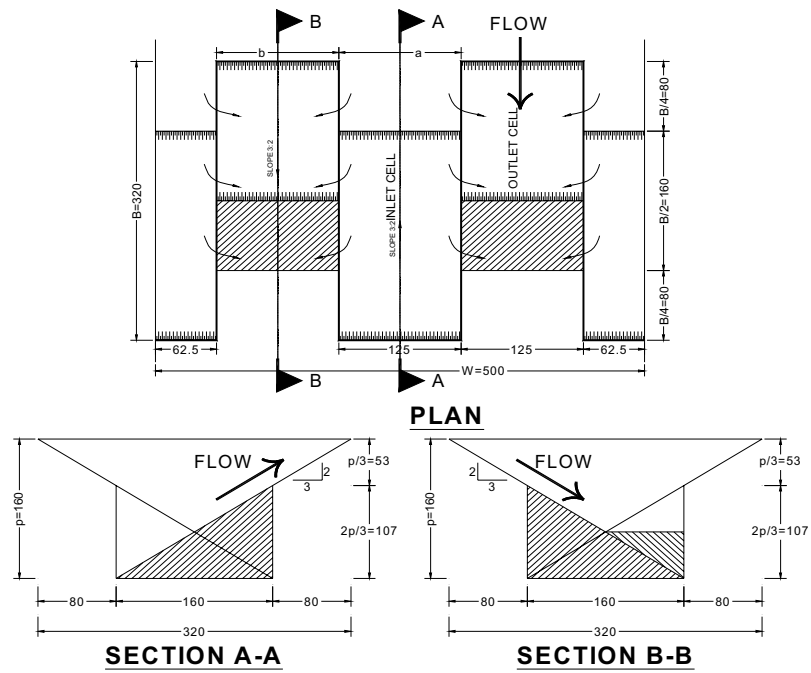
Fig. 3.33 Plan and section of model P₂M₅ with filling outlet cell modification (dimensions in mm)

3.9 SUMMARY

The experimental studies of Piano Key Weir model were performed in five different phases. A simple design of Piano Key Weir was investigated in the first phase experiments and modifications in the preliminary design of first phase model were added in subsequent phases. In order to increase the performance of Piano Key Weir, a ramp is provided in the preliminary designed model in first phase and thus sets the basis for the second phase experiments. Increase in discharge passing capacity was obtained in particular model of second phase experiments. Thereafter, it became obvious to select this particular model from second phase experiment and to carry out rigorous experimental analysis on this selected model. All these investigation were placed in the third phase experiments. Next, the fourth phase experiments were designed with downstream side over-hanging only. Finally model investigation with some modifications in few previous models were carried out and placed in the fifth phase experiments.

CHAPTER 4

DATA ANALYSIS AND PERFORMANCE

EVALUATION OF PIANO KEY WEIR

4.1   GENERAL

Considering the fact that Piano Key Weir of different shapes are to be used in field conditions, the objective of these experiments was to identify the Piano Key Weir in which the maximum discharge capacity at different L/W with p (height of weir) could be achieved. To achieve this for different flow conditions, length magnification ratio (L/W) is taken from 3.56 to 7.40. Also, other parameters are taken in different combinations for getting optimum configuration of Piano Key Weir for better performance. Few selected models of Piano Key Weir have been also used with certain modifications in the inlet and outlet cell for improving the performance. This chapter presents the experimental data processing of all these model results.

4.2   DATA ANALYSIS

Some of the steps of the data analysis consist of the following:

- Calculation of discharge through rectangular sharp crested weir is made by the formula,

$$Q_L = \frac{2}{3} C_d \sqrt{2g} . W h^{3/2} \tag{4.1}$$

where Q_L is the discharge through rectangular sharp crested weir, h is the head over the crest and C_d is coefficient of discharge, W is the width of channel. In Eq. (4.1)

$$C_d = \left[0.605 + \frac{0.08h}{p} + \frac{0.001}{h} \right] \tag{4.2}$$

and p is height of crest

- V-notch is used to measure the discharge through Piano Key Weir (Chow, 1959). The formula used for discharge of V-notch is

$$Q_{PK} = \frac{8}{15} C_d \sqrt{2g} \tan(\theta/2) H_e^{5/2} \tag{4.3}$$

where, $H_e = H + K_h$ \hfill (4.4)

Here, H_e is the effective depth of water above vertex at the upstream of V-notch, the quantity K_h represents the combined effects of fluid properties, taken as 0.0008m for 90^0 V-notch, C_d is coefficient of discharge, taken as 0.58 for a 90-degree V-notch only and θ is the angle of the V-notch.

- Difference of Piano Key Weir discharge and rectangular sharp crested weir discharge (ΔQ) is obtained as

$$\Delta Q = Q_{PK} - Q_L \qquad (4.5)$$

where, Q_{PK} is the discharge through Piano Key Weir and Q_L is the discharge through rectangular sharp crested weir

- Ratio (r) of Piano Key Weir discharge and linear Weir discharge is

$$r = \left(\frac{Q_{PK}}{Q_L}\right) \qquad (4.6)$$

- Calculation of h/p

h is the head over the crest (at one and half meter u/s of the Piano Key Weir) and p is height of Piano Key Weir.

- Calculation of length magnification ratio (L/W)

L is the length of Piano Key Weir crest and W is the effective linear width of element of Piano Key Weir.

Data processing and analysis have been done for each model.

4.3 VALIDITY OF DISCHARGE MEASURING THROUGH V-NOTCH AND SHARP CRESTED WEIR

Sharp crested weir discharge is calculated by Eq. (4.1) and coefficient of discharge for sharp crested weir is taken as 0.72. Discharge through the V-notch is calculated by Eq. (4.3) and coefficient of discharge for 90° V-notch is taken as 0.58 (Weber et al., 2001). Comparative results of V-notch and sharp crested weir are shown in table 1. From table 4.1, percentage of discharge variation between V-notch and Sharp Crested Weir is -1.0 to 5.5.

Table 4.1: Results on comparative study between V-notch and sharp crested weir

Head over V-Notch (m)	V-Notch Discharge (l/s)	Head over Sharp Crested Weir (m)	Sharp Crested Weir Discharge (l/s)	% of discharge variation
0.31	72.12	0.18	71.37	-1.05
0.29	64.53	0.17	65.06	0.80
0.28	57.09	0.16	57.51	0.72
0.27	50.56	0.15	51.85	2.48
0.25	41.88	0.13	43.37	3.43
0.23	33.57	0.11	35.09	4.33
0.20	25.82	0.10	27.36	5.63
0.19	20.45	0.08	21.60	5.33

4.4   EVALUATION OF FIRST PHASE EXPERIMENTS

The collected data from all six models have been analysed to find best geometric shape. Collected data have been analysed using Eq. 4.1 to 4.6. The graphical representation between discharge and (h/p) for all the six models is shown in Figs. (4.1-4.6). In Figs. 4.1 to 4.6, the discharge passing through Piano Key Weir (Q_{PK}) is observed to be more than the discharge passing through rectangular sharp crested weir because available water way length in Piano Key Weir is more than rectangular sharp crested weir. In Figs. 4.7 to 4.9, r vs h/p for same height of Piano Key Weir has been analysed. It can be seen from Figs. 4.7 to 4.9 that value of r increases with increasing L/W because water-way length increases with increasing L/W. In Figs. 4.10 to 4.11, for same length magnification ratio (L/W), the variation of r is shown with respect to h/p and indicates that r is high when h/p is low. Graphical plots between 'r' and h/p for all six models is shown in Fig. 4.12. From Fig. 4.12, model P_1M_2 is found to perform better.
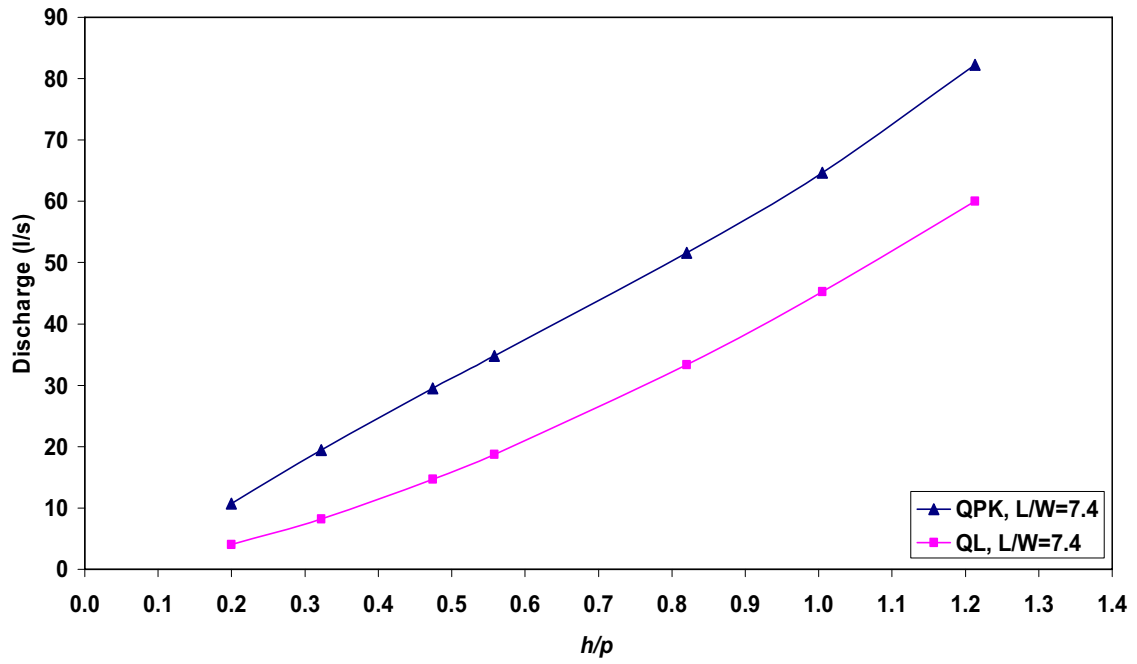
Fig. 4.1 Plot between Q_{PK}, Q_L and h/p for model P_1M_1
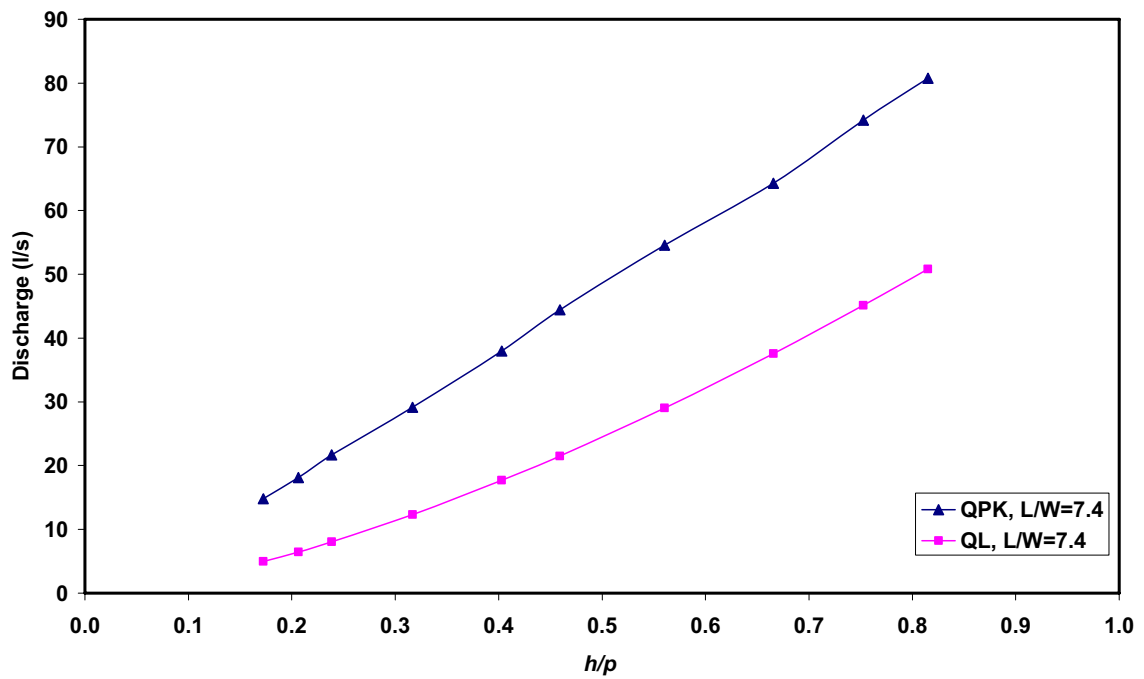
Fig. 4.2 Plot between Q_{PK}, Q_L and h/p for model P_1M_2

58
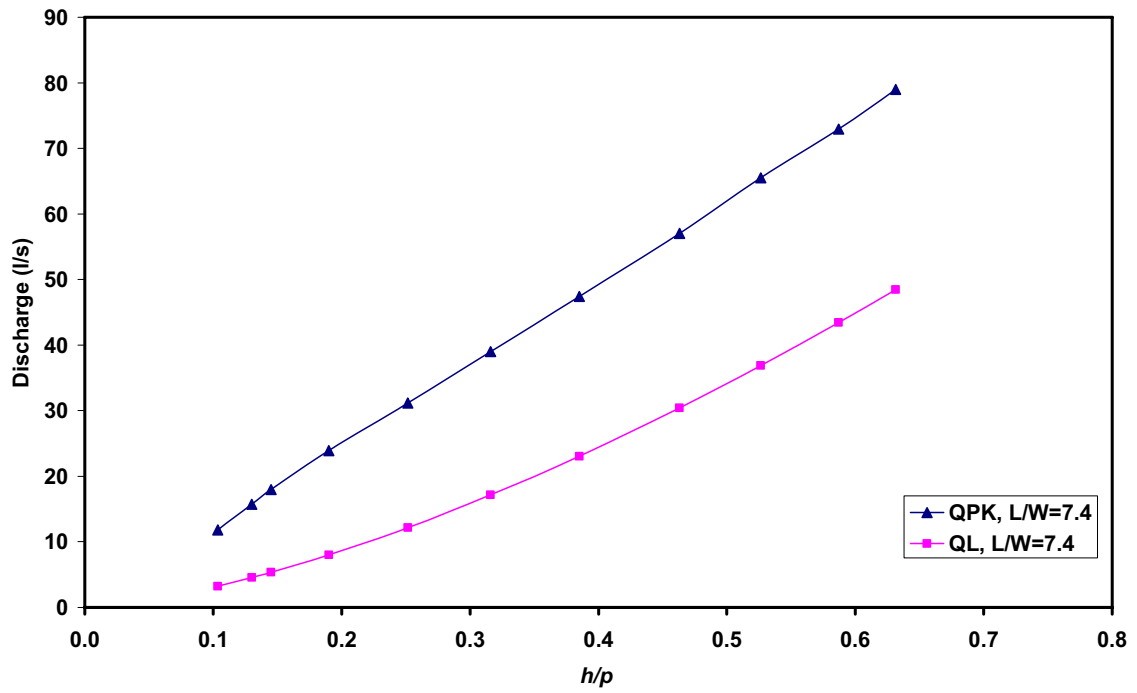
Fig. 4.3 Plot between Q_{PK}, Q_L and h/p for model P_1M_3
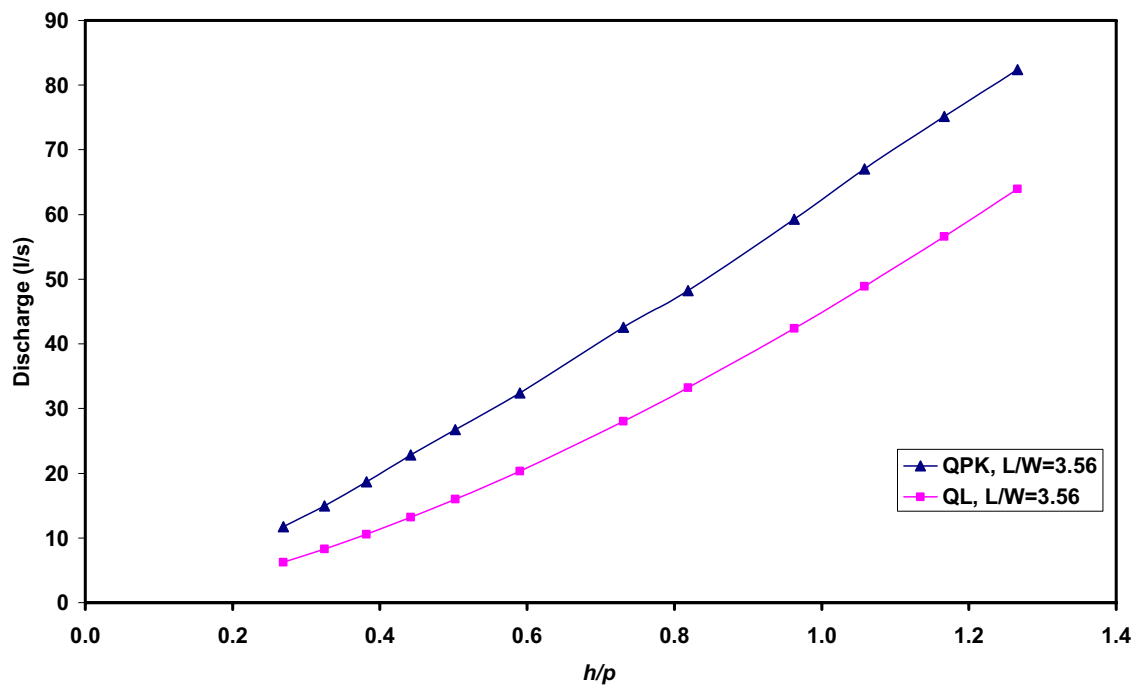
Fig. 4.4 Plot between Q_{PK}, Q_L and h/p for model P_1M_4
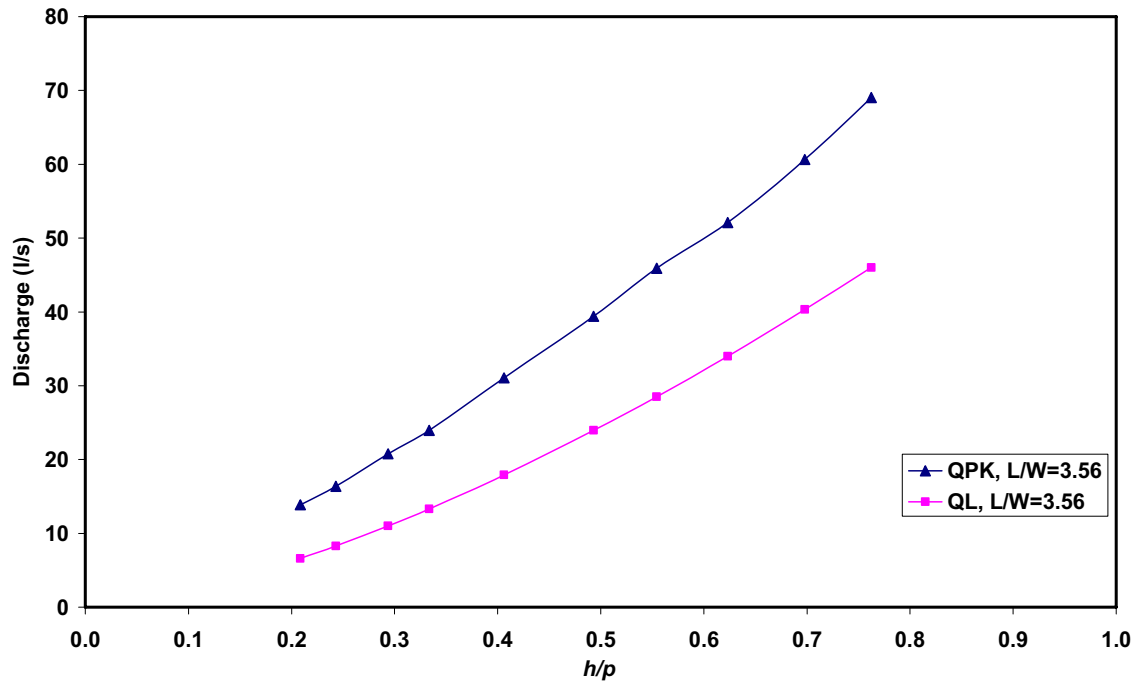
Fig. 4.5 Plot between Q_{PK}, Q_L and h/p for model P_1M_5
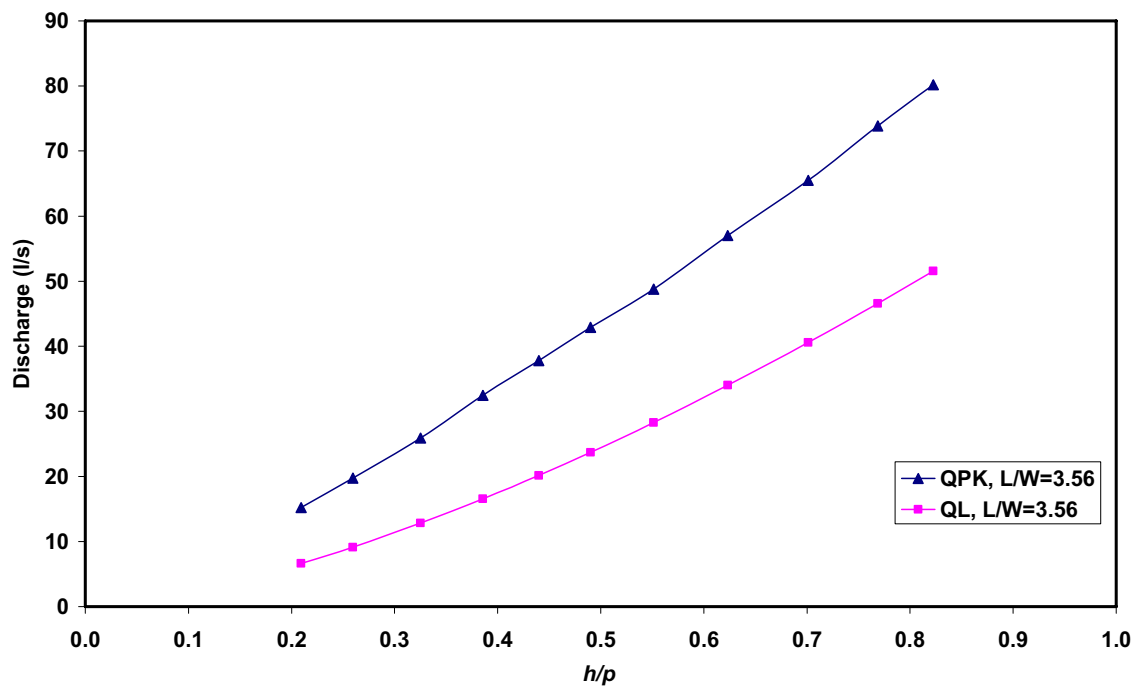
Fig. 4.6 Plot between Q_{PK}, Q_L and h/p for model P_1M_6
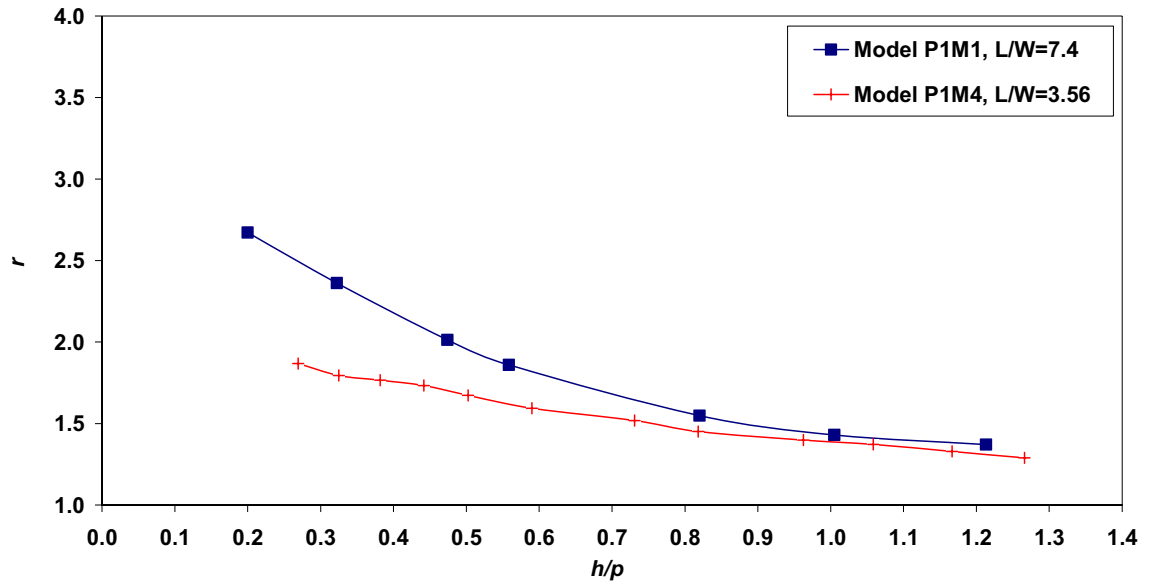
Fig. 4.7 Plot between *r* and *h/p* for model P₁M₁ & P₁M₄ with same *p* = 12 cm
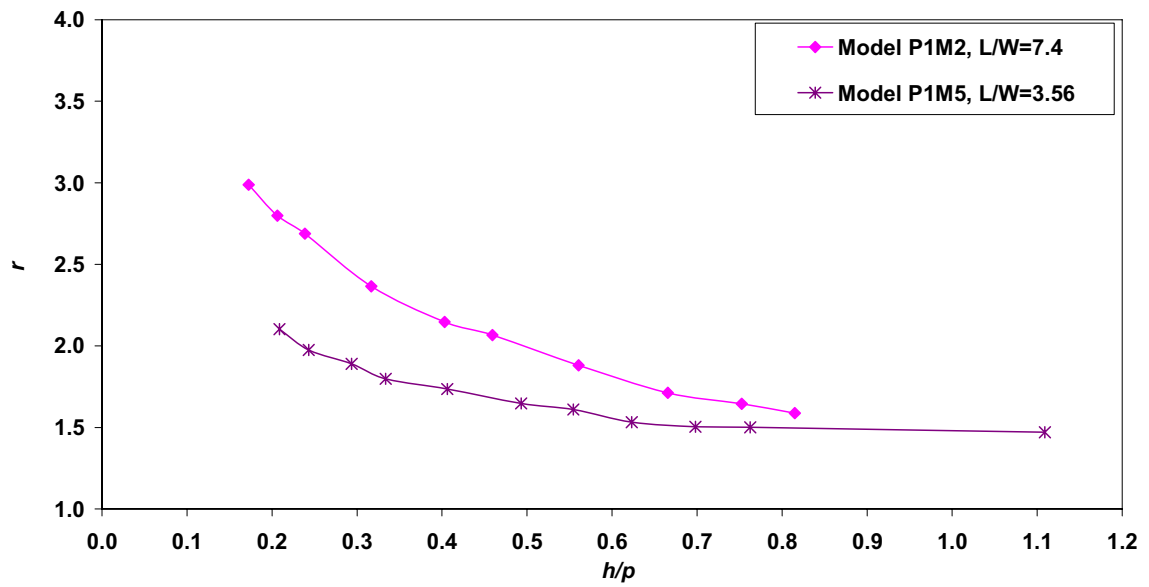
Fig. 4.8 Plot between *r* and *h/p* for model P₁M₂ & P₁M₅ with same *p* = 16 cm
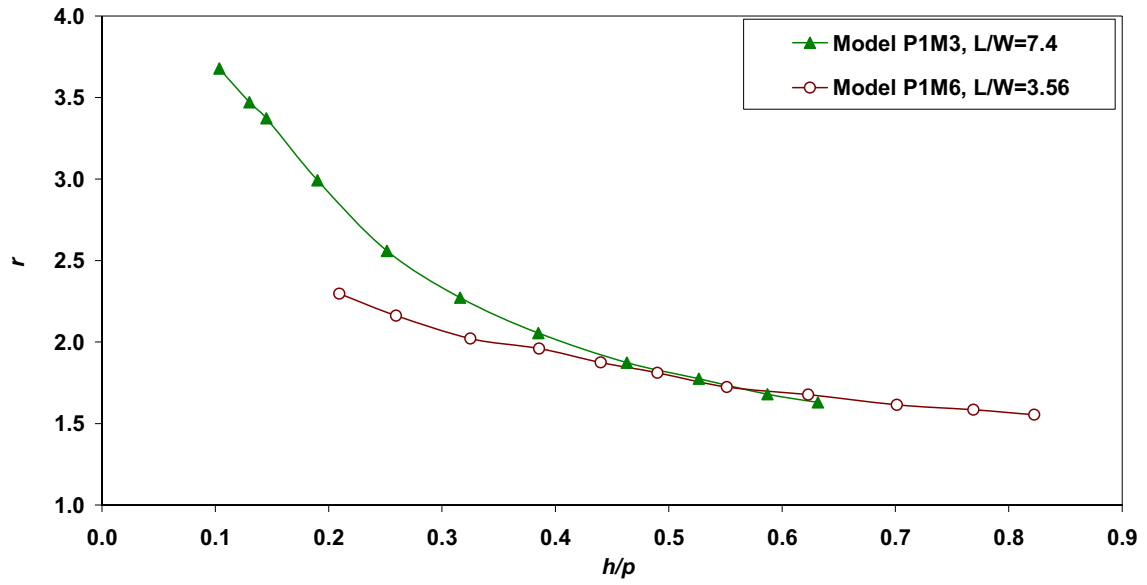
Fig. 4.9 Plot between *r* and *h/p* for model P₁M₃ & P₁M₆ with same *p* = 20 cm
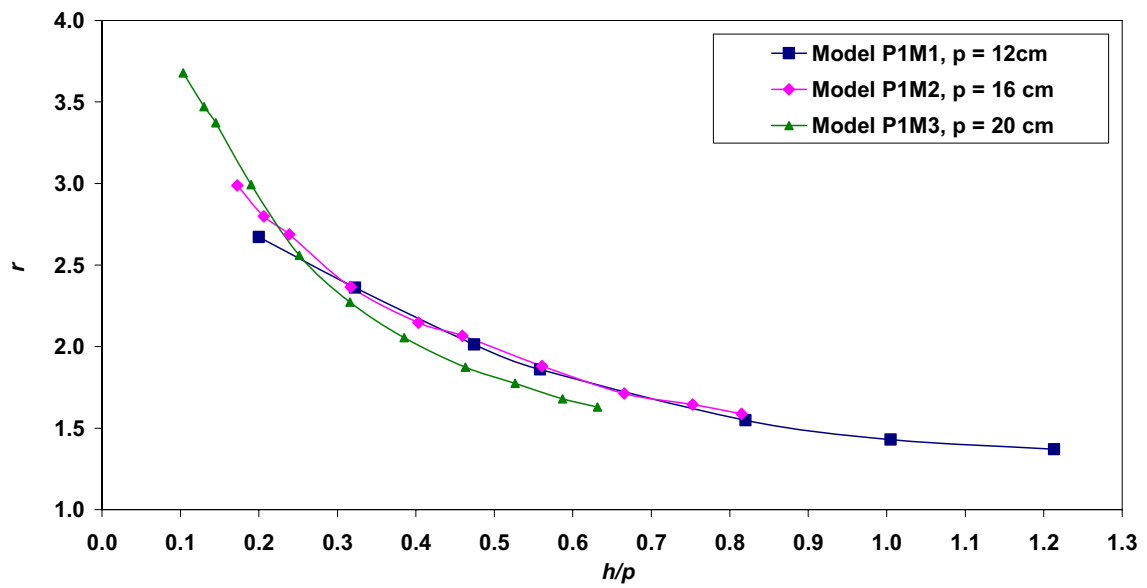
Fig. 4.10 Plot between *r* and *h/p* for same *L/W* = 7.4
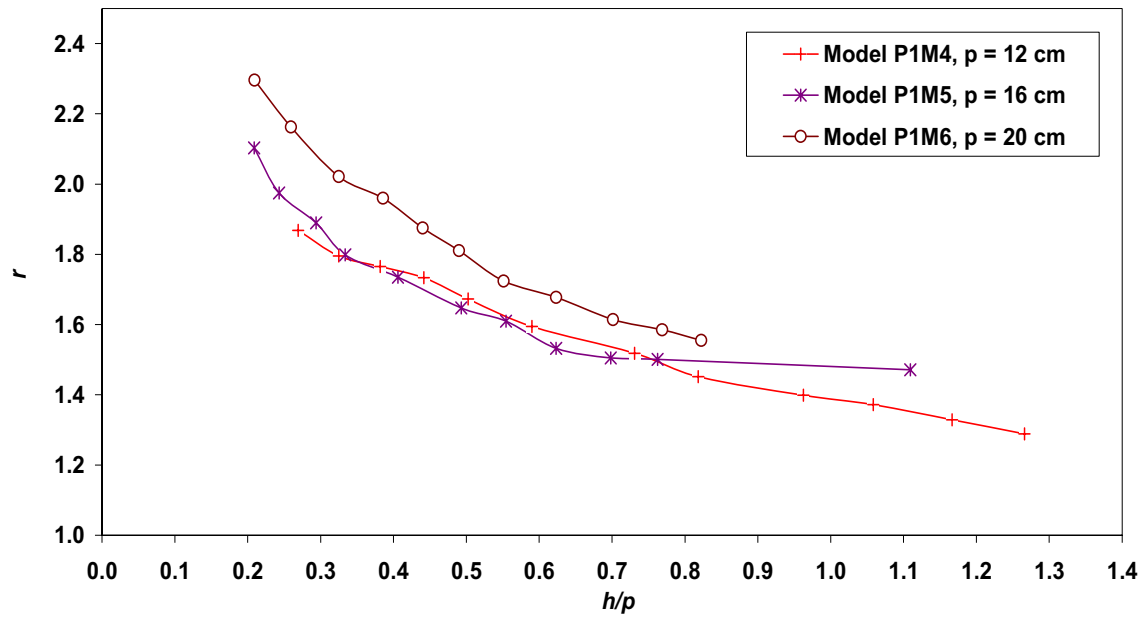
Fig. 4.11 Plot between *r* and *h/p* for same *L/W* = 3.56
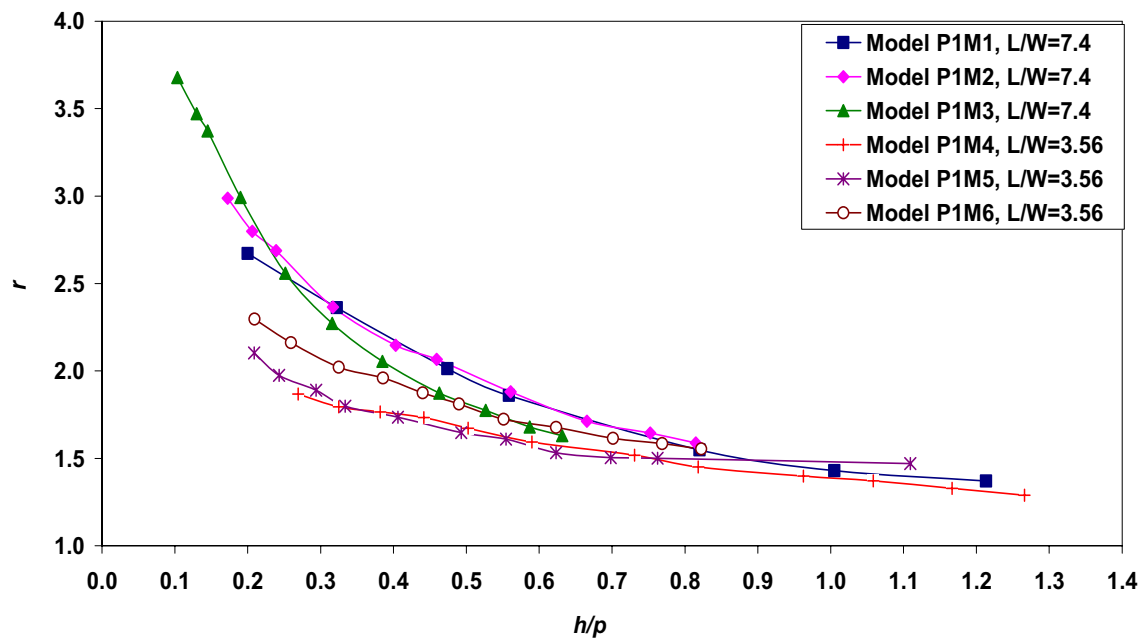
Fig. 4.12 Plot between *r* and *h/p* for all six models

4.5   EVALUATION OF SECOND PHASE EXPERIMENTS

In this phase of experiment, some modifications have been done in the first phase models for increased hydraulic efficiency. In this phase of the experiment, both sides ramps are provided in the first phase models.

The graphical representation between net absolute value of discharge increment (difference between ordinates of Q_L and Q_{PK}) for both side ramps and without ramps against (h/p) for all the six models is shown in Figs. 4.13-4.18. In Figs.4.13 to 4.18, one can see that net absolute value of discharge increment ΔQ is more for both side ramps than without ramps. It can be seen that the discharge increment increases in the presence of ramps. Graphical plots between 'r' and h/p for all six models are shown in Fig. 4.19. From Fig. 4.19, model P_2M_2 is found to perform better.
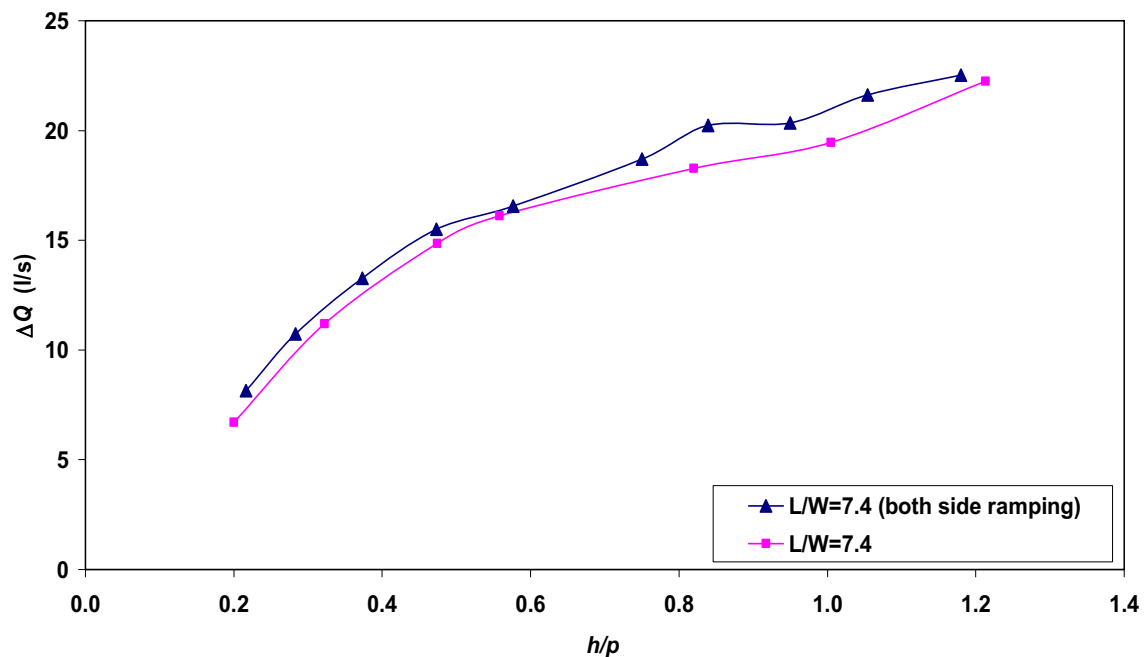
Fig. 4.13 Plot between ΔQ and h/p for model P_2M_1 with both side ramps and without ramps.
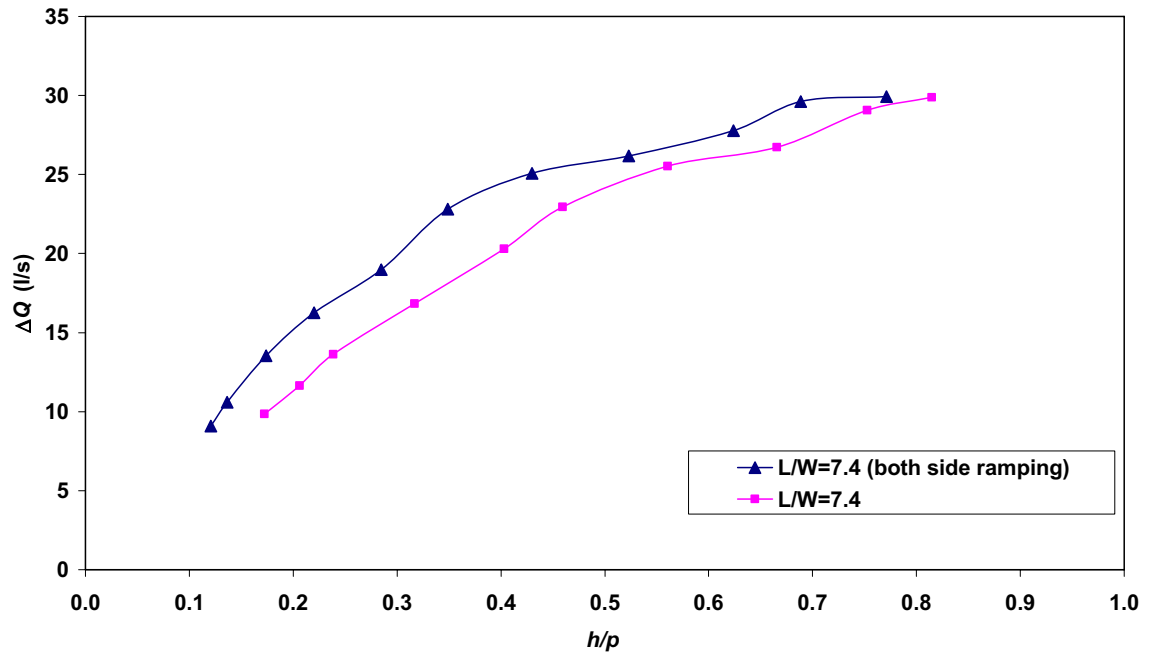
Fig. 4.14 Plot between ΔQ and _h/p_ for model P₂M₂ with both side ramps and without ramps
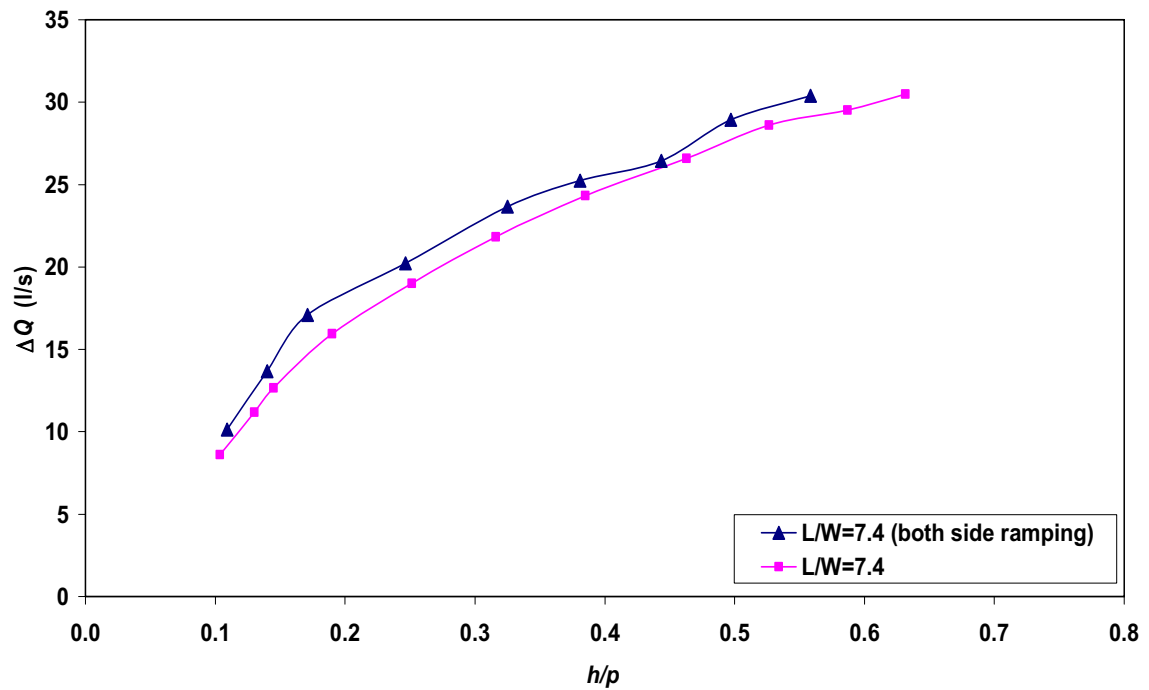
Fig. 4.15 Plot between ΔQ and _h/p_ for model P₂M₃ with both side ramps and without ramps
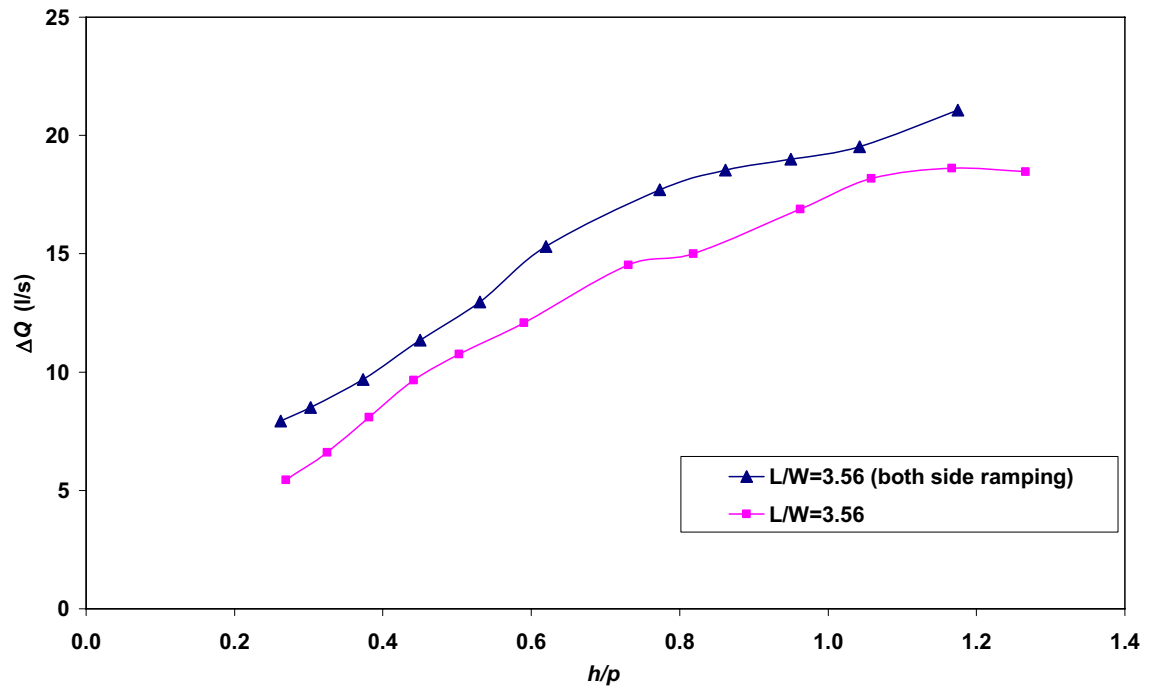
Fig. 4.16 Plot between ΔQ and *h/p* for model P₂M₄with both side ramps and without ramps
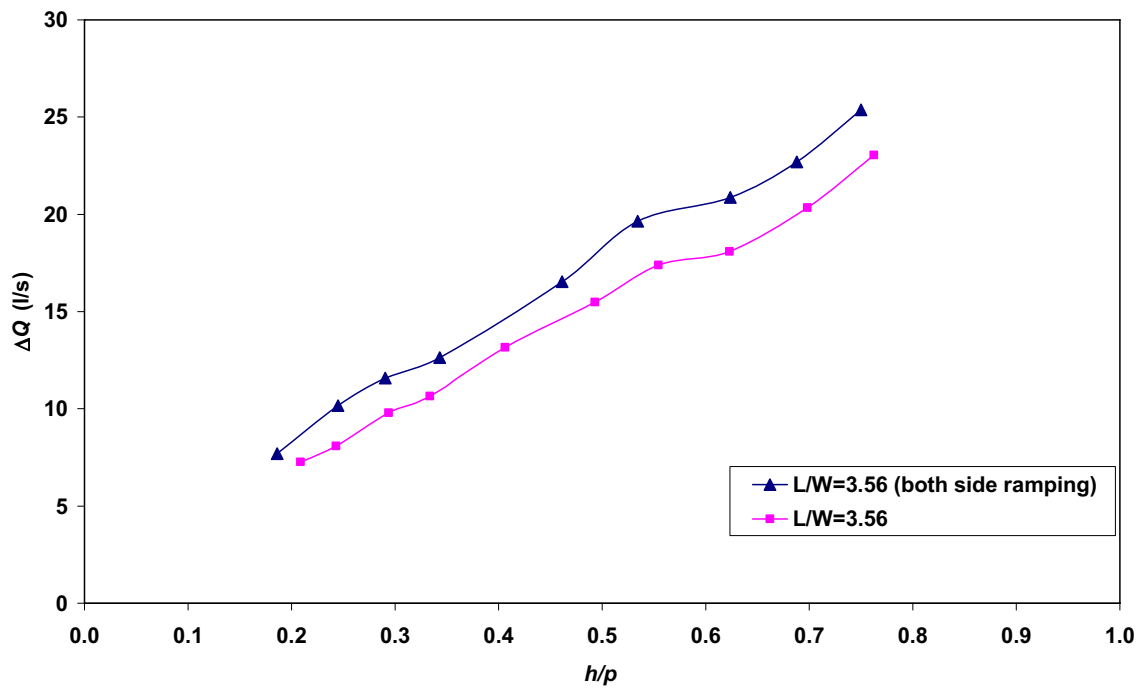
Fig. 4.17 Plot between ΔQ and *h/p* for model P₂M₅ with both side ramps and without ramps
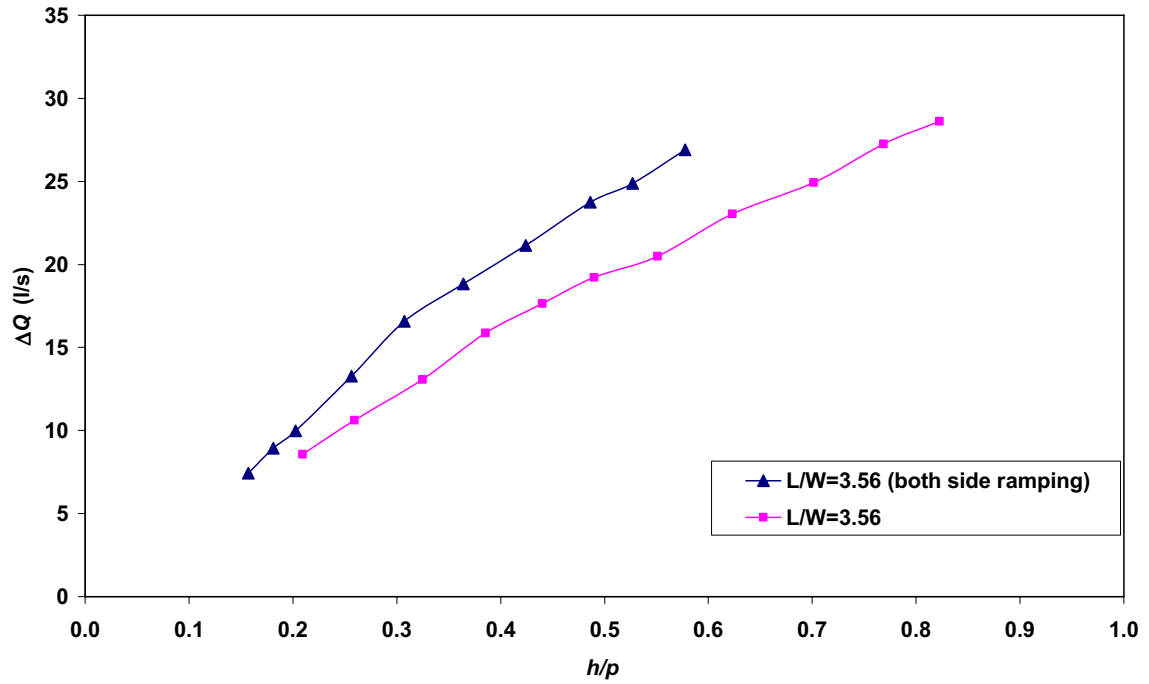
Fig. 4.18 Plot between ΔQ and h/p for model P₂M₆ with both side ramps and without ramps
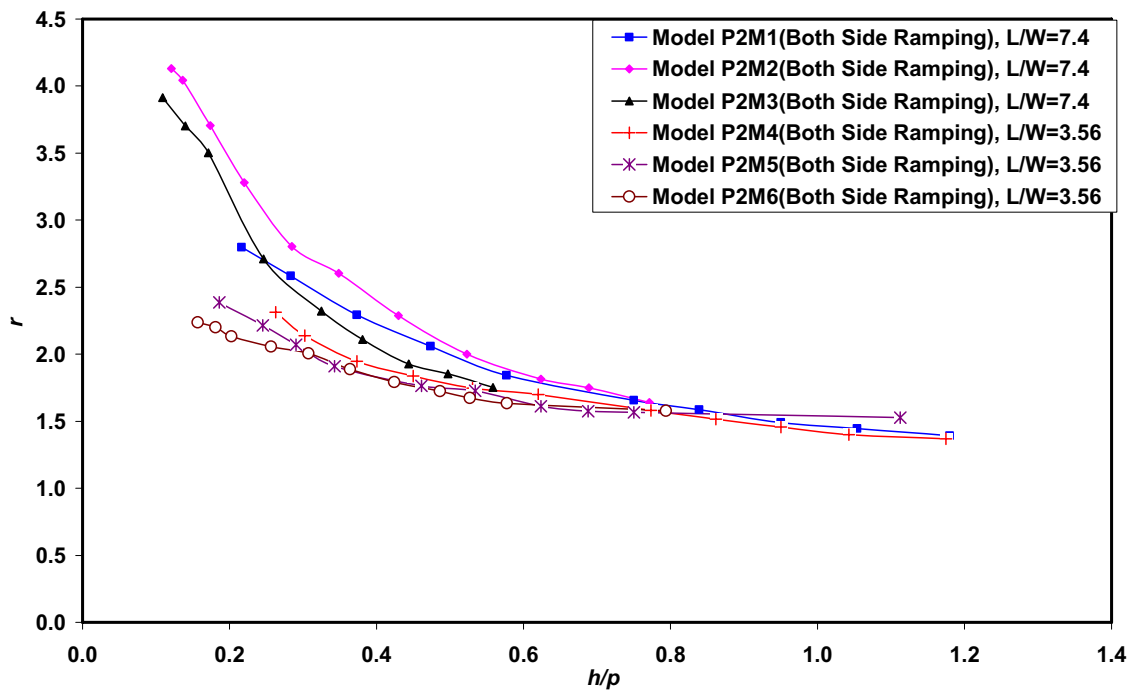
Fig. 4.19 Plot between r and h/p for all six models with both side ramps

4.6 EVALUATION OF THIRD PHASE EXPERIMENTS

The effect of changing widths of inlet and outlet cells has been studied in this phase of experiments. Here, the ratio of inlet to outlet cell is varied from 0.667 to 1.33. The model height is kept as 16 cm and in total six models having ramps and both side overhanging are fabricated and used.

Graphical plots between 'r' and h/p for all six models in this phase are shown in Fig. 4.20. From Fig. 4.20, model P_3M_1 is found to perform better. It is also observed that effect of length magnification ratio L/W does not appear significant at h/p higher than 0.6.

Graphical plots between 'r' and $h/(a+b)$ for all six models is shown in Fig. 4.21 and this graph highlights the effect of inlet cell width (a) and outlet cell width (b). In Fig. 4.21, all 16 cm height of Piano Key Weir models have been considered including two second phase models P_2M_2 & P_2M_5 also. It can be seen from Fig. 4.21 that the value of 'r' increases with increasing a/b. But for L/W 7.4, it is found that value of 'r' increases with increasing a/b value upto 1, and after that there is no increment in value of r. Thus, a/b as unity appears to be a reasonable choice for larger L/W ratio.
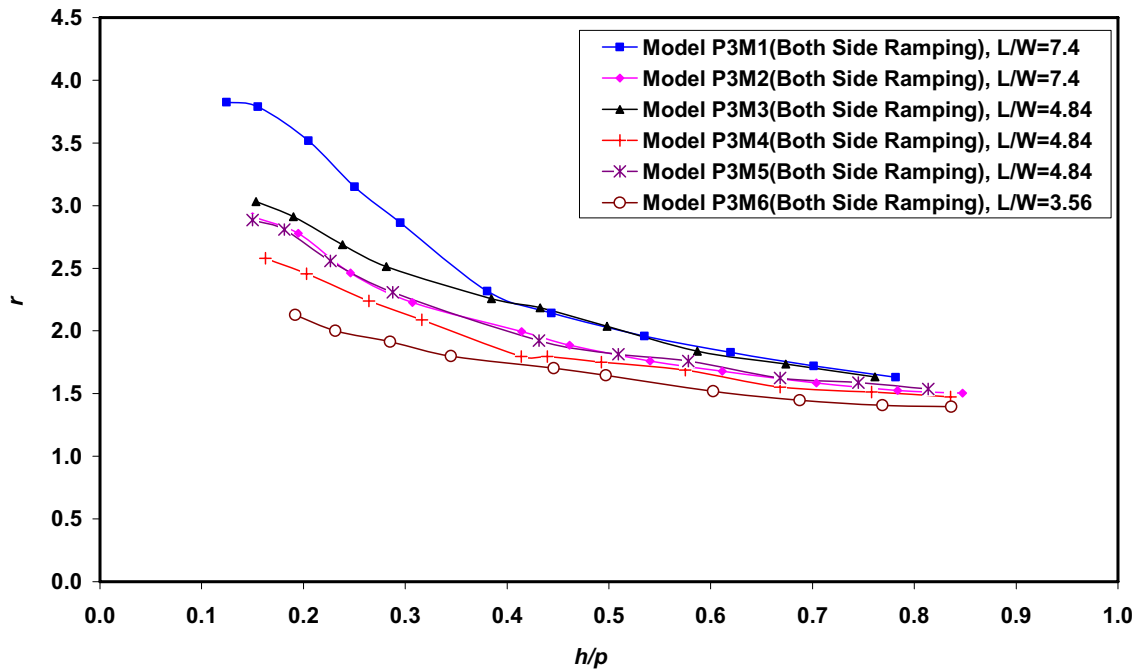
Fig. 4.20 Plot between _r_ and _h/p_ for all six Models of phase three
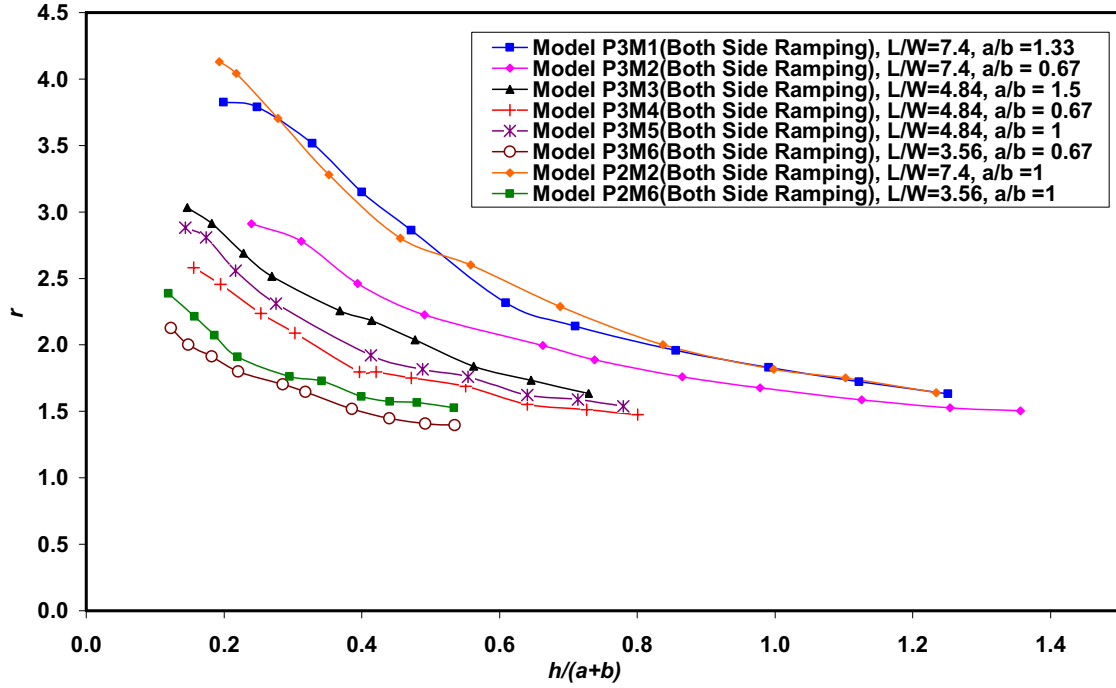
Fig. 4.21 Plot between *r* and *h/(a+b)*

4.7   EVALUATION OF FOURTH PHASE EXPERIMENTS

In the fourth phase of the experiment programme, the models of Piano Key Weir having only downstream side over hanging only are used. Details of the models used in this phase are given in Chapter 3. All the models used are having ratio of inlet to outlet cell widths as unity and mainly, the effect of varying *L/W* is studied.

The graphical representation between discharge and (h/p) for all the six models is shown in Figs. (4.22-4.26). In Figs. 4.22 to 4.26, it can be seen that discharge passing through Piano Key Weir (Q_{PK}) is more than discharge passing through rectangular sharp crested weir. Graphical plots between '*r*' and h/p for all five models is shown in Fig. 4.27. From Fig. 4.27, model P_4M_4 is found to perform better. It is observed from Fig. 4.27 that effect of length magnification ratio *L/W* reduces as h/p becomes greater than 0.6.
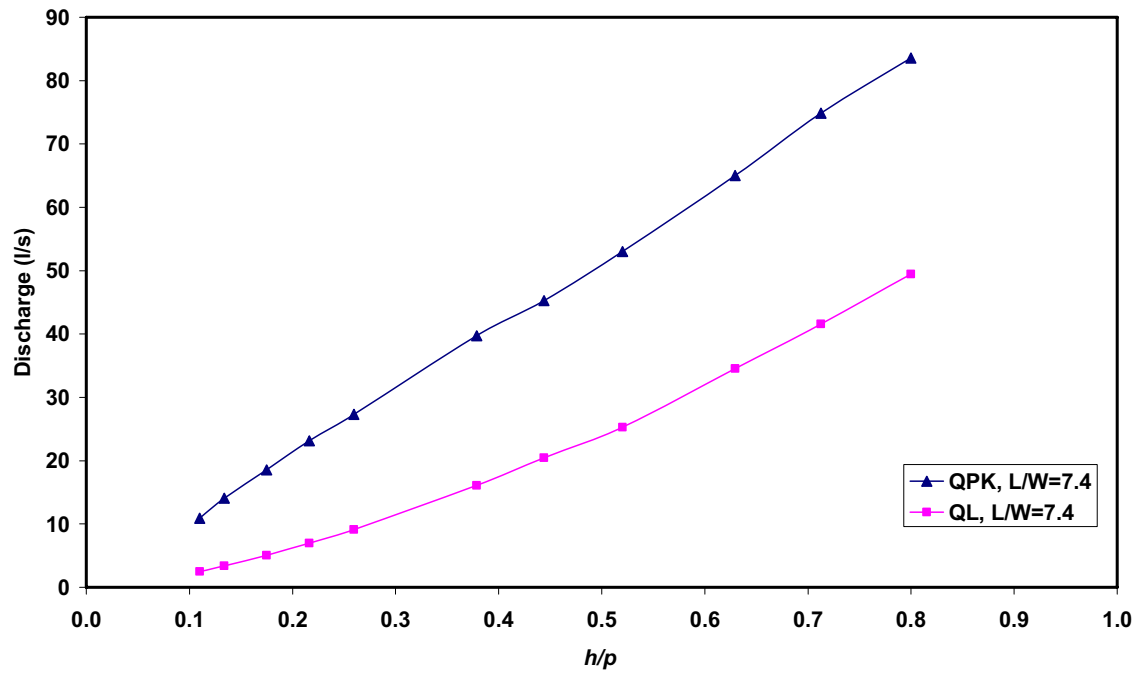
Fig. 4.22 Plot between Q_{PK}, Q_L and h/p for model P_4M_1 with both side ramps
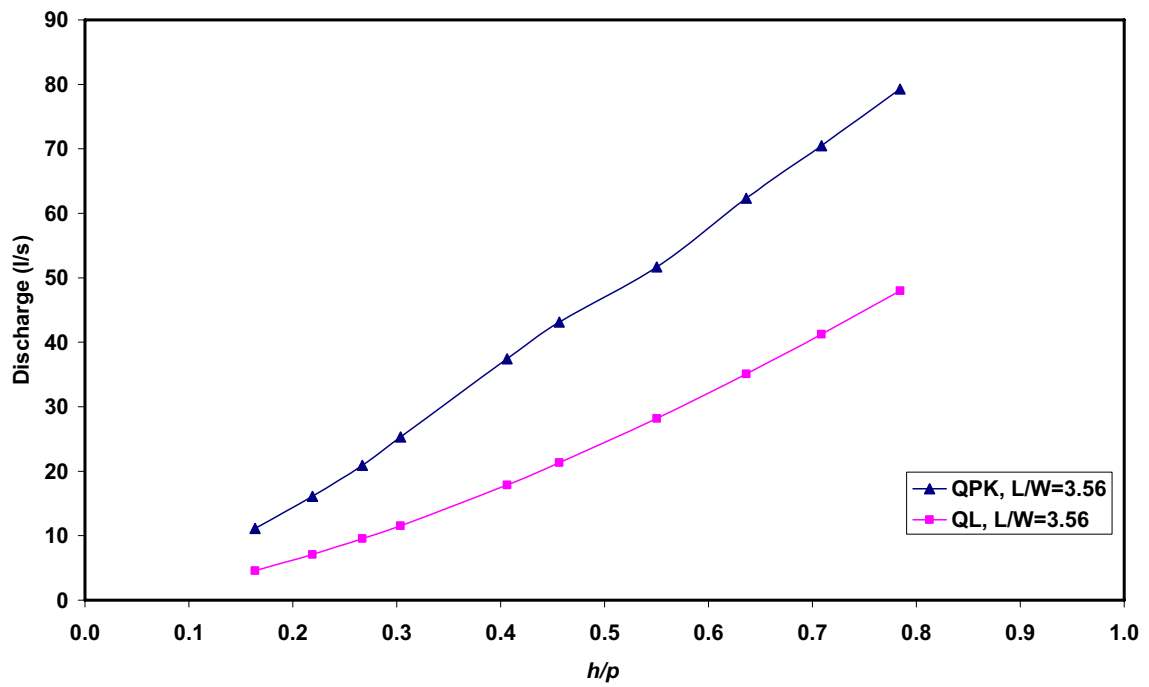
Fig. 4.23 Plot between Q_{PK}, Q_L and h/p for model P_4M_2 with both side ramps
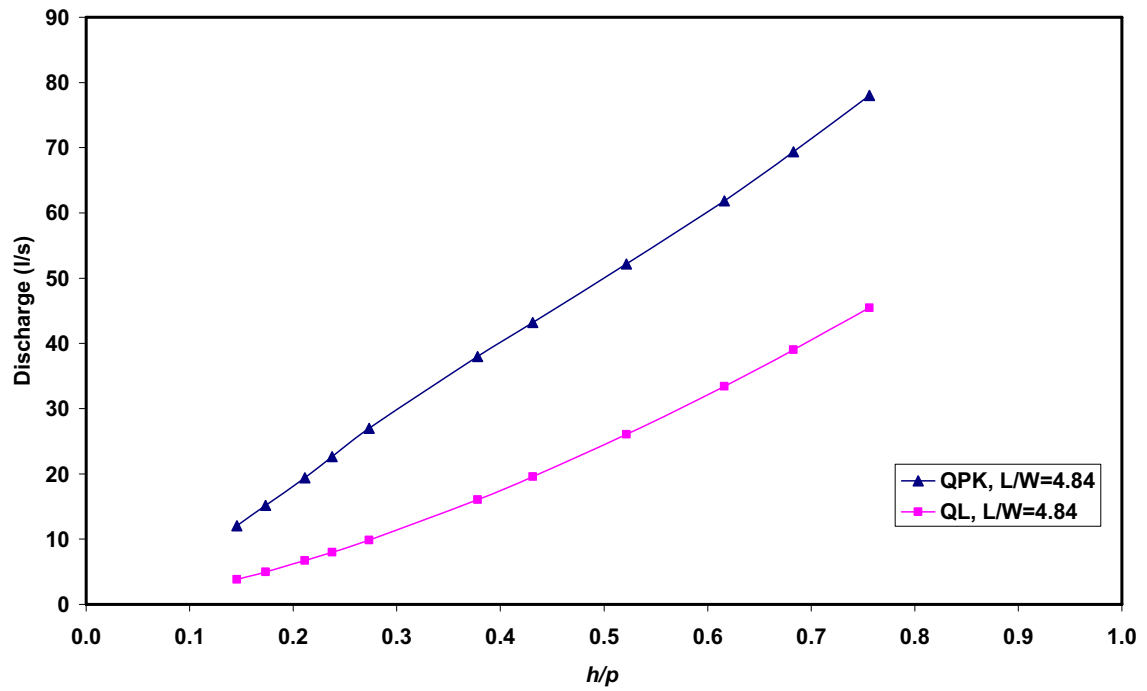
Fig. 4.24 Plot between Q_{PK}, Q_L and h/p for model P_4M_3 with both side ramps
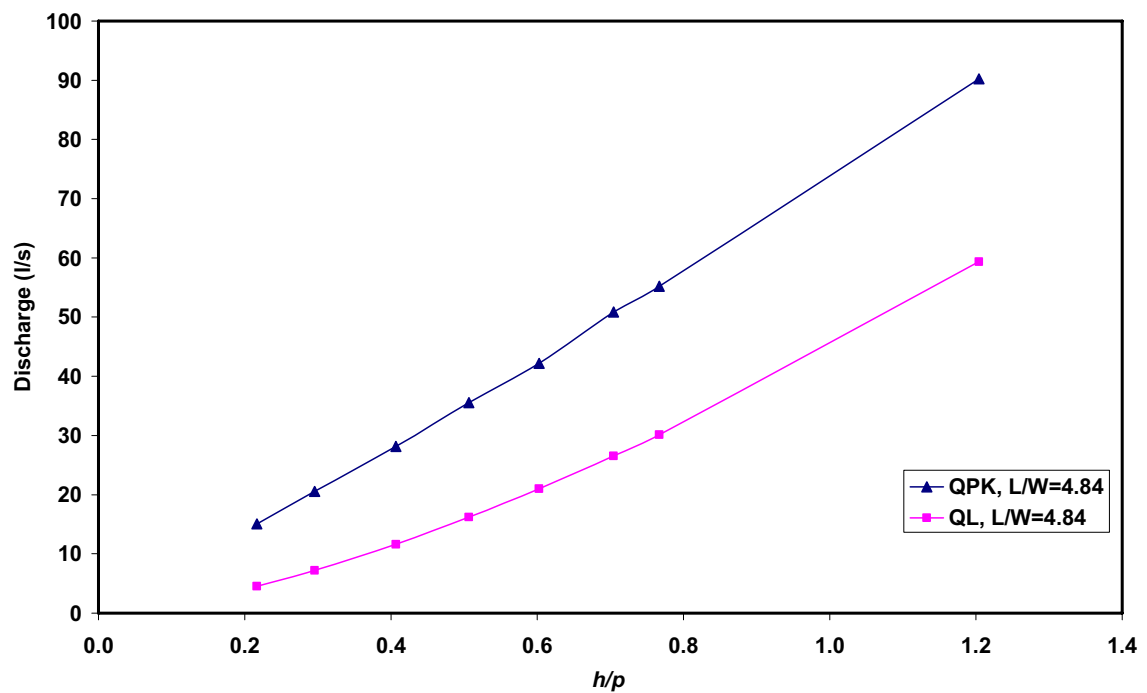
Fig. 4.25 Plot between Q_{PK}, Q_L and h/p for model P_4M_4 with both side ramps

71
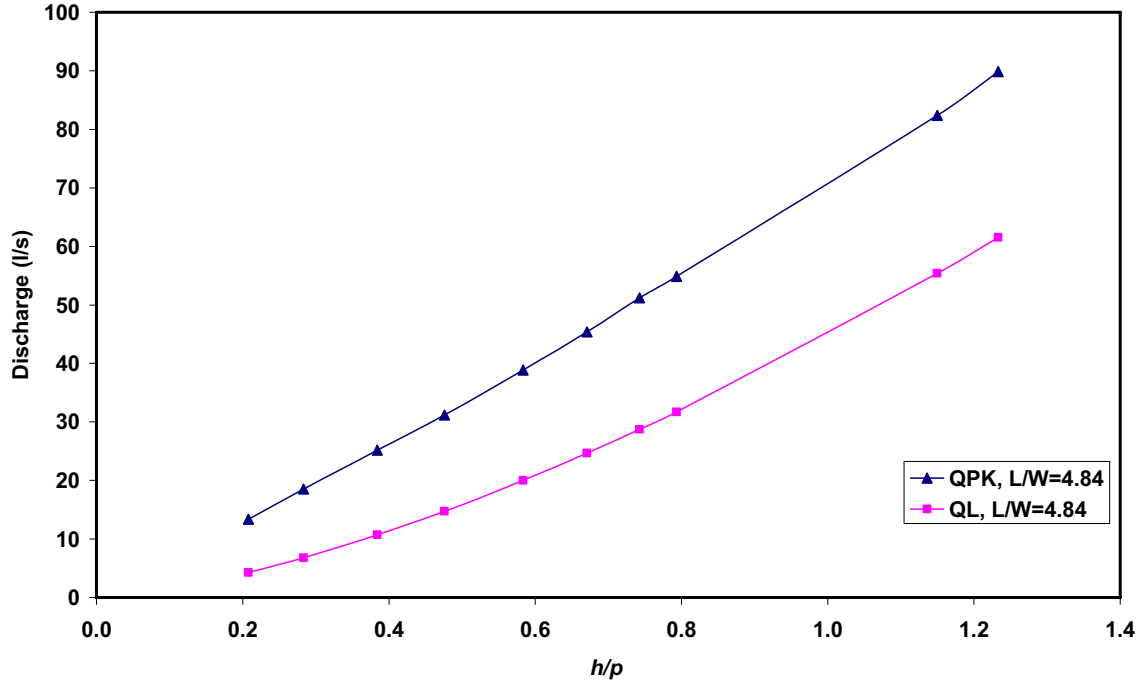
Fig. 4.26 Plot between Q_{PK}, Q_L and h/p for model P_4M_5 with both side ramps
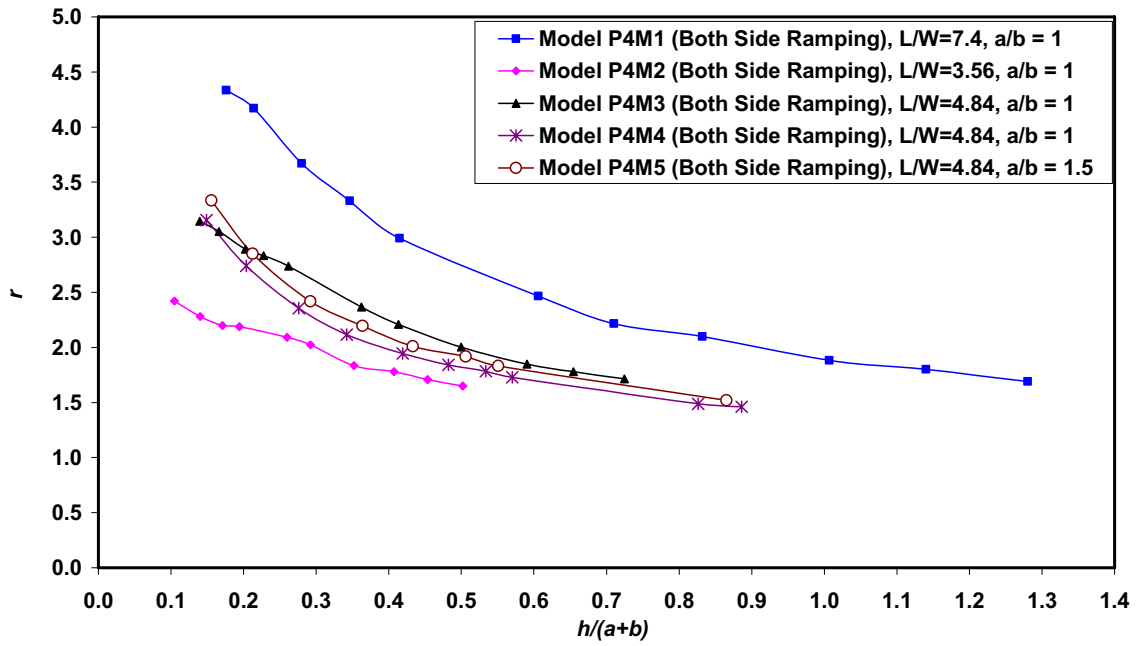
Fig. 4.27 Plot between r and h/p for all five models of phase four

4.8   EVALUATION OF FIFTH PHASE EXPERIMENTS

Here, the focus is modification of inlet and outlet cells by providing filling to ramps so that one ramp now consists of two steps and thus, a planar discontinuity. In total, three models are fabricated. Also, in two models, inlet portion is modified from a flat plate to a triangular prism shaped configuration. Details of these models are given in preceding chapter.

In Figs. 4.28 to 4.32, it could be seen that net absolute value of discharge increment ΔQ is not normally increased for all the modified models.
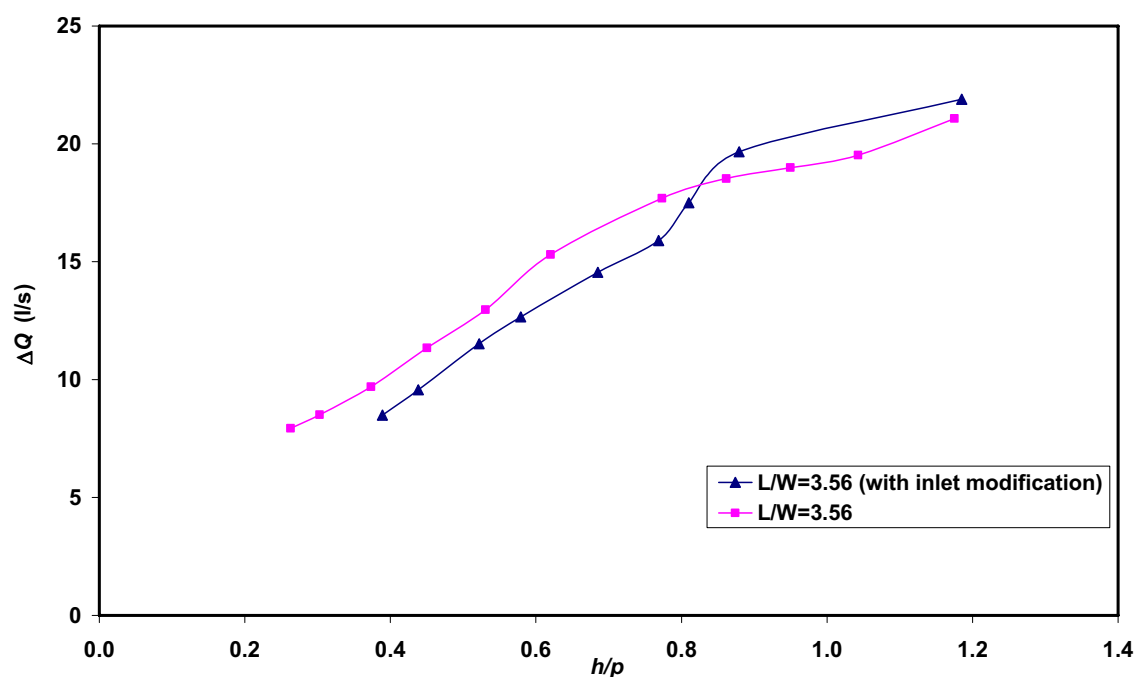
Fig. 4.28 Plot between ΔQ and h/p for model P_2M_4 & model P_2M_4 (with improving the hydraulic shape of inlet)
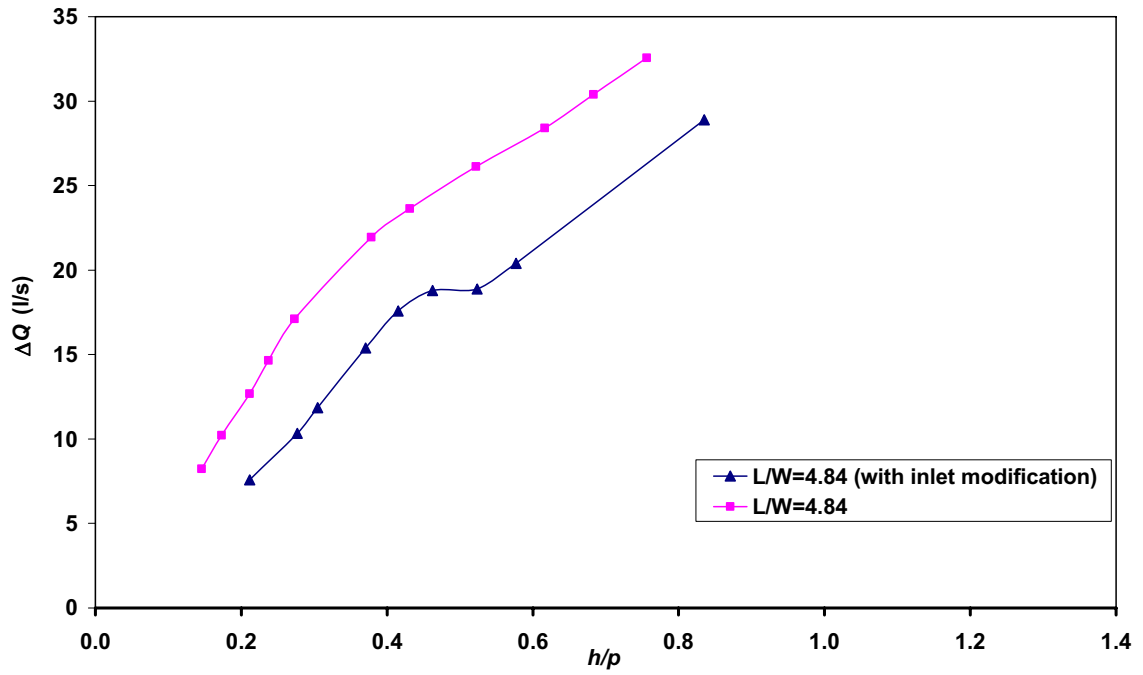
Fig. 4.29 Plot between ΔQ and *h/p* for model P$_4$M$_3$ & model P$_4$M$_3$ (with improving the hydraulic shape of inlet)
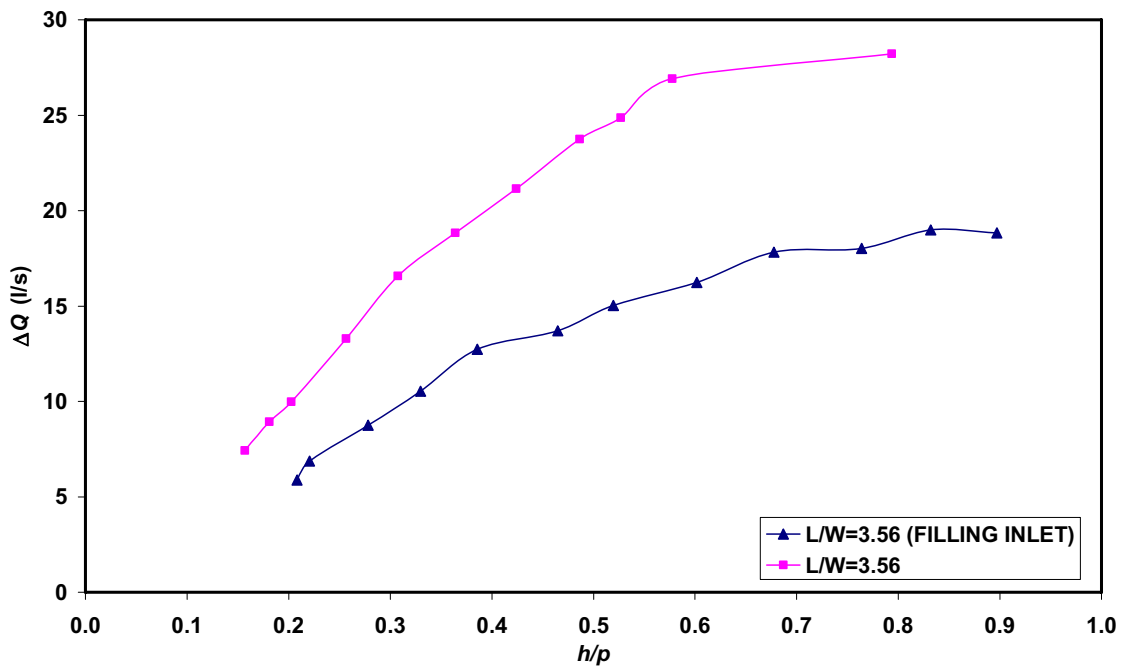
Fig. 4.30 Plot between ΔQ and *h/p* for model P$_2$M$_6$ (filling inlet cell)
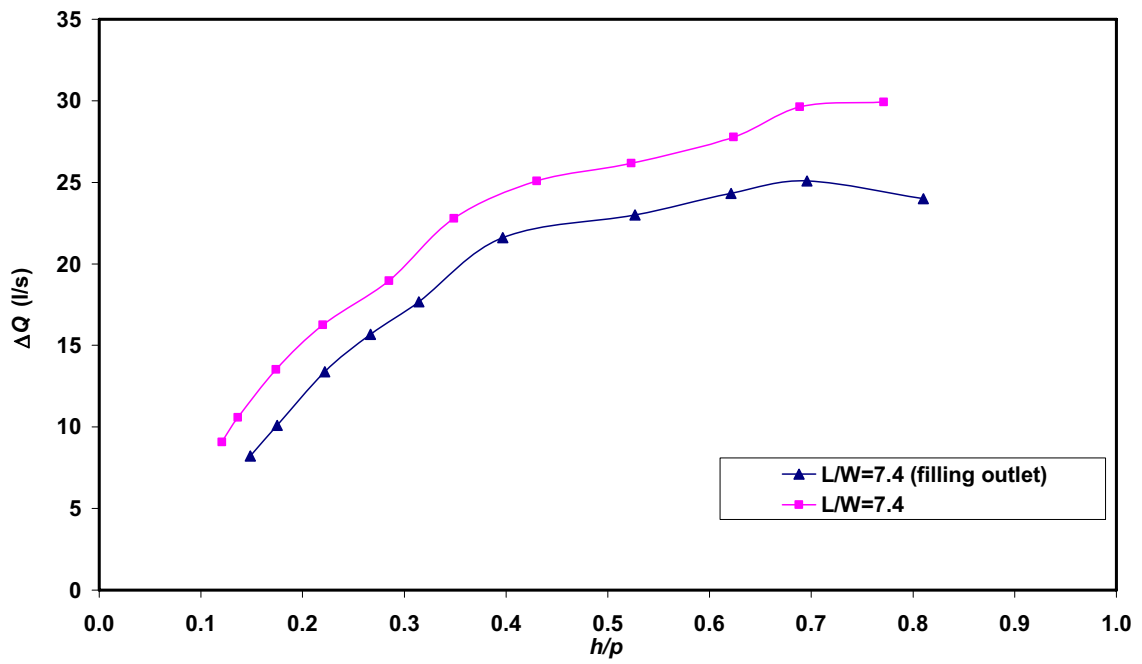
Fig. 4.31 Plot between ΔQ and *h/p* for model P$_2$M$_2$ (filling outlet cell)
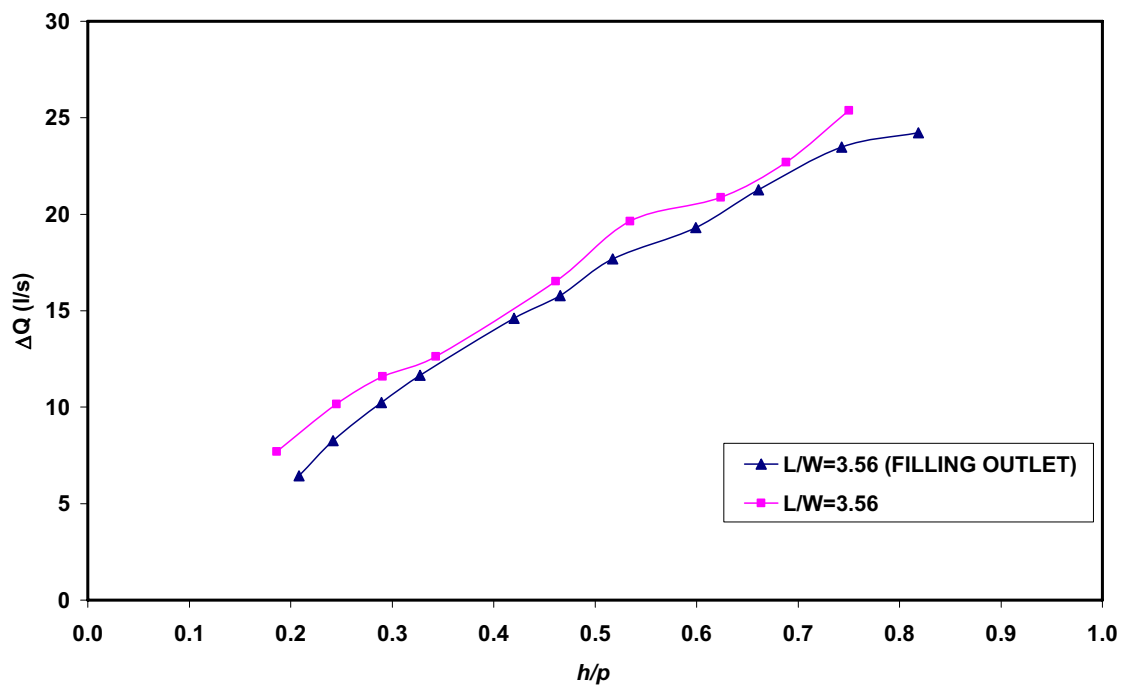
Fig. 4.32 Plot between ΔQ and *h/p* for model P$_2$M$_5$ (filling outlet cell)

4.9 SUMMARY

In this chapter, the experimental data collected in the present study towards evaluation of a most efficient shape of Piano Key Weir are subjected to a preliminary analysis. It is found that during all the phases of experiments, Piano Key Weir discharge is higher than linear weir discharge for a given head. Similarly, the discharge passing capacity of Piano Key Weir at a given head improves with increasing L/W ratio and for this reason, the choice of inlet to outlet cell width should be kept as unity, as deviation from this is not helpful in the magnification of discharge. Various modifications to inlet and outlet cells are also not found useful. Piano Key Weir with ramps and having overhanging sides are found to perform better.

CHAPTER – 5

PIANO KEY WEIR –A CASE STUDY

5.1   GENERAL

This chapter presents investigation related to application of typical Piano Key Weir for Sawra Kuddu Hydro Electric Project. Sawra Kuddu HEP with an installed capacity of 111 MW is located on Pabbar River in Himachal Pradesh. Laugier (2007) has studied other form of Piano Key Weir for Goulours Dam in France. He conducted the model test in flume with geometrical similar scale based on Froude law. Laugier has reported that Piano Key Weir is used for rehabilitation project in Goulours dam. In Sawra Kuddu HEP, the flow diversion structure consists of four under-sluices bays on the left and three on the right bank, each of 8.00 m width with 1.50 m thick intermediate piers. A 138 m long Piano Key Weir is proposed in between the two sets of under-sluices. The design discharge of the project is 6880 m^3/s. The Piano Key Weir is designed to handle 3900 m^3/s and the balance discharge 2980 m^3/s passes through under-sluices. This chapter focuses on the experimental results and optimization procedure of the evacuation system of Sawra Kuddu HEP with the Piano Key Weir. The physical modeling has been carried out at the laboratory of River engineering at the Water Resources Development and Management department (WRD&M), IITR, Roorkee, India. A comprehensive investigation based on physical model studies on a flume has been undertaken to evolve the best suitable Piano Key Weir elements to assess the behaviour of the Sawra Kuddu HEP.

5.2   EXPERIMENTAL STUDIES

Combining the experience of preceding experiments, some more physical model studies have been conducted to evolve optimal Piano Key Weir elements of the Sawra Kuddu HEP. A wide flume having perspex walls to visualize the flow was installed at River Engineering Lab of WRD&M IIT-Roorkee. Six Piano Key Weir models built to non-distorted geometrically similar scale of 1:50 molded in transparent acrylic sheet were installed in the flume during experimentation. The models were developed based on Froude law. These models represent a gross waterway of 50.00 m. The dimensions of Piano Key Weir for physical model study in laboratory are indicated in Table 5.1. The plan and sectional view of Piano Key Weir for physical model study are shown in Figs.

5.1 to 5.6. 1.00 m out of 2.76 m width of Piano Key Weir is selected from centre for physical model study in the flume. The total width of Piano Key Weir is 2.76 m. The maximum discharge adopted for model studies was 2500 m^3/s. The discharge scale as per Froude Law was worked out to 1/17678. Using this, the maximum flume discharge was found as 51.23 l/s. The studies were aimed mainly on assessing the better hydraulic efficiency.

The discharge was measured over a V-notch installed at the downstream of the flume. The water levels were measured by pointer gauge having least count of 0.01 cm. All the models were run for 8 to 10 different nappe heights. Pictorial view of all the models is shown in plate no. 5.1 to 5.6.

A comprehensive investigation has been done based on physical model studies on a flume to evolve best suitable Piano Key Weir elements to assess the behaviour of the Sawra Kuddu Barrage system. Comprehensive model constructed at outdoor lab of WRD&M, IIT, Roorkee has reproduced the actual topography of the valley including part of reservoir, designed Piano Key Weir and down stream side of weir. The model extends approximately 400 m upstream of the weir and 150 m down stream of the weir. Here, the Piano Key Weir is installed with full width of 2.76 m in geometric similar model i.e. 138.00 m in Prototype dimension.

The dimensions of Piano Key Weir for prototype are as indicated below in Table 5.2. The plan and sectional view of Piano Key Weir for comprehensive physical model study are shown in Fig. 5.7 and the plan and sectional view of Piano Key Weir for prototype with dimension are shown in Figs. 5.8. The pictorial view of model C_1M_6 in field is shown in Plate No. 5.7.

Table 5.1: Piano Key Weir dimensions for model study

Model No.	Height of Model (p) (cm)	a (cm)	b (cm)	$a + b$ (cm)	L/W	No. of Element
C_1M_1	18.40	14.80	26.28	41.08	3.74	2.5
C_1M_2	18.40	26.30	26.3	52.6	2.96	2
C_1M_3	18.40	19.72	19.72	39.44	3.74	2.5
C_1M_4	18.40	13.14	13.14	26.28	5.10	4
C_1M_5	18.40	16.00	11.60	27.6	4.91	3.5
C_1M_6	18.40	13.80	13.80	27.6	4.91	3.5

Table 5.2: Piano Key Weir dimensions for prototype

Model No.	Height of Model (p) (m)	a (m)	b (m)	$a + b$ (m)	L/W	No. of Element
C_1M_6	9.20	6.90	6.90	13.82	4.91	10
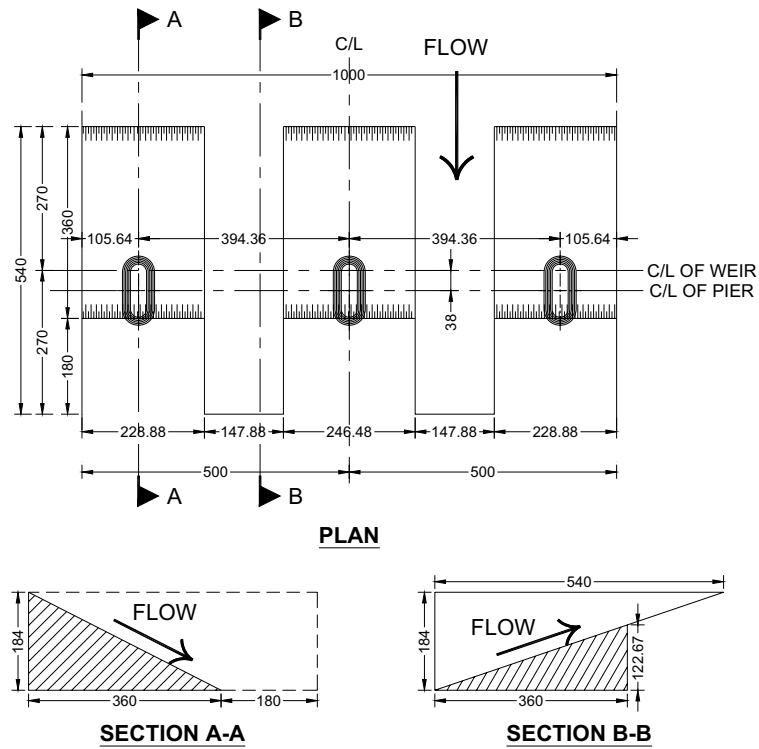
Fig. 5.1 Plan and section of model C₁M₁ for physical model study

(dimensions in mm)

Plate No. 5.1 Model C₁M₁

B ◄ ▲ A
C/L
FLOW

1000

270
360
105.64   394.36   394.36   105.64
540   C/L OF WEIR
                                         C/L OF PIER
270
180   38

171.63   262.91   262.91   262.91
                                         39.65
500   500

B ◄ ▲ A

PLAN

184
FLOW
360   180

540
184   122.67
FLOW
360

SECTION A-A   **SECTION B-B**

Fig. 5.2 Plan and section of model C_1M_2 for physical model study (dimensions in mm)

Plate No. 5.2 Model C_1M_2
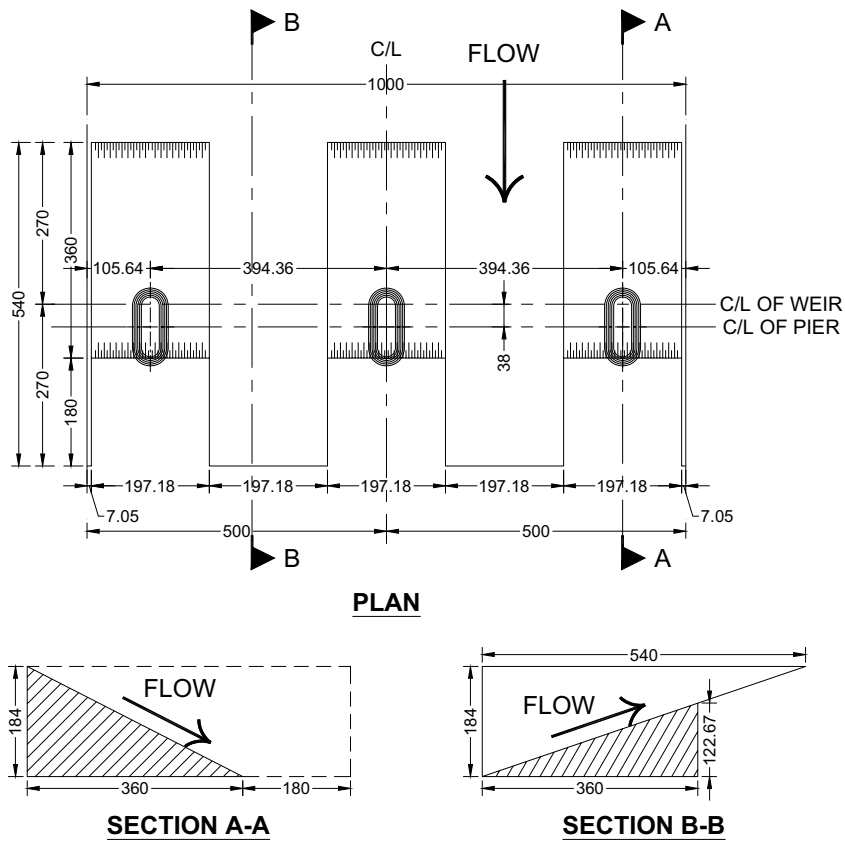
Fig. 5.3 Plan and section of model C₁M₃ for physical model study

(dimensions in mm)

Plate No. 5.3 Model C₁M₃
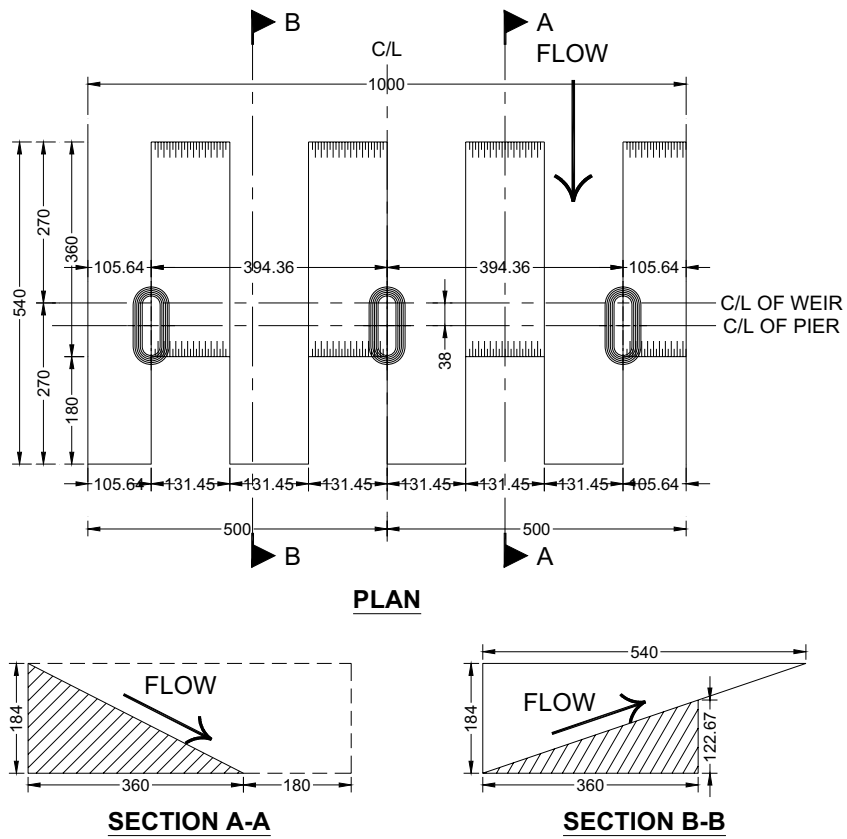
Fig. 5.4 Plan and section of model C₁M₄ for physical model study
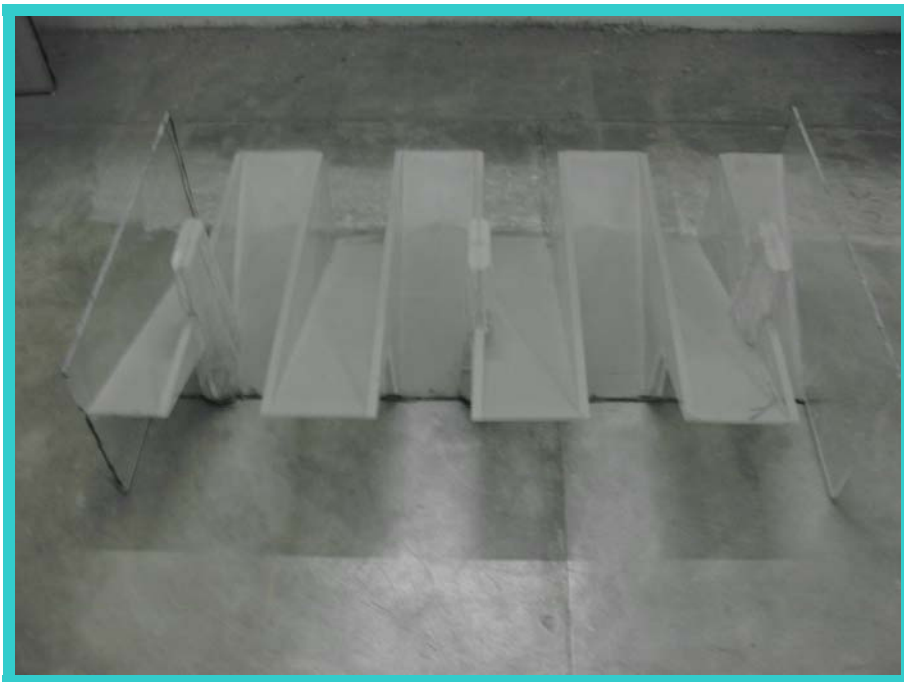
(dimensions in mm)

Plate No. 5.4 Model C₁M₄

Fig. 5.5 Plan and section of model C₁M₅ for physical model study

(dimensions in mm)

Plate No. 5.5 Model C₁M₅

83

Fig. 5.6 Plan and section of model C_1M_6 for physical model study

(dimensions in mm)

Plate No. 5.6 Model C_1M_6
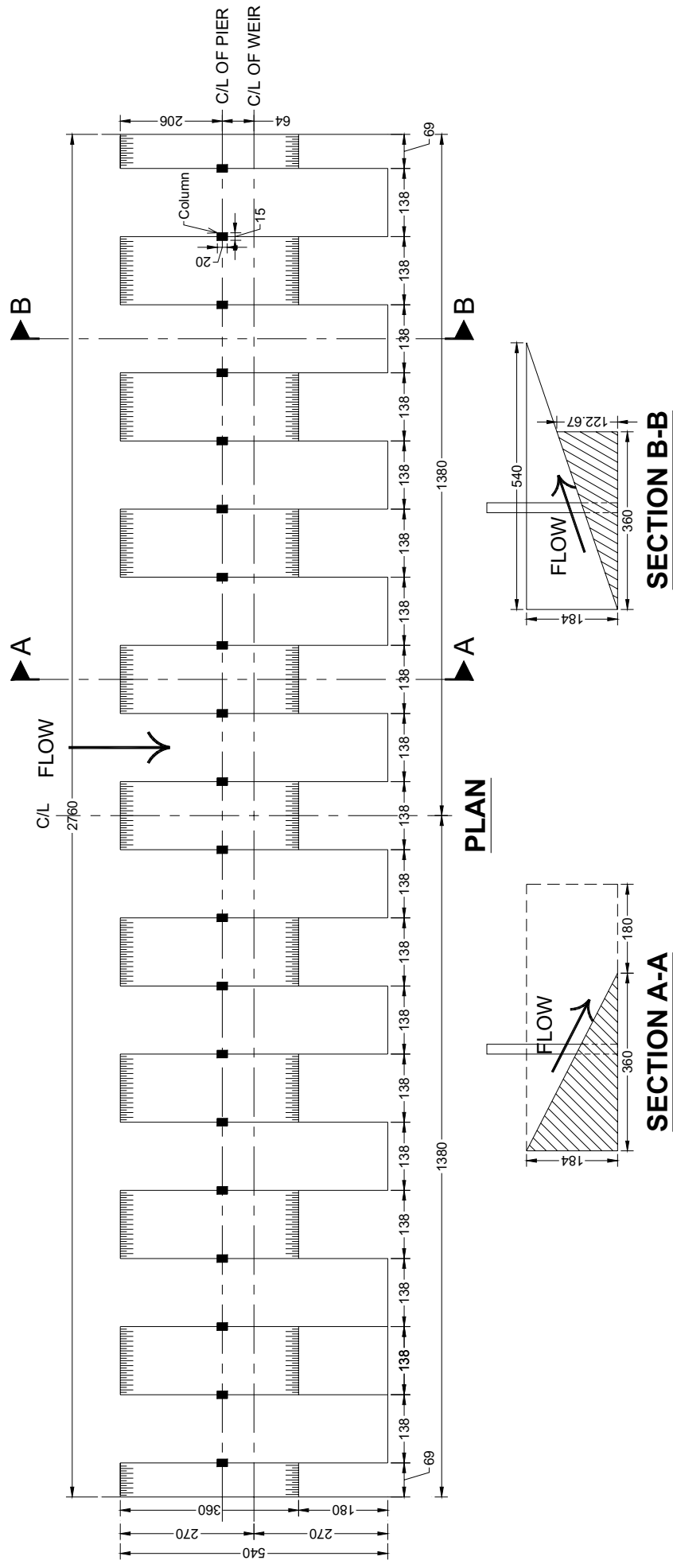
Fig. 5.7 Plan and section of model C_1M_6 for comprehensive model study (dimensions in mm)

85
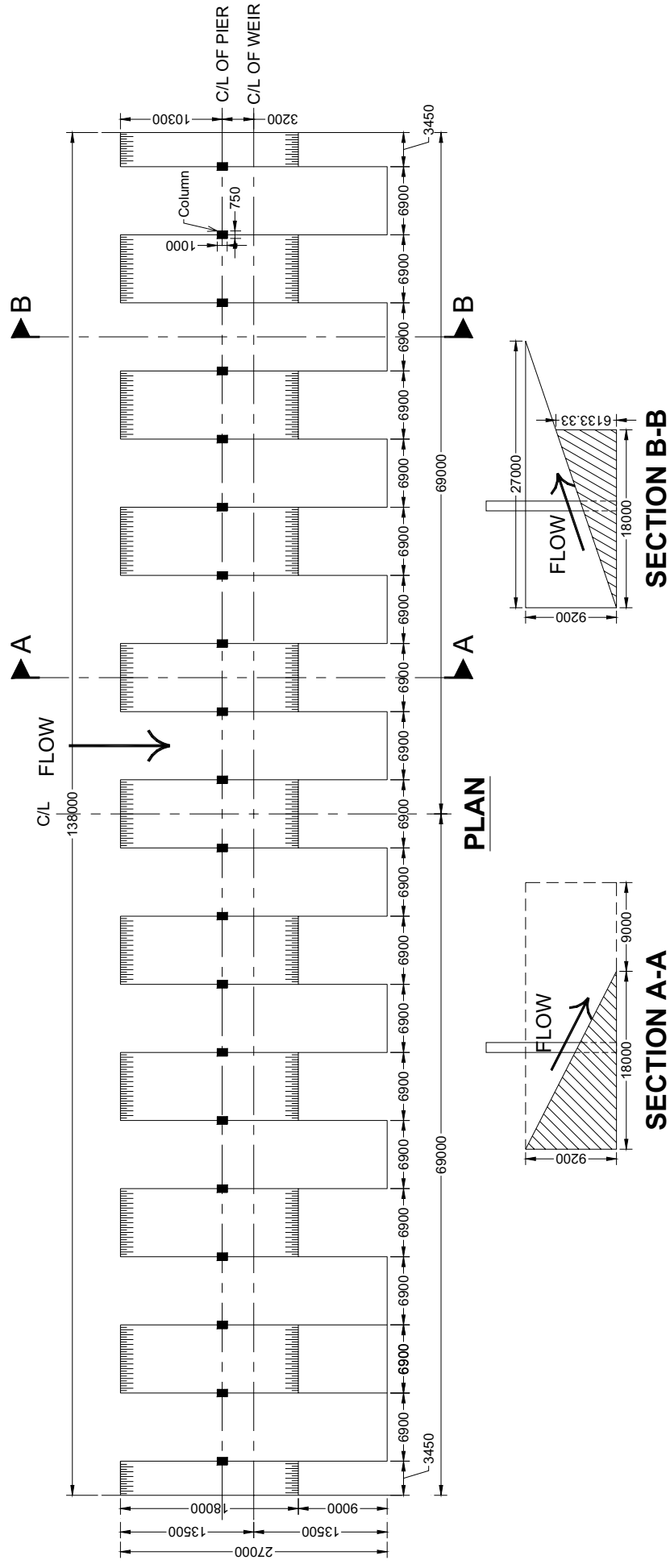
Fig. 5.8 Plan and section of model C_1M_6 for prototype (dimensions in mm)

86

Plate No. 5.7 Pictorial view of Piano Key Weir model C_1M_6 for comprehensive model study

5.3   ANALYSIS OF LAB-BASED MODEL EXPERIMENTS

This is done in two steps. Six different configurations of models are tested for their performance in lab based experiments. The test results in the form of discharge passing capacity as net absolute discharge increment is shown in Fig. 5.9, in which the ordinate 'ΔQ' represents the difference between discharge passing over a Piano Key Weir and sharp crested weir for same h/p. The net absolute value of discharge increment for different models is in the range of 5.00 to 30.00 l/s.

The test results for discharge passing capacity is shown in Fig. 5.10 where in the ordinate 'r' represents the ratio of discharge passing over a Piano Key Weir and sharp crested weir. Fig. 5.10 shows that discharge passing over a Piano Key Weir is 1.54 to 4 times higher than the sharp crested weir. From Figs. 5.9 and 5.10, it is found that lab based model C_1M_6 performs best in terms of r. For field scale testing, this model is used for construction.
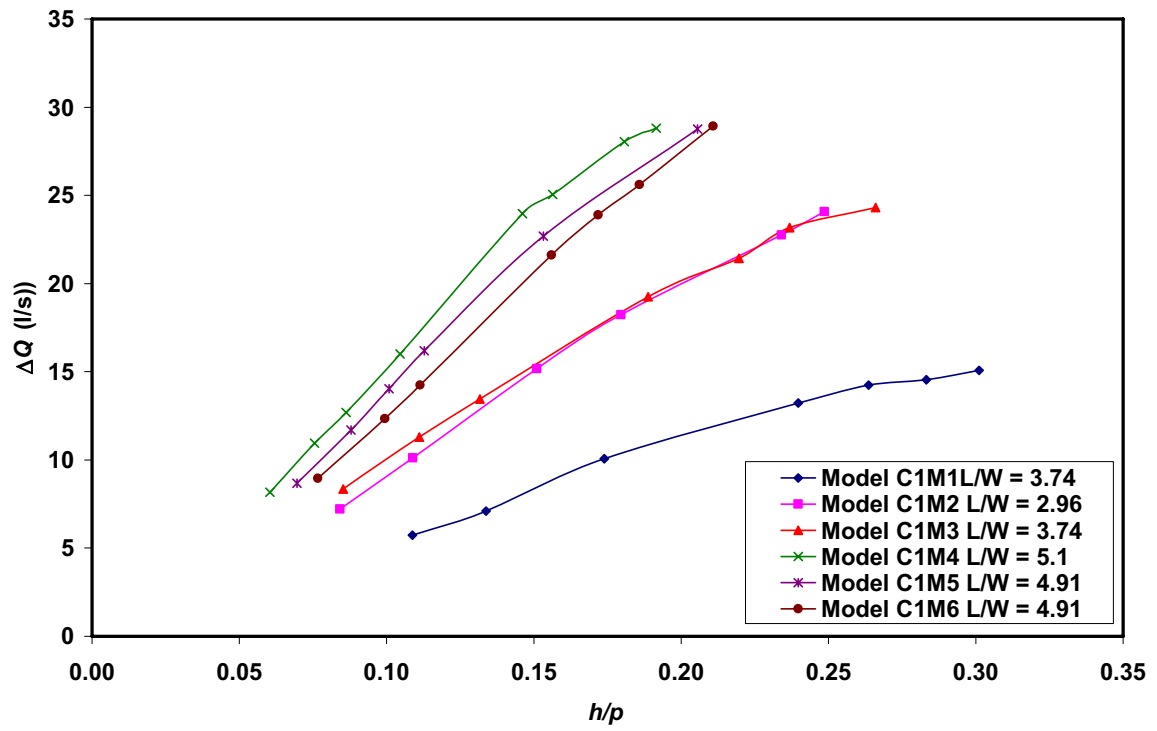
Fig. 5.9 Plot between ΔQ and *h/p* for all six models
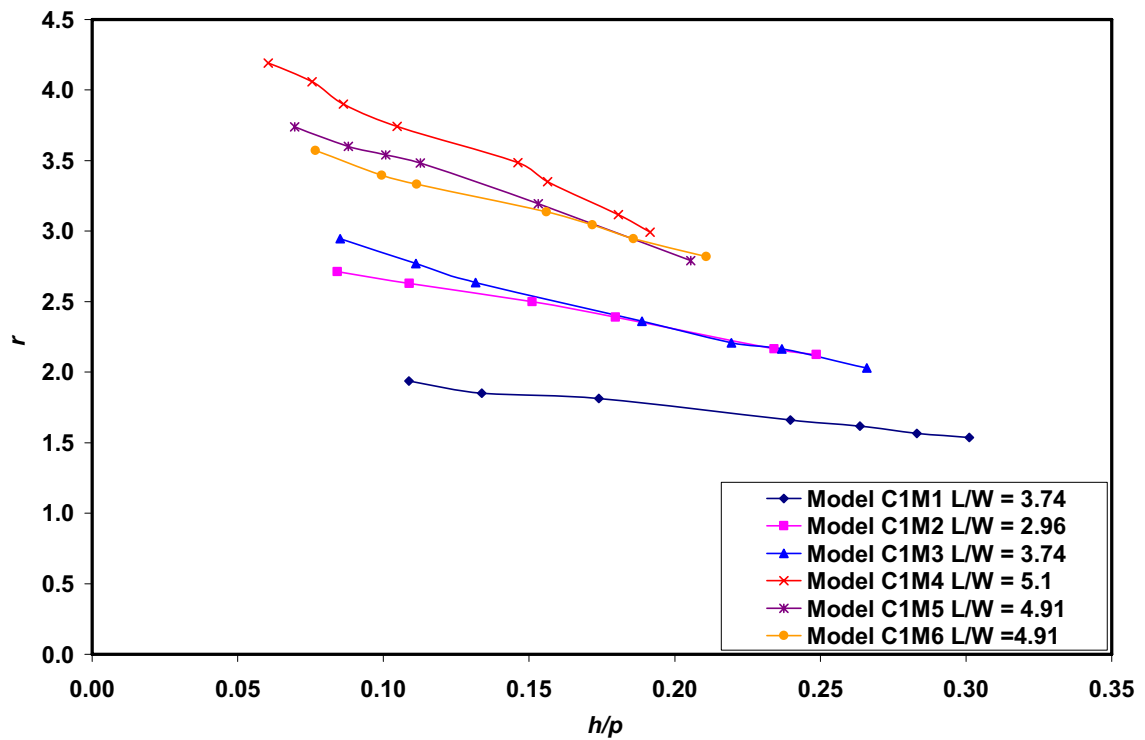
Fig. 5.10 Plot between *r* and *h/p* for all six models

5.4   ANALYSIS OF COMPREHENSIVE MODEL EXPERIMENTS RESULTS

From laboratory physical model studies, model C_1M_6 is preferred shape of Piano Key Weir. So this model C_1M_6 of Piano Key Weir is used for comprehensive model experiments. Full length of Piano Key Weir is used in comprehensive model study for better analyses of weir with reservoir area in upstream and downstream of weir.

The test results in the form of discharge passing capacity as net absolute discharge increment is shown in Fig. 5.11, where in the ordinate 'ΔQ' represents the difference between discharge passing over a Piano Key Weir and sharp crested weir for same h/p. The net absolute value of discharge increment for model C_1M_6 lies in the range of 450 to 1550 m^3/sec of prototype discharge.

The test results for discharge passing capacity is shown in Fig. 5.12 in which the ordinate 'r' represents the ratio of discharge passing over a Piano Key Weir and sharp crested weir. Fig. 5.12 shows that discharge passing over a Piano Key Weir is 2.65 to 4.00 times higher than sharp crested weir.

Fig. 5.13 represents the saving of head over the crest of Piano Key Weir against sharp crested weir. This graph shows that saving of head over the crest is 0.80 m (i.e. 58.6 %) in Piano Key Weir against sharp crested weir for lower range of discharge (i.e. 500 m^3/sec) and is 2.00 m (i.e. 47.6 %) in Piano Key Weir against sharp crested weir for higher range of discharge (i.e. 2500 m^3/sec). The running view of the models is shown in Plate no. 5.8 from downstream side of weir and in plate No. 5.9 from upstream side of weir.
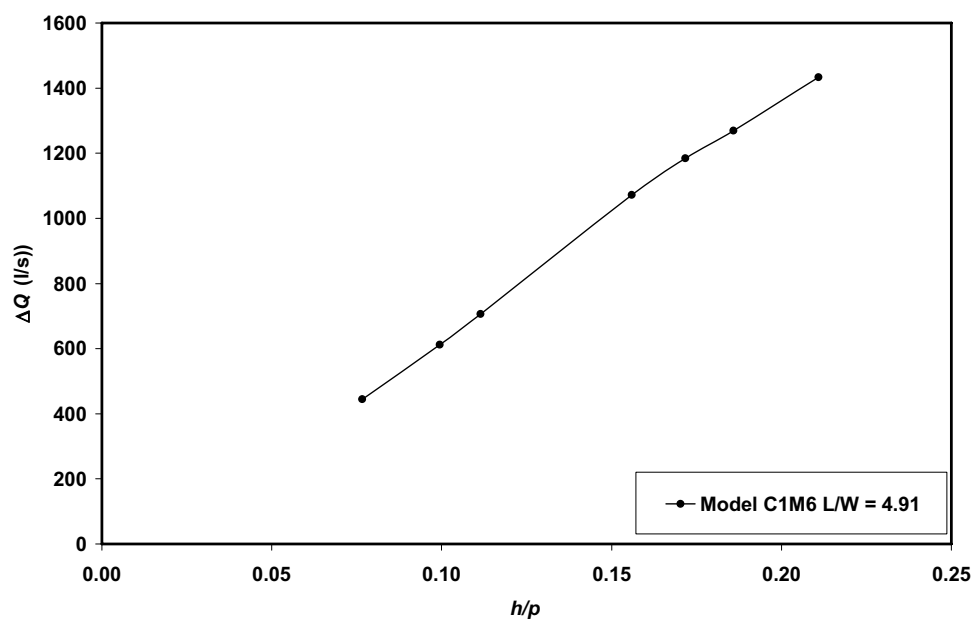
Fig. 5.11 Plot between r and h/p for model C_1M_6
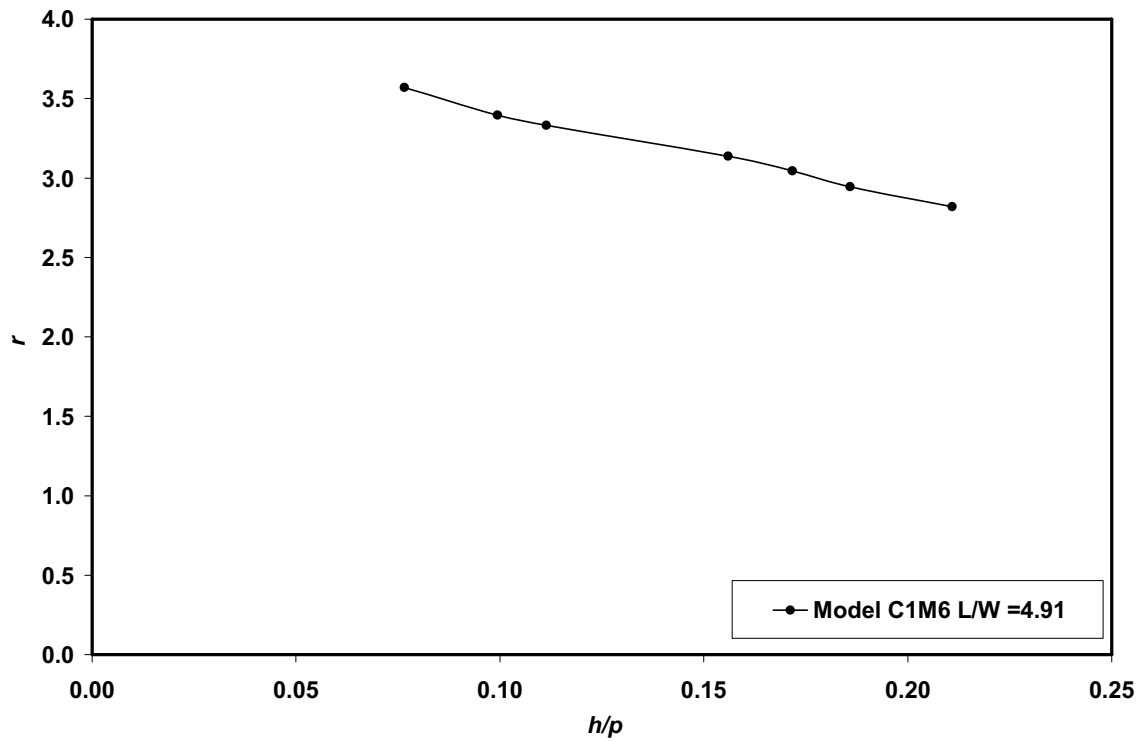
Fig. 5.12 Plot between ΔQ and *h/p* for model C_1M_6
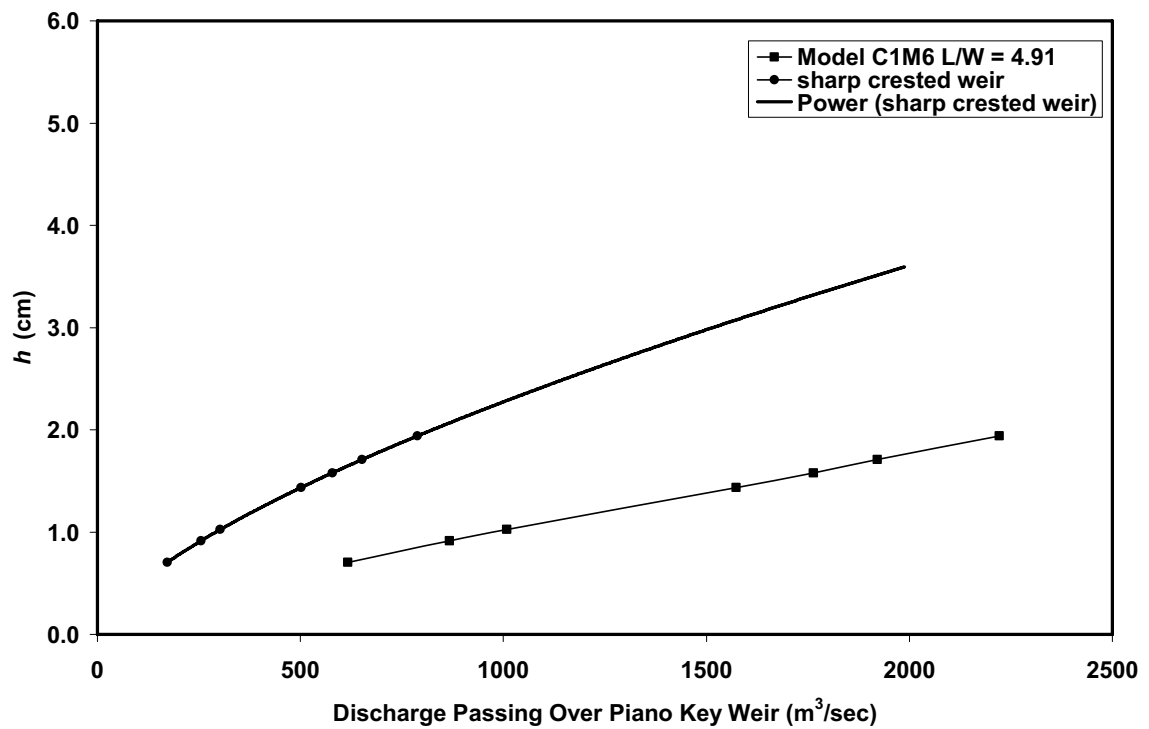
Fig. 5.13 Comparison of Piano Key Weir by to sharp crested weir with head over the crest for model C_1M_6

Plate No. 5.8 Running view of Piano Key Weir from d/s with under sluice gate

Plate No. 5.9 Running view of Piano Key Weir from u/s with under sluice gate

The maximum water level (MWL) for design flood of 5240 m^3/s was found at El 1423.12 from model study. The rating curve for the discharge passing over Piano Key Weir is depicted in adjoining Fig. 5.14. Reservoir level for 4000 m^3/s passes over Piano Key Weir is 1421.25 m.
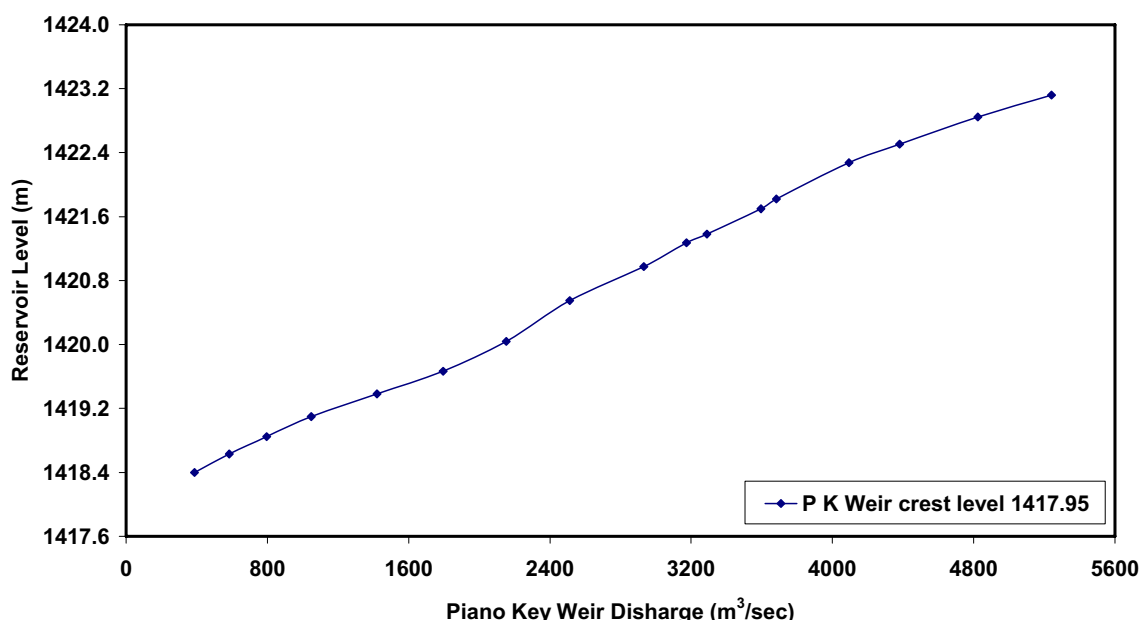
Fig. 5.14 Discharge passing over Piano Key Weir and corresponding reservoir level

5.5   SUMMARY

Design flood of the Sawara Kuddu HEP is 6880 m^3/s and requires high spilling capacity through weir in limited space. Piano Key Weir is designed with geometrically similar scale factor of 1:50. Six different geometries of Piano Key Weirs have been investigated in the lab. Among them, model C_1M_6 was found to be the most efficient with regard to the weir capacity. Study of model C_1M_6 indicated that the Piano Key Weir gives about 2.62 to 4.20 times higher discharge than sharp crested weir for corresponding head. The best evolved shape of Piano Key Weir from laboratory model study has been used for comprehensive model study. Comprehensive model study shows very interesting result that saving of head over the crest in Piano Key Weir lies in the range of 45 to 58 % of sharp crested weir.

CHAPTER 6
CONCLUSIONS AND FUTURE SCOPE OF WORK

6.1 CONCLUSIONS

Based on this study, the following conclusions can be inferred:

1. Different phase of experiments (phase -I to IV) which were planned with different configurations of Piano Key Weir, i.e. with or without ramp and one or two side overhanging (u/s & d/s) indicate that Piano Key Weir with presence of ramp and two sides overhanging provides a higher discharge under same head when compared with other Piano Key Weir configurations with lesser number of ramps and/or over-hangings. Different phase of experiments (phase -I to IV) which were planned with different configurations of Piano Key Weir, i.e. with or without ramp and one or two side overhanging (u/s & d/s) indicate that discharge through Piano Key Weir gets increased with increasing h/p upto unity

2. The hydraulic effect of P. K. Weir on discharge passing capacity at higher value of head over crest to crest height ratio h/p may depend upon height of model only and not the L/W ratio. Because at higher value of h/p, the net discharge increment for the best model seems to coincide at constant model height, and variable L/W ratio does not coincide at variable values of model height and constant value of L/W ratio.

3. At higher range of h/p, nappe formation occurs due to hydraulic effect triggered by upstream Piano Key shape between two elements. At medium range of h/p, depths of nappe formation that occur from upstream direction of elements are smaller than higher discharge due to effect of Piano key shape. Two more nappe formation between each element occurs sideways from the element, resulting in collision of lateral jets at the brink of each wall. At lower ranges of h/p, nappe formation phenomenon is less pronounced due to combined effect of (i) upstream piano key shape and (ii) two nappes plunging from the sideways of each element, which are more than that of medium range discharges and no occurrence of jet collision is observed at the brink of each wall.

4. The discharge magnification ratio of 'r' value is increasing with the length magnification L/W ratio for different h/p values. But as can be discerned from the plot, at higher h/p values (i..e 0.75), the 'r' value does not display any significant increase with L/W ratio. Also, it is seen from graphs of different phase experiments that the discharge magnification ratio (r) was found to increase with magnification ratio L/W. However, at larger value of L/W, the ratio (r) was observed to tend to approach a limiting value in the proximity of four.

5. From graphical plot of Phases I-IV, it is seen that at lower h/p value the sensitivity of crest height parameter 'p' is clearly discernible. The lower value of 'p' gives higher magnitude of 'r' in the lower range of h/p ratio.

6. In phase-V experiments, fillings were introduced in the ramps but these were not found to increase the discharge. Thus, ramps with no planar discontinuity were found to be best performing. In phase-V experiments, modifications were introduced into inlet limb of Piano Key Weir but it was again observed (experiment set P5M1 & P5M2) that such inlet modification was of no practical significance as it did not lead to any increase in the discharge.

7. Comprehensive model study of Piano Key Weir for Sawara Kuddu HEP as an adopted case study shows very interesting result that energy loss behaviour in downstream of Piano Key Weir is sufficient with providing steps in downstream of Piano Key Weir and it is also shown in Plate No. 5.8.

6.2 FUTURE SCOPE OF WORK

- Detailed flow characteristics over a typical Piano Key Weir model may be studied to provide an insight into the internal flow distribution characteristics through the different flow paths constituting the overall magnified crest length and the flow characteristics in the upstream of the Piano Key Weir.

- The model study is required for higher discharges.

- Detailed study on crest shape of Piano Key Weir is also required.

REFERENCES

1. Afshar, A., (1988) "The Development of Labyrinth Weir Design", Water Power and Dam Construction, 40(5), 36-39.

2. Baud O., Hager W.H., Minor H.-E. (2002) "Non-intrusive Discharge Measurements During Floods" Proc. Int. Conf. Flood Estimation March, 6-8, Berne, Switzerland.

3. Blanc, P., and Lemperiere, F., (2001) "Labyrinth Spillways Have a Promising Future", International Journal of Hydropower & Dams, Issue 4.

4. Borghei S.M., Jalili M.R. and Ghodsian M. (1999) "Discharge Coefficient for Sharp Crested Weir in Subcritical Flow", American Society of Civil Engineering, Journal of Hydraulic Engineering, 125(10), 1051-1056.

5. Chi Hien, T., Thanh Son, H. and Ho Ta Khanh, M. (2006) "Results of Some Piano Keys Weir Hydraulic Model Tests in Vietnam", CIGB/ICOLD, Barcelona, Spain.

6. Chow V.T. (1959), "Open Channel Hydraulics", Mc Graw-Hill, Inc., New York.

7. Cohen J, Cohen P, Aiken L, & West S. (2003) "Applied Multiple Regression/Correlation Analysis for the Behavioral Sciences", 3rd ed. Hillsdale NJ: Lawrence Erlbaum.

8. Darvas, L. A. (1971) "Performance and Design of Labyrinth Weirs", American Society of Civil Engineering, Journal of Hydraulic Engineering, 97(80), 1246-1251.

9. Emiroglu, M. E. and A. Baylar (2005) "Influence of Included Angle and Sill Slope of Air Entrainment of Triangular Planform Labyrinth Weirs", American Society of Civil Engineering, Journal of Hydrualic Engineering, 131(3): 184-189.

10. Falvey H.T. (2003) "Hydraulic Design of Labyrinth Weir", ACSE Press, USA.

11. Hay, N., and Taylor, G., (1970) "Performance and Design of Labyrinth Weirs", American Society of Civil Engineering, Journal of Hydraulic Engineering, 96(11), 2237-2357.

12. Kindsvater, C. E., and Carter R. W. (1959), "discharge characteristics of rectangular thin plate weirs", American Society of Civil Engineering, Journal of Hydraulic Engineering, 124, 772-822.

13. Laugier, F. (2007) "Design and Construction of the First Piano Key Weir (PKW) Spillway at the Goulours Dam", Hydropower & Dams. Issue 5,

14. Leite Ribeiro M., Bieri M., Boillat J.-L., Schleiss A., Laugier F., (2009) "Improving Hydraulic Capacity of existing spillway, Pani key weir design", Q.90-R.1, International Commission on the Large Barrage, Brasilia, Mai.

15. Leite Ribeiro M., Boillat J.-L., Kantoush S., Albalat C., Laugier F., Lochu A. (2007) "Rehabilitation of St-Marc dam: Model studies for the spillways", Hydro 2007 "New approaches for a new era", Granada, Spain,15-17 October 2007.

16. Lempérière F. and Jun G. (2005) "Low Cost Increase of Dams Storage and Flood Mitigation: The Piano Keys Weir", Q. 53 R. 2.06 International Commission on Irrigation and Drainage Nineteenth Congress Beijing.

17. Lempérière, F. and Ouamane, A. (2003) "The Piano Keys weir: a new cost-effective solution for spillways", Hydropower & Dams Issue 5, 144-149.

18. Lux, F., (1989) "Design and Application of Labyrinth weir", Design of Hydraulic Structures 89, Balkema/Rotterdam/Brookfield.

19. Lux, F., and Hinchliff, D.L., (1985) "Design and construction of labyrinth spillways", 15th Congress ICOLD, Vol. IV, Q59-R15, Lausanne, Switzerland, 249-274.

20. Magalhaes, A. P., and M. Lorena (1989) "Hydraulic Design of Labyrinth Weir", Report No. 736, National Laboratory of Civil Engineering, Lisbon, Portugal.

21. Meglhaes, A. P., (1985) "Labyrinth weir spillway", Transactions of the 15th Congress ICOLD, Vol. VI, Q59-R24, Lausanne, Switzerland, 395-407.

22. Modi P.N. and seth S.M. (1991) "Hydraulics and Fluid Mechanics", Edition 10, Standard Book House, New Delhi.

23. Ouamane, A. and Lempérière F. (2006) "Design of a new economic shape of weir", Proceedings of the International Symposium on Dams in the Societies of the 21st Century, 463-470. Barcelona, Spain,

24. Pinheiro, A.N., and Silva, I., (1999) "Discharge coefficient of side weirs, Experimental study and comparative analysis of different formulas", XXVIII IAHR Proceedings, Garz, Austria.

25. Taylor G. (1968), "The Performance of Labyrinth Weir", Ph.D. Thesis, University of Nottingham, Nottingham, U.K.

26. Tullis, J. P., Nosratollah, A., and Waldron, D., (1995). "Design of labyrinth spillways", American Society of Civil Engineering, Journal of Hydraulic Engineering, 121(3), 247-255.

27. Weber, L.J., Shumate, E.D. and Mawer, (2001) "Experimental on Flow at a 90° Open-Channel Junction", Journal of Hydraulic Engineering, ASCE, Vol. 127, No. 5.

28. Wormleaton, P. R. and C. C. Tsang (2000) "Aeration performance of rectangular plan-form labyrinth weirs", Journal of Hydrualic Environmental Engineering 126(5): 456-465.

DATA RELATED TO FIVE PHASE EXPERIEMNTS

This appendix contains the experimental data collected in five phase experiments. The data presented here have been used in Chapter 4.

P	=	height of weir (cm)
L	=	Perimeter of Piano Key weir crest (cm)
W	=	Width of channel (cm)
Q_{PK}	=	Piano Key Weir discharge (l/s)
Q_L	=	Linear Weir discharge (l/s)
r	=	Q_{PK}/Q_L
ΔQ	=	$Q_{PK}-Q_L$

Table A.1: Data for discharge coefficient variation analysis for Model P_1M_1

h	h/p	Q_{PK}	Q_L	r	ΔQ
14.56	1.21	82.24	60.00	1.37	22.24
12.06	1.01	64.68	45.23	1.43	19.45
9.84	0.82	51.61	33.34	1.55	18.27
6.70	0.56	34.84	18.73	1.86	16.11
5.69	0.47	29.51	14.66	2.01	14.85
3.87	0.32	19.42	8.22	2.36	11.20
2.40	0.20	10.73	4.02	2.67	6.71

Table A.2: Data for discharge coefficient variation analysis for Model P_1M_2

h	h/p	Q_{PK}	Q_L	r	ΔQ
13.04	0.82	80.75	50.86	1.59	29.89
12.04	0.75	74.19	45.12	1.64	29.07
10.65	0.67	64.26	37.54	1.71	26.72
8.97	0.56	54.56	29.01	1.88	25.54
7.35	0.46	44.46	21.52	2.07	22.94
6.45	0.40	37.98	17.69	2.15	20.29
5.07	0.32	29.17	12.33	2.37	16.84
3.82	0.24	21.68	8.06	2.69	13.62
3.30	0.21	18.12	6.47	2.80	11.64
2.76	0.17	14.80	4.95	2.99	9.84

Table A.3: Data for discharge coefficient variation analysis for Model P₁M₃

h	h/p	Q_{PK}	Q_L	r	ΔQ
12.63	0.63	78.98	48.48	1.63	30.50
11.74	0.59	72.96	43.44	1.68	29.51
10.53	0.53	65.50	36.90	1.77	28.60
9.26	0.46	57.03	30.43	1.87	26.59
7.70	0.39	47.41	23.08	2.05	24.33
6.32	0.32	38.99	17.16	2.27	21.83
5.03	0.25	31.18	12.18	2.56	19.00
3.80	0.19	23.94	8.00	2.99	15.94
2.90	0.15	17.99	5.33	3.37	12.66
2.60	0.13	15.72	4.53	3.47	11.19
2.07	0.10	11.83	3.22	3.68	8.61

Table A.4: Data for discharge coefficient variation analysis for Model P₁M₄

h	h/p	Q_{PK}	Q_L	r	ΔQ
15.19	1.27	82.41	63.94	1.29	18.47
14.00	1.17	75.19	56.57	1.33	18.62
12.70	1.06	67.07	48.88	1.37	18.19
11.55	0.96	59.28	42.39	1.40	16.89
9.82	0.82	48.23	33.23	1.45	15.00
8.77	0.73	42.58	28.05	1.52	14.54
7.08	0.59	32.43	20.35	1.59	12.09
6.03	0.50	26.75	15.99	1.67	10.76
5.30	0.44	22.84	13.18	1.73	9.66
4.58	0.38	18.69	10.59	1.77	8.10
3.90	0.33	14.93	8.32	1.80	6.61
3.23	0.27	11.71	6.27	1.87	5.44

Table A.5: Data for discharge coefficient variation analysis for Model P₁M₅

h	h/p	Q_{PK}	Q_L	r	ΔQ
13.31	1.11	77.14	52.44	1.47	24.70
12.20	0.76	69.06	46.02	1.50	23.04
11.17	0.70	60.66	40.32	1.50	20.35
9.97	0.62	52.09	34.00	1.53	18.09
8.87	0.55	45.92	28.53	1.61	17.39
7.89	0.49	39.42	23.94	1.65	15.48
6.50	0.41	31.05	17.90	1.74	13.16
5.34	0.33	23.97	13.33	1.80	10.64
4.70	0.29	20.79	11.00	1.89	9.79
3.89	0.24	16.36	8.29	1.97	8.08
3.34	0.21	13.86	6.59	2.10	7.27

Table A.6: Data for discharge coefficient variation analysis for Model P_1M_6

h	h/p	Q_{PK}	Q_L	r	ΔQ
13.16	0.82	80.16	51.56	1.55	28.60
12.30	0.77	73.83	46.59	1.58	27.24
11.22	0.70	65.52	40.59	1.61	24.93
9.97	0.62	57.03	34.00	1.68	23.03
8.82	0.55	48.77	28.29	1.72	20.48
7.84	0.49	42.92	23.71	1.81	19.22
7.04	0.44	37.83	20.17	1.87	17.65
6.17	0.39	32.43	16.55	1.96	15.88
5.20	0.33	25.89	12.81	2.02	13.08
4.15	0.26	19.74	9.13	2.16	10.61
3.35	0.21	15.21	6.62	2.30	8.58

Table A.7: Data for discharge coefficient variation analysis for Model P_2M_1

h	h/p	Q_{PK}	Q_L	r	ΔQ
14.16	1.18	80.08	57.55	1.39	22.53
12.65	1.05	70.20	48.59	1.44	21.61
11.40	0.95	61.92	41.57	1.49	20.35
10.07	0.84	54.74	34.51	1.59	20.23
9.00	0.75	47.16	28.46	1.66	18.70
6.92	0.58	36.22	19.66	1.84	16.56
5.68	0.47	30.12	14.62	2.06	15.50
4.48	0.37	23.50	10.24	2.29	13.26
3.40	0.28	17.50	6.77	2.58	10.73
2.60	0.22	12.67	4.53	2.80	8.14

Table A.8: Data for discharge coefficient variation analysis for Model P_2M_2

h	h/p	Q_{PK}	Q_L	r	ΔQ
12.34	0.77	76.73	46.81	1.64	29.92
11.02	0.69	69.12	39.50	1.75	29.62
9.98	0.62	61.83	34.05	1.82	27.78
8.37	0.52	52.32	26.15	2.00	26.17
6.88	0.43	44.58	19.49	2.29	25.09
5.58	0.35	37.03	14.23	2.60	22.80
4.56	0.29	29.50	10.52	2.80	18.98
3.52	0.22	23.38	7.13	3.28	16.25
2.78	0.17	18.52	5.00	3.70	13.52
2.18	0.14	14.07	3.48	4.04	10.59
1.93	0.12	11.98	2.90	4.13	9.08

Table A.9: Data for discharge coefficient variation analysis for Model P₂M₃

h	h/p	Q_{PK}	Q_L	r	ΔQ
11.17	0.56	70.72	40.32	1.75	30.40
9.94	0.50	62.77	33.84	1.85	28.93
8.87	0.44	54.98	28.53	1.93	26.45
7.62	0.38	47.97	22.72	2.11	25.25
6.50	0.33	41.56	17.90	2.32	23.66
4.93	0.25	32.05	11.82	2.71	20.23
3.42	0.17	23.92	6.83	3.50	17.09
2.80	0.14	18.73	5.06	3.70	13.67
2.18	0.11	13.62	3.48	3.91	10.14

Table A.10: Data for discharge coefficient variation analysis for Model P₂M₄

h	h/p	Q_{PK}	Q_L	r	ΔQ
14.10	1.18	78.25	57.18	1.37	21.07
12.51	1.04	68.31	48.79	1.40	19.52
11.40	0.95	60.56	41.57	1.46	18.99
10.34	0.86	54.43	35.90	1.52	18.53
9.28	0.77	48.23	30.53	1.58	17.70
7.44	0.62	37.23	21.92	1.70	15.31
6.37	0.53	30.32	17.36	1.75	12.96
5.40	0.45	24.90	13.55	1.84	11.35
4.48	0.37	19.93	10.24	1.95	9.69
3.63	0.30	15.98	7.47	2.14	8.51
3.15	0.26	13.98	6.04	2.31	7.94

Table A.11: Data for discharge coefficient variation analysis for Model P₂M₅

h	h/p	Q_{PK}	Q_L	r	ΔQ
13.35	1.11	80.49	52.68	1.53	27.81
12.00	0.75	70.27	44.89	1.57	25.38
11.01	0.69	62.15	39.45	1.58	22.70
9.98	0.62	54.92	34.05	1.61	20.87
8.55	0.53	46.64	27.00	1.73	19.64
7.38	0.46	38.18	21.65	1.76	16.53
5.49	0.34	26.52	13.89	1.91	12.63
4.65	0.29	22.41	10.82	2.07	11.59
3.92	0.25	18.55	8.38	2.21	10.17
2.98	0.19	13.25	5.55	2.39	7.70

Table A.12: Data for discharge coefficient variation analysis for Model P$_2$M$_6$

h	h/p	Q$_{PK}$	Q$_L$	r	ΔQ
12.70	0.79	77.10	48.88	1.58	28.22
11.55	0.58	69.30	42.39	1.63	26.91
10.54	0.53	61.83	36.95	1.67	24.88
9.73	0.49	56.53	32.78	1.72	23.75
8.48	0.42	47.81	26.67	1.79	21.14
7.28	0.36	40.05	21.21	1.89	18.84
6.15	0.31	33.05	16.47	2.01	16.58
5.13	0.26	25.83	12.55	2.06	13.28
4.05	0.20	18.78	8.80	2.13	9.98
3.62	0.18	16.37	7.44	2.20	8.93
3.14	0.16	13.43	6.00	2.24	7.43

Table A.13: Data for discharge coefficient variation analysis for Model P$_3$M$_1$

h	h/p	Q$_{PK}$	Q$_L$	r	ΔQ
12.51	0.78	77.98	47.78	1.63	30.20
11.22	0.70	69.90	40.58	1.72	29.32
9.91	0.62	61.68	33.69	1.83	27.99
8.56	0.54	52.95	27.04	1.96	25.91
7.10	0.44	43.76	20.43	2.14	23.33
6.09	0.38	37.62	16.23	2.32	21.39
4.72	0.30	29.11	10.17	2.86	18.94
4.00	0.25	24.60	7.81	3.15	16.79
3.28	0.21	19.94	5.67	3.52	14.27
2.48	0.16	14.63	3.86	3.79	10.77
1.99	0.12	11.59	3.03	3.83	8.56

Table A.14: Data for discharge coefficient variation analysis for Model P$_3$M$_2$

h	h/p	Q$_{PK}$	Q$_L$	r	ΔQ
13.56	0.85	81.12	53.92	1.50	27.20
12.54	0.78	73.19	47.96	1.53	25.23
11.26	0.70	64.70	40.80	1.59	23.90
9.78	0.61	55.42	33.03	1.68	22.39
8.65	0.54	48.32	27.47	1.76	20.85
7.38	0.46	40.88	21.65	1.89	19.23
6.63	0.41	36.64	18.35	2.00	18.29
4.91	0.31	26.16	11.75	2.23	14.41
3.94	0.25	20.80	8.45	2.46	12.35
3.12	0.20	16.37	5.89	2.78	10.48
2.40	0.15	11.67	4.01	2.91	7.66

Table A.15: Data for discharge coefficient variation analysis for Model P₃M₃

h	h/p	Q_{PK}	Q_L	r	ΔQ
12.18	0.76	74.98	45.90	1.63	29.08
10.78	0.67	66.30	38.22	1.73	28.08
9.39	0.59	57.14	31.07	1.84	26.07
7.97	0.50	48.40	23.75	2.04	24.65
6.92	0.43	42.00	19.23	2.18	22.77
6.15	0.38	37.17	16.47	2.26	20.70
4.50	0.28	25.90	10.30	2.51	15.60
3.81	0.24	21.60	8.03	2.69	13.57
3.04	0.19	16.66	5.72	2.91	10.94
2.45	0.15	12.19	4.02	3.03	8.17

Table A.16: Data for discharge coefficient variation analysis for Model P₃M₄

h	h/p	Q_{PK}	Q_L	r	ΔQ
13.37	0.84	77.83	52.80	1.47	25.03
12.13	0.76	69.01	45.63	1.51	23.38
10.69	0.67	58.57	37.74	1.55	20.83
9.20	0.58	50.03	29.65	1.69	20.38
7.88	0.49	41.84	23.89	1.75	17.95
7.03	0.44	36.14	20.13	1.80	16.01
6.62	0.41	33.05	18.39	1.80	14.66
5.06	0.32	25.21	12.07	2.09	13.14
4.23	0.26	21.02	9.39	2.24	11.63
3.25	0.20	15.54	6.33	2.45	9.21
2.60	0.16	11.69	4.53	2.58	7.16

Table A.17: Data for discharge coefficient variation analysis for Model P₃M₅

h	h/p	Q_{PK}	Q_L	r	ΔQ
13.02	0.81	78.02	50.73	1.54	27.29
11.92	0.75	70.56	44.44	1.59	26.12
10.69	0.67	61.30	37.74	1.62	23.56
9.25	0.58	52.18	29.64	1.76	22.54
8.15	0.51	45.60	25.12	1.82	20.48
6.90	0.43	37.62	19.57	1.92	18.05
4.60	0.29	24.60	10.65	2.31	13.95
3.62	0.23	19.04	7.44	2.56	11.60
2.90	0.18	14.97	5.33	2.81	9.64
2.40	0.15	11.59	4.02	2.88	7.57

Table A.18: Data for discharge coefficient variation analysis for Model P₃M₆

h	h/p	Q_{PK}	Q_L	r	ΔQ
13.38	0.84	73.78	52.85	1.40	20.93
12.30	0.77	65.53	46.59	1.41	18.94
11.00	0.69	57.03	39.40	1.45	17.63
9.64	0.60	49.05	32.32	1.52	16.73
7.95	0.50	39.84	24.21	1.65	15.63
7.13	0.45	34.99	20.56	1.70	14.43
5.52	0.35	25.21	14.00	1.80	11.21
4.56	0.29	20.14	10.52	1.91	9.62
3.70	0.23	15.38	7.68	2.00	7.70
3.07	0.19	12.38	5.82	2.13	6.56

Table A.19: Data for discharge coefficient variation analysis for Model P₄M₁

h	h/p	Q_{PK}	Q_L	r	ΔQ
12.80	0.80	83.56	49.45	1.69	34.11
11.40	0.71	74.83	41.57	1.80	33.26
10.07	0.63	65.03	34.51	1.88	30.52
8.32	0.52	53.00	25.26	2.10	27.74
7.10	0.44	45.28	20.43	2.22	24.85
6.06	0.38	39.70	16.11	2.46	23.59
4.15	0.26	27.29	9.13	2.99	18.16
3.46	0.22	23.15	6.95	3.33	16.20
2.80	0.18	18.57	5.06	3.67	13.51
2.14	0.13	14.10	3.38	4.17	10.72
1.76	0.11	10.92	2.52	4.33	8.40

Table A.20: Data for discharge coefficient variation analysis for Model P₄M₂

h	h/p	Q_{PK}	Q_L	r	ΔQ
12.55	0.78	79.27	48.01	1.65	31.26
11.34	0.71	70.46	41.24	1.71	29.22
10.18	0.64	62.36	35.07	1.78	27.29
8.80	0.55	51.70	28.19	1.83	23.51
7.30	0.46	43.11	21.30	2.02	21.81
6.50	0.41	37.43	17.89	2.09	19.54
4.86	0.30	25.30	11.57	2.19	13.73
4.27	0.27	20.94	9.53	2.20	11.41
3.50	0.22	16.13	7.07	2.28	9.06
2.62	0.16	11.11	4.59	2.42	6.52

Table A.21: Data for discharge coefficient variation analysis for Model P$_4$M$_3$

h	h/p	Q$_{PK}$	Q$_L$	r	ΔQ
12.10	0.76	78.01	45.45	1.72	32.56
10.93	0.68	69.41	39.02	1.78	30.39
9.86	0.62	61.83	33.43	1.85	28.40
8.35	0.52	52.18	26.05	2.00	26.13
6.90	0.43	43.20	19.57	2.21	23.63
6.05	0.38	38.02	16.07	2.37	21.95
4.37	0.27	26.97	9.86	2.74	17.11
3.80	0.24	22.65	8.00	2.83	14.65
3.38	0.21	19.40	6.71	2.89	12.69
2.77	0.17	15.20	4.98	3.05	10.22
2.33	0.15	12.07	3.84	3.14	8.23

Table A.22: Data for discharge coefficient variation analysis for Model P$_4$M$_4$

h	h/p	Q$_{PK}$	Q$_L$	r	ΔQ
14.45	1.20	90.22	59.32	1.52	30.90
9.20	0.77	55.22	30.14	1.83	25.08
8.45	0.70	50.84	26.53	1.92	24.31
7.23	0.60	42.21	21.00	2.01	21.21
6.08	0.51	35.56	16.19	2.20	19.37
4.88	0.41	28.16	11.64	2.42	16.52
3.55	0.30	20.58	7.22	2.85	13.36
2.60	0.22	15.09	4.53	3.33	10.56

Table A.23: Data for discharge coefficient variation analysis for Model P$_4$M$_5$

h	h/p	Q$_{PK}$	Q$_L$	r	ΔQ
14.80	1.23	89.88	61.49	1.46	28.39
13.80	1.15	82.39	55.37	1.49	27.02
9.52	0.79	54.87	31.72	1.73	23.15
8.91	0.74	51.22	28.72	1.78	22.50
8.05	0.67	45.39	24.67	1.84	20.72
7.00	0.58	38.87	20.00	1.94	18.86
5.71	0.48	31.20	14.74	2.12	16.46
4.61	0.38	25.17	10.69	2.35	14.48
3.40	0.28	18.54	6.77	2.74	11.77

Table A.24: Data for discharge coefficient variation analysis for Model P$_5$M$_1$

h	h/p	Q_{PK}	Q_L	r	ΔQ
14.22	1.19	79.81	57.91	1.38	21.90
10.55	0.88	56.68	37.01	1.53	19.67
9.72	0.81	50.23	32.73	1.53	17.50
9.22	0.77	46.14	30.24	1.53	15.90
8.22	0.69	40.00	25.45	1.57	14.55
6.95	0.58	32.45	19.79	1.64	12.66
6.26	0.52	28.44	16.92	1.68	11.53
5.26	0.44	22.60	13.03	1.73	9.57
4.67	0.39	19.40	10.90	1.78	8.50

Table A.25: Data for discharge coefficient variation analysis for Model P$_5$M$_2$

h	h/p	Q_{PK}	Q_L	r	ΔQ
13.36	0.84	81.63	52.74	1.55	28.89
9.23	0.58	50.69	30.28	1.67	20.41
8.38	0.52	45.07	26.20	1.72	18.87
7.40	0.46	40.53	21.74	1.86	18.79
6.64	0.42	36.06	18.48	1.95	17.58
5.93	0.37	30.99	15.60	1.99	15.39
4.88	0.31	23.50	11.64	2.02	11.86
4.43	0.28	20.41	10.07	2.03	10.34
3.38	0.21	14.30	6.71	2.13	7.59

Table A.26: Data for discharge coefficient variation analysis for Model P$_5$M$_3$

h	h/p	Q_{PK}	Q_L	r	ΔQ
14.35	0.90	78.63	59.80	1.31	18.83
13.31	0.83	71.43	52.44	1.36	18.99
12.22	0.76	64.15	46.13	1.39	18.02
10.84	0.68	56.37	38.54	1.46	17.83
9.63	0.60	48.60	32.37	1.50	16.23
8.31	0.52	40.89	25.87	1.58	15.02
7.44	0.47	35.61	21.91	1.63	13.70
6.17	0.39	29.28	16.55	1.77	12.73
5.28	0.33	23.64	13.10	1.80	10.54
4.45	0.28	18.88	10.13	1.86	8.75
3.53	0.22	14.03	7.16	1.96	6.87

Table A.27: Data for discharge coefficient variation analysis for Model P$_5$M$_4$

h	h/p	Q_{PK}	Q_L	r	ΔQ
12.96	0.81	74.38	50.38	1.48	24.00
11.13	0.70	65.19	40.10	1.63	25.09
9.94	0.62	58.16	33.84	1.72	24.32
8.43	0.53	49.42	26.43	1.87	22.99
6.35	0.40	38.89	17.28	2.25	21.61
5.03	0.31	29.85	12.18	2.45	17.67
4.27	0.27	25.21	9.53	2.65	15.68
3.55	0.22	20.60	7.22	2.85	13.38
2.80	0.18	15.17	5.06	3.00	10.11
2.38	0.15	12.19	3.96	3.08	8.23

Table A.28: Data for discharge coefficient variation analysis for Model P$_5$M$_5$

h	h/p	Q_{PK}	Q_L	r	ΔQ
13.10	0.82	75.43	51.20	1.47	24.23
11.89	0.74	67.75	44.27	1.53	23.48
10.58	0.66	58.42	37.16	1.57	21.26
9.59	0.60	51.37	32.07	1.60	19.30
8.28	0.52	43.42	25.73	1.69	17.69
7.45	0.47	37.74	21.96	1.72	15.78
6.72	0.42	33.42	18.81	1.78	14.61
5.24	0.33	24.60	12.95	1.90	11.65
4.63	0.29	21.00	10.76	1.95	10.24
3.87	0.24	16.49	8.22	2.01	8.27
3.33	0.21	13.00	6.56	1.98	6.44

DATA RELATED TO CASE STUDY

This appendix contains the experimental data collected in case study experiments. The data presented here have been used in Chapter 5.

P	$=$	height of weir (cm)
L	$=$	Perimeter of Piano Key weir crest (cm)
W	$=$	Width of channel (cm)
Q_{PK}	$=$	Piano Key Weir discharge (l/s)
Q_L	$=$	Linear Weir discharge (l/s)
r	$=$	Q_{PK}/Q_L
ΔQ	$=$	$Q_{PK}-Q_L$

Table B.1: Data for discharge coefficient variation analysis for Model C_1M_1

h	h/p	Q_L	Q_{PK}	r	ΔQ
5.540	0.301	28.166	43.251	1.536	15.086
5.210	0.283	25.687	40.222	1.566	14.535
4.850	0.264	23.071	37.323	1.618	14.252
4.410	0.240	20.004	33.217	1.661	13.213
3.200	0.174	12.365	22.423	1.814	10.059
2.460	0.134	8.334	15.432	1.852	7.098
2.000	0.109	6.109	11.836	1.937	5.727

Table B.2: Data for discharge coefficient variation analysis for Model C_1M_2

h	h/p	Q_L	Q_{PK}	r	ΔQ
4.610	0.249	21.380	45.451	2.126	24.071
4.340	0.234	19.529	42.285	2.165	22.756
3.330	0.180	13.126	31.362	2.389	18.236
2.800	0.151	10.120	25.300	2.500	15.180
2.020	0.109	6.201	16.304	2.629	10.103
1.560	0.084	4.209	11.414	2.712	7.205

Table B.3: Data for discharge coefficient variation analysis for Model C_1M_3

h	h/p	Q_L	Q_{PK}	r	ΔQ
4.930	0.266	23.644	47.952	2.028	24.307
4.390	0.237	19.868	43.031	2.166	23.163
4.070	0.220	17.736	39.172	2.209	21.436
3.500	0.189	14.143	33.406	2.362	19.263
2.440	0.132	8.233	21.685	2.634	13.453
2.060	0.111	6.386	17.693	2.770	11.306
1.580	0.085	4.290	12.645	2.948	8.355

Table B.4: Data for discharge coefficient variation analysis for Model C_1M_4

h	h/p	Q_L	Q_{PK}	r	ΔQ
3.550	0.191	14.448	43.251	2.994	28.804
3.350	0.181	13.244	41.289	3.118	28.045
2.900	0.156	10.667	35.725	3.349	25.058
2.710	0.146	9.636	33.596	3.486	23.960
1.940	0.105	5.837	21.832	3.741	15.995
1.600	0.086	4.372	17.053	3.901	12.682
1.400	0.076	3.578	14.519	4.058	10.941
1.120	0.060	2.560	10.731	4.191	8.170

Table B.5: Data for discharge coefficient variation analysis for Model C_1M_5

h	h/p	Q_L	Q_{PK}	r	ΔQ
3.810	0.206	16.064	44.816	2.790	28.752
2.840	0.153	10.338	33.029	3.195	22.691
2.090	0.113	6.526	22.723	3.482	16.196
1.870	0.101	5.524	19.559	3.541	14.036
1.630	0.088	4.495	16.181	3.600	11.686
1.290	0.070	3.165	11.836	3.740	8.671

Table B.6: Data for discharge coefficient variation analysis for Model C_1M_6

h	h/p	Q_L	Q_{PK}	r	ΔQ
3.880	0.211	15.897	44.816	2.819	28.919
3.420	0.186	13.155	38.756	2.946	25.601
3.160	0.172	11.684	35.568	3.044	23.884
2.870	0.156	10.113	31.728	3.137	21.615
2.050	0.111	6.105	20.338	3.331	14.232
1.830	0.099	5.149	17.486	3.396	12.337
1.410	0.077	3.483	12.434	3.570	8.952